

**Partitioning of inorganic contaminants between fluid fine tailings and cap water under end  
pit lake scenario:  
Biological, Chemical and Mineralogical processes**

by

Najmeh Samadi

A thesis submitted in partial fulfillment of the requirements for the degree of

Master of Science

in

Soil Science

Department of Renewable Resources  
University of Alberta

© Najmeh Samadi, 2019

## Abstract

Fluid fine tailings (FFT) are generated during bitumen extraction from surface mined oil sands ore (in Alberta, Canada) and comprised of oil sands process-affected water (OSPW), fine particles, unrecovered bitumen and residual diluent. For reclaiming huge volumes of FFT, a viable remediation option is to place FFT in open pit covered by a mix layer of OSPW and fresh water to form an end pit lake (EPL). A potential concern is the flux of constituents of concern (COCs) from underlying FFT to overlying cap water that could affect the quality and sustainability of EPLs. In this research, chemical, mineralogical and microbiological approaches were used to investigate how biogeochemical processes in underlying FFT would affect COCs transport to cap water. For this study, 10 L columns were filled with FFT (7 L) and cap water (1.4L), sealed anaerobically and incubated at room temperature in the dark. Labile hydrocarbons (a mixture of short chain *n*- and *iso*-alkanes and monoaromatics compound representing extraction diluent) endogenous to FFT were added to FFT (amended columns) to accelerate methanogenesis for the enhancement of biogeochemical processes in FFT. Some hydrocarbon-amended columns also received nutrients such as nitrogen (N) and phosphorus (P) at C: N: P ratio of 100:10:1 for optimal microbial growth, whereas others that did not receive any amendment as served as control (unamended) columns. The results demonstrated that hydrocarbon addition increased methane (CH<sub>4</sub>) and carbon dioxide (CO<sub>2</sub>) production in the FFT and N addition exhibited incremental effect on methanogenesis and all other subsequent biogeochemical processes. Molecular analysis (16S rRNA gene) revealed that *Syntrophaceae* and *Peptococcaceae* (Bacteria) syntrophically worked with acetoclastic (*Methanosaetaceae*) and hydrogenotrophic (*Methanoregulaceae*) methanogens (Archaea) to metabolize hydrocarbons into CH<sub>4</sub> and CO<sub>2</sub> under methanogenic conditions.

Methanogenesis in amended columns increased dewatering and consolidation of FFT by altering porewater chemistry and transforming iron (Fe) minerals. Biogenic CO<sub>2</sub> production

decreased pH that dissolved carbonate minerals in FFT and increased concentrations of  $\text{Ca}^{2+}$ ,  $\text{Mg}^{2+}$ ,  $\text{HCO}_3^-$  in the porewater. Some trace metals such strontium (Sr) and barium (Ba) also increased significantly in the porewater of amended columns. These soluble ions/metals were transported to cap water via porewater expression and  $\text{CH}_4$  ebullition. Iron fractionation in FFT revealed that methanogenesis also transformed crystalline  $\text{Fe}^{\text{III}}$  minerals to amorphous  $\text{Fe}^{\text{II}}$  minerals decreasing the concentrations of certain metals such as arsenic (As), antimony (Sb), chromium (Cr), vanadium (V) and molybdenum (Mo) in porewater and cap water probably through reduction and precipitation with newly formed amorphous Fe minerals. Sequential metal extraction from FFT showed that carbonate, Fe, and manganese (Mn) oxide minerals in FFT were the major source of Sr and Ba in the porewater. Naphthenic acids (NAs) concentrations were also decreased in the porewater and capwater of amended columns. These results can help assess the water quality in EPL and understand the role of indigenous microbial communities in the sustenance of methanogenesis and partitioning of COCs from underlying FFT to overlying cap water.

## **Preface**

The experimental setup was designed by myself, with the assistance of Associate Professor Dr. Tariq Siddique. All data collection and analysis in this thesis is my original work. No part of this thesis has been previously published.

## **Acknowledgements**

In the name of Allah, the Most Gracious and the Most Merciful Alhamdulillah, all praises to Allah for the strengths and His blessing in completing this thesis. None of my efforts will bear any fruit without the guidance and permission of Allah.

Special appreciation goes to my supervisor, Dr. Tariq Siddique, for his supervision and constant support. His invaluable help of constructive comments and suggestions throughout the experimental and thesis works have contributed to the success of this research. I would also like to thank Dr. Alsu Kuznetsova and Petr Kuznetsov for volunteering their advice and Dr. Gloria Okpala for her assistance.

I thank my supervisory committee member, Dr. Ania Ulrich. I would also like to thank my examiner, Dr. Guillermo Hernandez Ramirez, for giving their precious time and insight to improve my thesis.

I also would like to thank Syncrude for providing the scholarship and funding for my MSc program.

Last but not least, deepest gratitude goes to my dearest parents. I earnestly thank both of you for believing in me and for your never-ending prayers. I owe you my eternal gratitude for moulding me into who I am today and to my brother and sister in law for their endless love, prayers and encouragement. Also, not forgetting my friend, Kamran Asgari for his encouragement, care, and support. To those who indirectly contributed in this research, your kindness means a lot to me. Thank you very much.

**Table of Contents**

- 1 Introduction ..... 1**
  - 1.1 Oil sands industry ..... 1
    - 1.1.1 The Alberta oil sands ..... 1
    - 1.1.2. Bitumen Extraction ..... 1
    - 1.1.3. Extraction process ..... 2
    - 1.1.4. Environmental impacts of surface mining ..... 3
    - 1.1.5. Tailings management ..... 4
    - 1.1.6. End pit lakes in oil sands reclamation ..... 6
  - 1.2. Biogeochemical processes in tailings ponds/End Pit Lake ..... 6
    - 1.2.1. Methane emission from tailings ..... 6
    - 1.2.2. Microbial communities in the MFT ..... 9
    - 1.2.3. Effect of methanogenesis on the consolidation of tailings in tailings ponds and EPLs ..... 10
  - 1.3. Rationale of the current research project on the effect of methanogenesis on the partitioning of contaminants between solid and aqueous phases of tailings in end-pit lakes ..... 12
    - 1.3.1. Research objectives ..... 13
  - 1.4. References ..... 14
- 2 Nutrients’ impact on the methanogenesis in oil sand tailings under End Pit Lake scenario: I: co-occurrence of N cycling and methanogenesis ..... 20**
  - 2.1 Abstract ..... 20
  - 2.2 Introduction ..... 20
  - 2.3 Materials and methods ..... 23
    - 2.3.1 Chemicals and materials ..... 23
    - 2.3.2 Experimental setup ..... 23
    - 2.3.3 Chemical analysis ..... 25
    - 2.3.4 Characterization of the microbial community by 16S rRNA genes and its involvement in nitrogen cycling by NifH, NirS, NosZ, NrfA genes ..... 25
  - 2.4 Results ..... 27
    - 2.4.1 Biogas production in FFT amended with a mixture of hydrocarbons, with or without nutrients addition ..... 27
    - 2.4.2 Biodegradation of the hydrocarbons in the FFT ..... 28
    - 2.4.3 Characterization of microbial community in FFTs and cap water ..... 28
  - 2.5 Discussion ..... 32
  - 2.6 Conclusion ..... 38
  - 2.7 References ..... 40

<b>3</b>	<b>Nutrients' impact on the methanogenesis in oil sand tailings under End Pit Lake scenario: II. Flux of constituents of concern .....</b>	<b>65</b>
3.1	Abstract.....	65
3.2	Introduction .....	66
3.3	Materials and methods.....	68
3.3.1	Experimental setup and sampling scheme .....	68
3.3.2	Porewater recovery as cap water and FFT consolidation.....	69
3.3.3	Chemical analyses of the Cap water and FFT porewater.....	70
3.3.4	Chemical analyses of the FFT.....	71
3.4	Results .....	75
3.4.1	Biogenic gas production and changes in the porewater and cap water chemistry .....	75
3.4.2	Changes in trace metals mobility during methanogenesis .....	77
3.4.3	Transformation of Iron in Unamended and amended FFT as influenced by amendments ..	78
3.4.4	Influence of amendments on the fractionation of trace metals in FFT .....	79
3.4.5	Changes in NAs concentration in FFT and cap water after amendment.....	79
3.5	Discussion.....	80
3.6	Conclusion .....	88
3.7	References .....	90
<b>4</b>	<b>General Conclusions.....</b>	<b>118</b>
4.1	Research Summary .....	118
4.2	Recommendation for the future studies .....	120
	<b>Bibliography.....</b>	<b>121</b>
	<b>Appendix A.....</b>	<b>138</b>

## List of Tables

<b>Table 2-1:</b> Chemical characteristics of initial mature fine tailings used in 10-L column experiment before amendment and incubation. Values are presented as means $\pm$ standard deviation .....	<b>57</b>
<b>Table 2-2:</b> Chemical characteristics of initially collected water samples from BML and BCR before capping the 10-L column experiment. Values are presented as means $\pm$ standard deviation .....	<b>58</b>
<b>Table 2-3:</b> Primers used in PCR analysis.....	<b>59</b>
<b>Table 2-4:</b> PCR reaction conditions for various gene .....	<b>60</b>
<b>Table 2-5:</b> Archaeal community in the FFT and capwater at each treatment, organized at the family level. Inset heat map indicates U, HC, HCN, and HCNP samples with the highest OTU numbers. Not detected, INT-FFT, and Cap-INT left white.....	<b>61</b>
<b>Table 2-6:</b> Distribution of the 27 most abundant genera (%) in the FFT and capwater at each treatment. ....	<b>62</b>
<b>Table 2-7:</b> Composition of nifH, nrfA, nirS, and nosZ transcripts in the FFT and capwater of unamended and amended samples. Symbols + and - represents presence and absence of each gene in each sample, respectively. ....	<b>63</b>
<b>Table 3-1:</b> Fractionation iron (Fe) in initial FFT prior to amendment and incubation at day 0 and in unamended (U) and amended (HC, HCN, HCNP) FFTs at 600 days incubation. Data represent the mean ( $\pm$ standard deviation, SD) of replicates taken from the port 4 of each column. ....	<b>116</b>
<b>Table 3-2:</b> Relative distributions of Sr (a), Ba (b), As (c), Sb (d), Mo (e), V (f), and Cr (g) in initial, unamended(U) and amended FFTs (HC, HCN, and HCNP) according to BCR sequential extraction procedures; F1: soluble, weak acid soluble, carbonate bound; F2: Fe and Mn bound, F3: organic matter and sulfide bound; F4: Residual .....	<b>117</b>

## List of Figures

- Figure 2-1.** Experimental 10L columns used for measuring biogenic gas emission, microbial communities, and the COCs in the capwater, liquid and solid phases of FFT. Septum for measuring CH<sub>4</sub> and CO<sub>2</sub> gas. Four sampling ports for collecting capwater and FFT (cap water, Top, Mid, and Bot ports). Bottles 1 and 2 for monitoring pressure buildup in the columns and reducing the risk of columns ‘explosion. In some parts of second chapter, cap water, Top, Mid, and Bot ports respectively defined as P1, P2, P3, and P4. .... **48**
- Figure 2-2.** Cumulative emitted Methane (CH<sub>4</sub>) measured in the headspace of methanogenic unamended and amended columns (2columns per each treatment); U: unamended columns; HC: columns amended with hydrocarbon mixture; HCN: columns amended with hydrocarbon plus nitrogen; HCNP: columns amended with hydrocarbon plus nitrogen plus phosphorus ..... **49**
- Figure 2-3.** Percent degradation of hydrocarbons in initial FFT at day 0 and unamended and amended (HC, HCN, HCNP) FFT at days 190 and 350. Bars represent the mean from analysis of two FFT samples taken from Mid and Bot ports (see Fig 2.1) of each columns ((± 1 standard deviation). ..... **50**
- Figure 2-4.** Taxonomic composition of the Bacterial (Top figure (T)) and Archaeal (Bottom Figure (B)) community in the FFT and capwater at each treatment, organized at the phylum level. INT. initial FFT at day 0; U: unamended columns; HC: columns amended with hydrocarbon mixture; HCN: columns amended with hydrocarbon plus nitrogen; HCNP: columns amended with hydrocarbon plus nitrogen plus phosphorus. [Cap: capwater; Top, Mid and Bot: respectively, Top, Middle, and Bottom ports in each column, see Fig 2.1]..... **51**
- Figure 2-5.** Taxonomic composition of the Bacterial community in the FFT and capwater at each treatment, organized at the Class level. INT. initial FFT at day 0; U: unamended columns; HC: columns amended with hydrocarbon mixture; HCN: columns amended with hydrocarbon plus nitrogen; HCNP: columns amended with hydrocarbon plus nitrogen plus phosphorus. [Cap: capwater; Top, Mid and Bot: respectively, Top, Middle, and Bottom ports in each column, see Fig 2.1]. ..... **52**
- Figure 2-6.** Taxonomic composition of the Bacterial community in the FFT at each treatment, organized at the family level. INT. initial FFT at day 0; U: unamended columns; HC: columns amended with hydrocarbon mixture; HCN: columns amended with hydrocarbon plus nitrogen; HCNP: columns amended with hydrocarbon plus nitrogen plus phosphorus. [Top, Mid and Bot: respectively, Top, Middle, and Bottom ports in each column, see Fig 2.1]. ..... **53**
- Figure 2-7.** Taxonomic distribution of nifH-generated OTUs in the FFT and capwater at each treatment. INT. initial FFT at day 0; U: unamended columns; HC: columns amended with hydrocarbon

	mixture; HCN: columns amended with hydrocarbon plus nitrogen; HCNP: columns amended with hydrocarbon plus nitrogen plus phosphorus. [Cap: capwater; Top, Mid and Bot: respectively, Top, Middle, and Bottom ports in each column, see Fig 2.1]. .....	54
<b>Figure 3-1.</b>	Cumulative emitted Methane (CH <sub>4</sub> ) and carbon dioxide (CO <sub>2</sub> ) measured in the headspace of methanogenic unamended and amended columns (2columns per each treatment); U: unamended columns; HC: columns amended with hydrocarbon mixture; HCN: columns amended with hydrocarbon plus nitrogen; HCNP: columns amended with hydrocarbon plus nitrogen plus phosphorus.....	98
<b>Figure 3-2.</b>	Consolidation and recovery of water in unamended (U) and amended (HC, HCN, HCNP) FFTs over incubation period. U: unamended columns; HC: columns amended with hydrocarbon mixture; HCN: columns amended with hydrocarbon plus nitrogen; HCNP: columns amended with hydrocarbon plus nitrogen plus phosphorus .....	99
<b>Figure 3-3.</b>	pH values in the pore- and cap-water of unamended (U) and amended (HC, HCN, and HCNP) columns. P1 refers to Port 1 located in the capwater and P2, P3, and P4 were below the mudline and accessed FFT (see Fig 2.1. at chapter 2). pH values measured at P1 (capwater) and at P2, P3, and P4 (the mean pH value of these 3 ports is given as a representative of pH in the FFT porewater per sampling time; error bars, where visible, represent 1 standard deviation). ....	100
<b>Figure 3-4.</b>	Carbonate mineral content in unamended (U) and amended (HC, HCN, HCNP) FFTs at day 0 and 600 days incubation. Bars represent the mean value from analysis of four replicates taken from port 4 of each column and the error bars, where visible, represent 1 standard deviation; U: unamended columns; HC: columns amended with hydrocarbon mixture; HCN: columns amended with hydrocarbon plus nitrogen; HCNP: columns amended with hydrocarbon plus nitrogen plus phosphorus.....	101
<b>Figure 3-5.</b>	The concentrations of soluble cations and anions in the pore- and cap-water of unamended (U) and amended (HC, HCN, and HCNP) columns. P1 refers to Port 1 located in the capwater and P2, P3, and P4 were below the mudline and accessed FFT (see Fig 2.1. at Chapter 2). Left: Concentrations of major soluble cations in the cap- and porewater (Bars represent the mean from analysis of three replicates taken from each port and the error bars, where visible, represent 1 standard deviation). Right: Concentrations of major soluble carbonate and bicarbonate in the cap- and porewater.....	102
<b>Figure 3-6.</b>	The concentration of sulfate in the pore- and cap-water of unamended (U) and amended (HC, HCN, and HCNP) columns. P1 refers to Port 1 located in the capwater and P2, P3, and P4 were below the mudline and accessed FFT (see Fig 2.1. at Chapter2). .....	103

**Figure 3 -7.** Total Sr and Ba concentrations in the capwater (cw) and porewater (pw) of unamended (U) and amended (HC, HCN, and HCNP) columns. HC, HCN, and HCNP respectively represent columns amended by hydrocarbon, hydrocarbon plus nitrogen, and hydrocarbon plus nitrogen plus phosphorous. P1 refers to Port 1 located in the capwater and P2, P3, and P4 were below the mudline and accessed FFT (see Fig 2.1. at chapter 2). Bars represent the mean from analysis of three replicates taken from the same ports in two replicated columns and the error bars, where visible, represent 1 standard deviation..... **104**

**Figure 3-8.** Total As and Sb concentrations in the capwater (cw) and porewater (pw) of unamended (U) and amended (HC, HCN, and HCNP) columns. HC, HCN, and HCNP respectively represent columns amended by hydrocarbon, hydrocarbon plus nitrogen, and hydrocarbon plus nitrogen plus phosphorous. P1 refers to Port 1 located in the capwater and P2, P3, and P4 were below the mudline and accessed FFT (see Fig 2.1. at chapter 2). Bars represent the mean from analysis of three replicates taken from the same ports in two replicated columns and the error bars, where visible, represent 1 standard deviation..... **105**

**Figure 3-9.** Total Mo, V, and Cr concentrations in the capwater (cw) and porewater (pw) of unamended (U) and amended (HC, HCN, and HCNP) columns. HC, HCN, and HCNP respectively represent columns amended by hydrocarbon, hydrocarbon plus nitrogen, and hydrocarbon plus nitrogen plus phosphorous. P1 refers to Port 1 located in the capwater and P2, P3, and P4 were below the mudline and accessed FFT (see Fig 2.1. at chapter 2). Bars represent the mean from analysis of three replicates taken from the same ports in two replicated columns and the error bars, where visible, represent 1 standard deviation..... **107**

**Figure 3-10.** Transformation of Iron (Fe) in unamended (U) and amended (HC, HCN, HCNP) FFTs at day 0 and 600 days incubation. HC, HCN, and HCNP respectively represent columns amended by hydrocarbon, hydrocarbon plus nitrogen, and hydrocarbon plus nitrogen plus phosphorous and INT, represent the initial FFT. The data relative to iron fractionation has given at table 3.1. Fe (total) = Fe obtained from acid digestion method; Fe<sup>III</sup> = Fe (DCB) – Fe<sup>II</sup> (ferrozine); Fe<sup>III</sup> (amorphous) = Fe (AOD) – Fe (siderite) – Fe (acid volatile sulfides, AVS) – Fe (ferrozine); Fe<sup>III</sup> (crystalline) = Fe<sup>III</sup> – Fe<sup>III</sup> (amorphous); Fe<sup>II</sup> (crystalline) = Fe (pyrite) + Fe (vivianite) + Fe (siderite); and Fe<sup>II</sup> (amorphous) = Fe<sup>II</sup> – Fe<sup>II</sup> (crystalline). ..... **108**

**Figure 3-11.** Transformation of Iron (Fe) in unamended (U) and amended (HC, HCN, HCNP) FFTs at day 0 and 600 days incubation. HC, HCN, and HCNP respectively represent columns amended by hydrocarbon, hydrocarbon plus nitrogen, and hydrocarbon plus nitrogen plus phosphorous and INT, represent the initial FFT. The data relative to iron fractionation has given at table 3.1. Siderite represent FeCO<sub>3</sub>, and amorphous sulfides (FeS), and vivianite (Fe<sub>3</sub> (PO<sub>4</sub>)<sub>2</sub>.8H<sub>2</sub>O)

represent the iron content in newly formed Fe<sup>II</sup> minerals. Bars represent the mean from analysis of three replicates taken from the port 4 of each column and the error bars, where visible, represent 1 standard deviation. .... 109

**Figure 3-12.** Relative distributions of Sr, and Ba in initial, unamended (U) and amended FFTs (HC, HCN, and HCNP) according to BCR sequential extraction procedures; F1: soluble, weak acid soluble, carbonate bound; F2: Fe and Mn bound, F3: organic matter and sulfide bound; F4: Residual ..... 110

**Figure 3-13.** Relative distributions of As, and Sb in initial, unamended (U) and amended FFTs (HC, HCN, and HCNP) according to BCR sequential extraction procedures; F1: soluble, weak acid soluble, carbonate bound; F2: Fe and Mn bound, F3: organic matter and sulfide bound; F4: Residual ..... 111

**Figure 3-14.** Relative distributions of Mo, V, and Cr in initial, unamended(U) and amended FFTs (HC, HCN, and HCNP) according to BCR sequential extraction procedures; F1: soluble, weak acid soluble, carbonate bound; F2: Fe and Mn bound, F3: organic matter and sulfide bound; F4: Residual ..... 112

**Figure 3-15.** The concentrations of Naphthenic acid, in the pore and cap water of unamended (U) and amended (HC, HCN, and HCNP) columns at day 0 and 190 days incubation. Bars represent the mean value from the analysis of three replicates taken from port 1 (cap water) and port 4 (pore water) of each column, and the error bars, where visible, represent 1 standard deviation; U: unamended columns; HC: columns amended with hydrocarbon mixture; HCN: columns amended with hydrocarbon plus nitrogen; HCNP: columns amended with hydrocarbon plus nitrogen plus phosphorus..... 113

**Figure 3-16.** Calculated ionic strength of the porewater and capwater in unamended (U) and amended (HC, HCN, and HCNP) columns. Ionic strength was calculated using the cations and anions concentrations at P1 (capwater) and at P2, P3, and P4 (the mean ionic strength value of these 3 ports is given as a representative of ionic strength in the FFT porewater; error bars, where visible, represent 1 standard deviation) after 600 days incubation. .... 114

**Figure 3-17.** The concentrations of As species, As III and As V, in the pore and capwater of unamended (U) and amended (HC, HCN, and HCNP) columns after 190 incubation. Soil bars represent capwater, hatched bars represent porewater. The species of As was measured at at P1 (capwater) and at P2, P3, and P4 (the mean value of these 3 ports is given as a representative of As species in the FFT porewater; error bars, where visible, represent 1 standard deviation) ..... 115

## List of abbreviation

AAS	Atomic Absorption Spectroscopy
AER	Alberta Energy Regulator
AO	Ammonium Oxalate
AOSR	Athabasca Oil Sands Region
AVS	Acid Volatile Sulfide
BIOS	Biogenic Iron Oxides
BML	Base Mine Lake
BTEX	Benzene, Toluene, Ethyl benzene, and Xylenes
CCME	Canadian Council of Ministers of the Environment
CEC	Council of the European Communities
CEMA	Cumulative Environmental Management Association
CNRL	Canada Natural Resources Limited
COC	Chemicals of Concern
COCs	Constituents of Concerns
CRS	Chromium Reducible Sulfide
CSS	Cyclic Steam Stimulation
CT	Consolidated Tailings
DCB	Dithionite-Citrate-Bicarbonate
DDL	Diffuse Double Layer
DNRA	Dissimilatory Nitrate Reduction to Ammonium
EPLs	End Pit Lakes
FFT <sub>s</sub>	Fluid Fine Tailings
GC-FID	Gas Chromatography- Flame Ionization Detector
HC	FFT <sub>s</sub> amended with a hydrocarbon
HCN	FFT <sub>s</sub> amended with hydrocarbon plus N
HCNP	FFT <sub>s</sub> amended with hydrocarbon plus N plus P

ICP-MS	Inductively Coupled Plasma Mass Spectrometry
ICP-OES	Inductively Coupled Plasma Optical Emission Spectrometry
MFTs	Mature Fine Tailings
MLSB	Mildred Lake Settling Basin
NAs	Naphthenic Acids
NifH	nitrogen fixation gene
NirS	nitrite reductase gene
NosZ	nitrous oxide reductase gene
NrfA	nitrate reductase gene
OSPW	Oil Sands Process-affected Water
OTUs	Operational Taxonomic Units
PAHs	Polycyclic Aromatic Hydrocarbons
rRNA	ribosomal ribonucleic acid
SAGD	Steam- Assisted Gravity Drainage
WCT	Water-Capped Tailings
WIP	West In-Pit

# **1 Introduction**

## **1.1 Oil sands industry**

### **1.1.1 The Alberta oil sands**

In recent decades, environmental concerns over fossil fuel consumption compelled societies to seek alternative sustainable and renewable energy sources. However, over 30% of total global primary energy is still provided by oil (CAPP, 2017). Alberta with an estimated 2.5 trillion barrels of recoverable bitumen (mainly in the Athabasca, Cold Lake and Peace River areas) is known to have the third largest oil reserve in the world (Li et al., 2017). Oil sands are naturally occurring petrochemical that typically consists of a mixture of 10% bitumen, 5% water and 85% solids. Bitumen is a heavy oil that is extremely viscous. It must be heated or diluted before it can be extracted, flown, pumped and be used by refineries to produce usable fuels such as gasoline and diesel. The presence of heavy metals in trace amounts, particularly nickel and vanadium and 4-5% sulfur have been reported in Alberta bitumen. Solid phase comprises sand primarily consisting of quartz (>80%) and a small fraction of potassium feldspar whereas Kaolinite, illite, chlorite and smectite are important clay minerals in oil sands depositions. Water portion in oil sands carries soluble ions (sodium, potassium, calcium and sulfate). Deposits with higher fine contents usually tend to have higher water content and lower bitumen content. Bitumen ore (oil sands ore) is found at different depths. Some oil sands ores lie within 70 meters (200 feet) from earth surface, but the majority deposit is located in deeper layers. Depending on the depth of the deposit, open pit mining (surface mining) and in situ drilling techniques have been employed to recover bitumen from the oil sands (CAPP, 2017).

### **1.1.2. Bitumen Extraction**

In the areas (20% of the total deposits) where the oil sands are located closer to the surface (up to 75 meters), surface mining is the only technique that is performed. After removing forest and layers of overburden (muskeg, glacial till and Cretaceous bedrock) from oil sands ore (Chalaturnyk et al., 2002), large power shovel scoop the ore into heavy trucks for transporting to crushers. The clumps of clay are broken down in crushers to prepare oil sands for extraction. In this stage, oil sands are diluted with warm water and then transported (hydrotransport) to the bitumen extraction plant. Athabasca oil sands have the largest deposits of oil rich bitumen in Northern Alberta. A portion (10%) of Athabasca deposit is shallow and close enough to the surface. Therefore, surface mining is a viable method that is used for extracting oil sands from this

part of Athabasca oil sands deposits. Currently, 5 active oil sands surface mining operators are conducting oil sands mining projects within Athabasca region 1) Syncrude Canada Ltd. (Syncrude), 2) Suncor Energy (Suncor), 3) Shell Albian Sands (Albian), 4) Canada Natural Resources Ltd. (CNRL) and 5) Imperial Oil Ltd (Imperial) (CAPP, 2017; The Government of Alberta, 2017).

Oil sands deposits which lie in deeper layers (more than 75 meters from the surface) can be extracted through in situ technology. Among several in situ methods that are being developed to improve the efficiency of bitumen extraction, Steam- Assisted Gravity Drainage (SAGD) (Foght et al. 2017) and Cyclic Steam Stimulation (CSS) are the most common techniques currently used in large-scale operations. In both methods, several wells are drilled into deposits, and then pressurized steam is continuously injected through underground horizontal well to warm and liquefy the bitumen. Then, the bitumen will be pumped to the surface through extraction wells. Within the Athabasca deposits, the SAGD has been chosen as the recovery process while SCC is used in cold lake deposits to recover bitumen (The Government of Alberta, 2017). Canadian Association of Petroleum Producers has been predicted an increase of in situ production from 1.4 million bbls/d in 2017 to 2.1 million bbls/d in 2030 (CAPP, 2017).

### **1.1.3. Extraction process**

Bitumen is extracted from surface-mined oil sands via hot water method developed by Dr. Karl Clark, a member of Alberta Research Council in the 1920s (Chalaturnyk et al., 2002). Through using this method, the oil sands are separated into its component parts. In the first separation step of bitumen, after the excavation of oil sands ore, the large boulders of oil sands are crushed to reduce the size. Then hot water at 50-80°C is added to the crushed oil to reduce the viscosity of heavy bitumen so bitumen can separate from the sand. The formed thick mixture called slurry (Chalaturnyk et al., 2002). To accelerate the separation process, the slurry is transported via hydrotransport lines which makes vigorous mechanical mixing, and also slurry is mixed with additional hot water before transferring to the primary separation vessel (Chalaturnyk et al., 2002). In the settling vessels, the coarse solids are settled in the bottom and then are removed and pumped into tailings ponds construction. However, the bitumen froth which was floated at the top of slurry is sent to extraction plant for the further processing and upgrading (Chalaturnyk et al., 2002). In the middle portion between floating and settling the sands, air is bubbled to the slurry to allow further bitumen is recovered as a product called bitumen froth (Chalaturnyk et al., 2002). The

bitumen froth is deaerated via heating and sent for the forth treatment. A mixture of low molecule weight of hydrocarbon solvent is initially used to dilute the bitumen forth and reduce its viscosity and density (Chalaturnyk et al., 2002). In this step, naphtha (a mixture of low molecule weight aliphatic and aromatic hydrocarbons) is used as extraction solvents by all oil sands operators except Albion(Albion Sands Energy Inc.) and Imperial (Imperial Oil Ltd.), which use a light paraffinic diluent comprising mainly C5–C6 n- and iso-alkanes (Siddique et al., 2018). The diluted bitumen is send to inclined plate settler for the further settling and then centrifuged to separate the heavier constituents (Chalaturnyk et al., 2002). After the completion of extraction process, the solids and water is left from the froth treatment process, together with all the residual water, solids, added chemicals and unrecovered bitumen which are called tailings are disposed to tailings ponds (Chalaturnyk et al., 2002). However, the remaining extraction solvents are recovered from the tailings before discharging them into tailings ponds for the long-term storage.

#### **1.1.4. Environmental impacts of surface mining**

While the growth in oil sands operations will be 60% (in situ) and 49% (in mining) in 2030, large-scale surface mining operations have greater environmental impacts as compared to in situ methods (CAPP, 2017). In surface mining, a large area of land is disturbed through oil sands excavation by removing an overburden layers overlaid on mineable bitumen deposits and creating pits and other structures after mining the oil sands deposits. Also, bitumen extraction process produces huge volumes of fluid tailings consist of sand, fine silt, clay, unrecovered hydrocarbons (diluent) added to oil sands during extraction process and dissolved constituents of concerns (trace metals, salts and soluble organic compounds) (MacKinnon et al., 2010). These tailings streams are transported into the constructed impoundments known as settling basins or tailings ponds. Once the coarse sand fraction is separated from tailings, the remaining fine silt and clay fractions form Fluid Fine Tailings (FFT). Over the years, fine fractions are also settled to some extent and form the suspension containing approximate 30% (w/w) solid content, known as Mature Fine Tailings (MFT) (Siddique et al., 2014a; Thompson et al., 2017). Settling of fine particles expresses porewater to the surface of tailings ponds that is recycled in the bitumen extraction process. Over half a century, more than 1 trillion L (1 billion m<sup>3</sup>) of ‘legacy’ fluid tailings has accumulated (McNeill and Lothian, 2017) by the oil sands industry in Alberta. These tailings are currently stored in tailing ponds that cover 98km<sup>2</sup> area (liquid surface area of ponds) in the Athabasca region which is continuing to grow (AEP, 2015a) (<http://osip.alberta.ca/map/>). In addition to the

challenges related to mining and tailings storage, significant amounts of fresh water are also consumed during bitumen extraction in surface mining compared to in situ operation (AEP, 2015b and CAPP, 2017). Oil sands mine operators recycle over 80-90% of water, which is used during bitumen separation process by utilizing the expressed porewater from tailings ponds. Based on Natural Resources Canada-Canmet Energy description (2010), every water which is in contact with oil sands is called oil sands process-affected water (OSPW) including the OSPW in active settling basins or tailings ponds, the water released from consolidated tailings (CT) after using the chemical/physical separation techniques for settling the fluid fine tailings; seepage drained water from settling basins; and released OSPW from wetlands and reclamation ponds (Mahaffey and Dube, 2016, Li et al; 2017). It can be conclude that different OSPWs has significantly different chemical composition. However, despite the differences observed in the water chemistry of OSPWs, they always contain several types of contaminates including naphthenic acids (NAs), polycyclic aromatic hydrocarbons (PAHs), BTEX (benzene, toluene, ethyl benzene, and xylenes), phenols, heavy metals and ions (Allen, 2008; Puttaswamy and Liber, 2012; van den Heuvel et al., 2012; Mahaffey and Dube, 2016). Recent studies showed the presence of chemicals of concern (COC) including dissolved organics, salts, and trace metals within OSPW and FFT cause toxicity effects on aquatic organisms (He et al., 2012; Kavanagh et al., 2011; Anderson et al., 2012; Leclair et al., 2013; McQueen et al., 2017; Li et al., 2017). To manage the volumes of fluid tailings and reduce the environmental risks of OSPW and FFTs on the landscape, tailings management and reclamation strategies as well as monitoring systems are being developed in the Alberta oil sands region for sustainable oil sands development.

#### **1.1.5. Tailings management**

As previously discussed, tailings as a byproduct of bitumen extraction process from oil sands deposits are placed in settling basins or tailings ponds by all surface mining operators. Once the tailings are deposited in tailings, the sand and coarse silt components settle rapidly over a few days. However, clay and fine silt particles' suspension (together known as Fluid Fine Tailings or FFTs) settle slowly. The fine tailings dewater and densify further over 1 to 2 years and form mature fine tailings (MFT). Further consolidation and dewatering of MFT is predicated to take centuries (COSIA, 2012). Reclamation treatment technologies should be used to reclaim these tailings in oil sand regions (OSTC and COSIA, 2012). In 2010, oil sands research and information network divided reclamation treatment technologies into two key technologies that would result in wet or

dry landscapes (BGC Engineering Inc, 2010). Based on a directive from Energy Resources Conservation Board, tailings managements should be conducted for the short-term storage of fluid tailings in reclamation sites, fluid tailings reduction, water recovery and fast creation of trafficable deposition (ERCB, 2009). The development of many tailings technologies are in progress to accelerate the fluid tailing consolidation including physical/mechanical methods (filtration, centrifuge), natural processes (evaporation, freeze/thaw) and chemical additives (Kasperski and Mikula, 2011; Sobkowicz, 2012). These methods would result in the production of tailings products to be used/reclaimed under dry landscapes. Some of these technologies are costly and energy consuming, and some have environmental impacts. In dry landscape reclamation after the dried MFT is stable enough to support heavy machinery and is covered with the top soil, the soil cover is revegetated to reclaim the tailings substrate under the typical boreal forest scenario (BGC Engineering Inc, 2010). However, in wet landscape reclamation, deposited MFT in pits is capped with a layer of fresh water or a mixture of fresh and OSPW. MFT consolidate over time and release porewater to the surface as cap water. This reclamation strategy has been defined as the establishment of End Pit Lakes (EPLs). EPLs are artificial lakes formed by deposited MFT in pits capped with a layer of fresh water or mixture of fresh and OSPW. MFT will settle over time and release porewater to the surface as cap water. Based on the achieved observations from several established pits and ponds on Syncrude site (1989-1993), it is expected that EPLs will form self-sustaining aquatic ecosystems (OSTC and COSIA, 2012). Among the various fines reclamation methods, which they are at different stages of their development, four commercial-scale deposits types which are actively developed are employed by oil sands mining industries: 1) Thin-layered fine dominated deposits (after the first stage of dewatering by chemical and mechanical treatments, the further dewatering will be affected by environmental processes such as atmospheric evaporation and freeze-thaw cycles); 2) Deep, fines-dominated deposits (after the first stage of dewatering by chemical and mechanical treatments, further dewatering will be done through self-weight consolidation) and 3) Fines-enriched sand deposits (the deposits will be dewatered through self-weight consolidation). Higher permeability of fines-enriched sand deposits cause quicker dewatering compared to fines-dominated deposits. 4) Water capped fines deposits, (water-capped tailings, WCT) where FFT is placed at the bottom of a completed mine pit and covered with overlying fresh water (COSIA, 2012). Among four treatments above and reclamation options, some distinct advantages including efficient FFT storage, gradual FFT consolidation without using

the chemical and mechanical treatments, and large water reservoirs creation by using readily available and low cost materials, FFT and OSPW, are provided by WCT method. The same advantages would be expected for the end pit lakes (EPLs) reclamation strategy (COSIA, 2012).

#### **1.1.6. End pit lakes in oil sands reclamation**

The application of WCT reclamation method results in creating aquatic reclamation area by placing FFT and water in closed mine pits which resemble artificial lakes called end pit lakes (EPLs). These EPLs have some distinct advantages over other methods, as it is expected to develop into self-sustaining and multi trophic ecosystems. However, the successful performance of EPLs is depended on the quality of surface water (COSIA, 2012). This makes several concerns about the feasibility of EPLs including (a) the possibility of mixing or resuspension of underlying FFT and overlying cap water and generation of turbidity; b) the interaction of ground water and/or the surrounding watersheds with EPLs; c) the movement of contaminants of concerns (including ions, soluble metals and organic constituents) from the FFT to overlying water cap; and finally d) the potential impact of water surface toxicity on aquatic life and ecological development (COSIA, 2012). Therefore, the behaviors of anaerobic FFTs and biogeochemical properties of tailings are important to determine the feasibility of EPLs for tailings reclamation. These findings may also be applied to solve similar problems with tailings ponds. Syncrude as one of the companies that use various methods to handle its tailings is leading in the use of WCT and EPLs within the Alberta oil sands region. This company started its laboratory testing on a small-scale WCT and EPL more than two decades ago to assess the potential at field scale. To confirm the potential benefits and concerns associated with EPLs and assess the feasibility of this method, a commercial scale EPL known as the Base Mine Lake (BML) has been initiated by Syncrude at Syncrude Mildred Lake mine since 2012 (COSIA, 2012).

### **1.2. Biogeochemical processes in tailings ponds/End Pit Lake**

#### **1.2.1. Methane emission from tailings**

Tailings as the main material deposited in tailings ponds and end pit lakes are highly anaerobic. The factors like the usage of high temperature in bitumen extraction process, the deposition depth of tailings in tailings ponds and EPLs, and the properties of tailing in preventing light and oxygen into the ponds create mostly anaerobic conditions in tailings ponds and EPLs (Li, 2010). For the first time, methane release from tailings was observed in Mildred Lake Settling Basin (MLSB), one of the main tailings ponds of Syncrude (COSIA, 2012). The production of

methane (methanogenesis) was due to the metabolic activities of methanogens, the microorganisms identified as Archaea that lives in syntrophic association with anaerobic bacteria, in tailings. Methanogenesis as a relatively complex process is the final step in the decomposition of available substrates in tailings and releasing the methane and Carbon dioxide from tailings ponds and EPLs. Observations on the release of methane in MLSB indicate that various microorganisms exist in the MFT and operate in the production of methane (Li, 2010). From past decade, research moved towards identifying the available substrates, key microbes and their functions in tailings regarding methane production. Also, these microbial activities (methanogenesis) influence geochemical processes in tailings ponds, and EPLs that are important in tailings management and reclamation.

The carbon source for microbial activities in tailings is the unrecovered bitumen, and the extraction solvents remained in the tailings after bitumen extraction (MacKinnon, 1989; Siddique et al., 2012). Bitumen as a complex mixture of the high molecular weight of hydrocarbon is not a readily available and easily degradable carbon source for indigenous microbes in tailings. However, residual extraction solvents composed of simple and low molecular weight hydrocarbon in tailings are more favorable for the microbial metabolism (Siddique et al., 2006). Earlier laboratory studies conducted for a year using MFT collected from MLSB and spiked with naphtha (extraction diluent used by Syncrude) or its major hydrocarbon groups (monoaromatics and *n*-alkanes) revealed that indigenous microorganisms metabolized about 23% of added naphtha into methane in a year-long incubation. Upon detailed analyses of naphtha in the microcosms producing methane, it was observed that *n*-alkanes (C<sub>6</sub>-C<sub>10</sub>) and monoaromatics (toluene and isomers of xylenes) were completely metabolized to methane. Other major fractions of naphtha hydrocarbons (*iso*-alkanes cycloalkanes) remained undegraded during a year-long incubation (Siddique et al. 2007). The complete biodegradation of *n*-alkanes and monoaromatics added to Syncrude MFT in separate microcosms (Siddique et al. 2006; Siddique et al. 2007) also substantiated the methanogenic biodegradation of these hydrocarbon groups in the naphtha (Siddique et al. 2007). These results suggested that labile hydrocarbons in extraction diluent (naphtha) sustained methanogenic activities in oil sands tailings ponds. Subsequently, long-term studies were performed to assess the biodegradation of *iso*-alkanes and cycloalkanes in naphtha. Multiple laboratory experiments were conducted using MFT from other tailings ponds such as Muskeg River tailings pond (Shell Albian) and Horizon tailings pond (CNRL). These MFTs were

spiked separately with both the diluents (naphtha; C<sub>3</sub>-C<sub>14</sub>, and paraffinic solvent; C<sub>5</sub>-C<sub>6</sub>) used by different oil sands operators. The research findings revealed that *iso*-alkanes that comprised a significant portion of diluents were biodegraded but longer incubations were required for microbial acclimation (Siddique et al. 2015; Mohamad Shahimin and Siddique 2017a, b). The long-term studies where Syncrude, Shell Albian and CNRL MFTs were spiked with diluents and incubated for more than 4 years revealed the biodegradation of major *iso*-alkanes (2-methylpentane, 2-methylhexane 3-methylhexane, 2-methylheptane, 4-methylheptane, 2-methyl octanes and various methyl nonanes) in the diluents. However, a few cycloalkanes showed the biodegradability during long incubations (Tan et al. 2015; Siddique et al. 2015; Mohamad Shahimin and Siddique 2017a, b). Bitumen can release some hydrocarbons with passage of time and be a source of carbon for microbial metabolism. Longer-chain *n*-alkanes released from bitumen is also a source of methane. Syncrude MFT spiked with longer-chain *n*-alkanes (C<sub>14</sub>-C<sub>18</sub>) also produce methane during metabolism of these added *n*-alkanes (Siddique et al., 2011).

Besides the carbon source, inorganic nutrients in particular nitrogen (N) and phosphorus (P) are also essential for microbial metabolism. The positive effect of amending hydrocarbon contaminated sites by appropriate amounts of N and P on the growth and activity of indigenous microorganisms has been reported in some previous studies (Smith et al., 2015; Zhang and Lo, 2015). In some research on biodiesel where wastewater contains high amounts of oil and low concentration of N and P, very limited biological activities have been observed (Vidal *et al.*, 2000; Siles *et al.*, 2010). It has also been observed that the available N influence the microorganism's abundance and microbial community structure (Liang et al., 2011; Mendelsohn et al., 2012). The low concentrations of N and P have been reported in mature fine tailings (Fedorak et al., 2003; Penner and Foght, 2010) and other hydrocarbon contaminated environments (Mendelsohn et al., 2012). However, the continuous methane emission from tailings ponds indicate that the available concentrations of N and P in tailings are enough for the microbial activities under methanogenic conditions or the nutrients (N and P) requirements of microorganisms are provided from the other biogeochemical processes occurring under methanogenic conditions. As an example, Collins et al. (2016) reported the concurrence of nitrogen fixation process and methanogenesis in oil sands tailings. It means that the fixed N through nitrogen fixation process is used as an important N source for supporting methanogenic activities in the tailings ponds. This finding signify the role of nutrients in addition to a carbon source in the production of methane in tailings ponds. The

availability of nutrients (N and P) may affect the biodegradation of hydrocarbons and methanogenesis in oil sand tailings and EPLs. Thus, it is important to determine the effect of nutrients' availability on methane production in oil sands tailings.

### **1.2.2. Microbial communities in the MFT**

The initial researches to identify microbial communities in MLSB tailings samples indicated the presence of diverse anaerobic microorganisms including methanogens, denitrifiers, sulfate and iron reducing bacteria in these tailings (Holowenko et al., 2000; Penner and Foght, 2010). In the early research conducted on the examination of microbial communities in MFT collected from MLSB and West In-Pit (WIP), Proteobacteria and acetoclastic methanogens were distinguished as a dominant population in bacterial and archaeal communities, respectively (Penner and Foght, 2010). However, under anaerobic conditions, different types of hydrocarbons can be degraded by different microbial players (Widdel et al. 2010).

However, in this chapter, the key microorganisms enriched during the biodegradation of different groups of hydrocarbons in diluents are discussed to highlight their involvement in the hydrocarbon biodegradation process. The study on anaerobic biodegradation of short-chain *n*-alkanes (C<sub>6</sub>-C<sub>10</sub>), monoaromatics (toluene and xylenes), and whole naphtha revealed the dominance of Firmicutes (*Peptococcaceae*) and Proteobacteria (*Syntrophus/Smithella*) among the bacterial community in Syncrude MFT (Siddique et al. 2012). The high abundance of *Peptococcaceae* was also reported during the biodegradation of shorter *n*-alkane (C<sub>5</sub>-C<sub>6</sub>) and *iso*-alkane (C<sub>5</sub>-C<sub>8</sub>) (Abu Laban et al., 2015; Siddique et al. 2015; Tan et al., 2015). Similar results were also observed during the biodegradation of shorter-chain *n*- and *iso*-alkanes (C<sub>5</sub>-C<sub>6</sub>) and paraffinic solvent (comprised of shorter-chain *n*- and *iso*-alkanes (C<sub>5</sub>-C<sub>6</sub>)) in CNRL MFT (Mohamad Shahimin et al. 2016; Mohamad Shahimin and Siddique 2017a). During the biodegradation of longer chain *n*-alkanes (C<sub>6</sub>-C<sub>18</sub>) in different MFTs, a more diverse bacterial community (*Syntrophaceae*, *Anaerolineaceae*, and *Desulfobacteraceae*) were dominant (Siddique et al. 2011; Mohamad Shahimin et al. 2016; Mohamad Shahimin and Siddique 2017b).

In the process of methanogenesis, bacteria and archaea work in syntrophic relationship. Complex organic substrates are initially biodegraded by bacteria into the simple products such as acetate, hydrogen and carbon dioxide. These are substrate for methanogens to produce methane. One group, known as acetoclastic methanogens, utilizes acetate to produce methane, whereas hydrogenotrophic methanogens consume hydrogen and carbon dioxide to produce methane

(Siddique et al. 2012; Siddique et al. 2018). During the degradation of hydrocarbons, the acetate generated by the actogens or fermenters is converted to methane whereas hydrogenotrophic methanogens reduce carbon dioxide to methane by using hydrogen. The energy released during the acetoclastic methanogenesis ( $\Delta G^\circ = -36.0$  kJ/mol methane) is less than hydrogenotrophic methanogenesis ( $\Delta G^\circ = -131.0$  kJ/mol methane) (Li, 2010). However, in addition to free energy yield, the dominance of one methanogenic pathway during the hydrocarbon biodegradation is also depended on the concentration of acetate, hydrogen, formate (the products of initial biodegradation of hydrocarbons), pH, and temperature (Li, 2010). In overall, there is a syntrophic relationship between bacteria and methanogens during hydrocarbon biodegradation (Siddique et al., 2012).

Methanogens as a group of the archaeal community were also observed dominantly in all MFTs. Among methanogens, both acetoclastic and hydrogenotrophic methanogens were identified as prevalent methanogens within oil sands tailings (Penner, 2006). Subsequent studies indicated that during the biodegradation of short chain *n*-alkanes (C<sub>6</sub>-C<sub>10</sub>) in Syncrude MFT, acetoclastic methanogens were dominant (Siddique et al. 2012). However in most studies on the biodegradation of different hydrocarbons, the codominance of both acetoclastic and hydrogenotrophic methanogens was observed in MFT collected from different ponds and amended with naphtha, BTEX, long-chain *n*-alkanes (C<sub>14</sub>-C<sub>18</sub>), and some iso-alkanes (Siddique et al. 2012; Mohamad Shahimin and Siddique 2017 a and b).

The findings from the above mentioned studies indicate that the availability and the type of carbon sources influence microbial community compositions and their activities in oil sand tailings under methanogenic conditions. However, the influence of nutrients (N and P) on the structures and activities of microbial communities is still not clear in oil sands tailings. Thus, it is important to determine how microbial communities in tailings are affected by the availability of nutrients and consequently, influence methane production in tailings ponds and EPLs.

### **1.2.3. Effect of methanogenesis on the consolidation of tailings in tailings ponds and EPLs**

The positive impact of biogenic gas production on the consolidation rate of fine particles in MFT was initially observed in a laboratory experiment was conducted by Fedorak et al., (2003) and Guo (2009). As mentioned in previous sections, MFT is about 85% water by volume, and the remaining part comprises solid phase: coarse and fine particles where fine particles take decades to settle. The rapid consolidation of fine particles is important because it enhances the recovery of porewater from tailings and reduces the usage of fresh water in the bitumen extraction process as

recovered porewater (OSPW) is recycled back in the bitumen extraction process. Secondly, consolidation of tailings facilitates reclamation process because the densified tailings can be used in the reclamation of land disturbed by mining under different land reclamation scenarios. More recent studies investigating the effect of methanogenesis on MFT consolidation revealed the biogeochemical pathways that accelerated consolidation of fine tailings (Siddique et al., 2014a; Siddique et al., 2014b; Arkell et al., 2015). These studies have suggested two pathways for the effect of methanogenesis on the consolidation of MFT. In Pathway I where changes in porewater chemistry occur, it has been observed that the increased biogenic CO<sub>2</sub> produced during methanogenesis decreases the pH of MFT. The decrease in pH increases the dissolution of carbonate minerals in MFT and releases divalent cations as calcium (Ca<sup>2+</sup>) and magnesium (Mg<sup>2+</sup>) into the porewater of MFT. By increasing the concentrations of Ca<sup>2+</sup> and Mg<sup>2+</sup> in the porewater, the ionic strength of the porewater increases. In addition, relatively higher concentrations of Ca<sup>2+</sup> and Mg<sup>2+</sup> in the porewater exchange the adsorbed Na<sup>+</sup> on the clay surfaces. Increased ionic strength and higher Ca<sup>2+</sup> and Mg<sup>2+</sup> on the clay surfaces decrease the thickness of the diffuse double layer that increases the densification of fine particles in MFT (Siddique et al., 2014a; Arkell et al., 2015). Concurrently occurring with Pathway 1 is pathway II that relates to solid phase chemistry. Microbial metabolism under methanogenic conditions transforms crystalline Fe<sup>III</sup> minerals to more amorphous Fe<sup>II</sup> minerals by transferring electrons from organic substrates to Fe<sup>III</sup> minerals. The newly produced amorphous Fe<sup>II</sup> minerals mask the clay surfaces shielding their surface potentials. This process causes a great reduction in the negative potential on the clay surfaces and therefore enhances the consolidation and dewatering of tailings (Siddique et al., 2014b).

The microbially accelerated dewatering and consolidation of tailings has been suggested as a more cost effective in situ method as compared to other chemical and physical treatments. Therefore, investigation of the factors (such as carbon source, nutrient availability, temperature, etc.) that can affect methanogenesis in tailings ponds and EPLs is not only important to evaluate the consolidation and dewatering of oil sands tailings and also the partitioning of contaminants in MFT solid and aqueous phases.

### **1.3. Rationale of the current research project on the effect of methanogenesis on the partitioning of contaminants between solid and aqueous phases of tailings in end-pit lakes**

As previously discussed that in the creation end-pit-lakes (EPLs) as a wet landscape reclamation method, FFT is placed into mined-out pits and capped with water. Despite several advantages of EPLs which are discussed in section 1.1.5, the primary performance factor for the EPLs is the quality of surface water (COSIA, 2012). As discussed in section 1.2.3 that the active methanogenesis in 50 L column study accelerated the consolidation and dewatering of tailings. Active methanogenesis altered the chemical composition of FFT porewater. The pH was decreased and the concentration of  $\text{Ca}^{2+}$ ,  $\text{Mg}^{2+}$ , and  $\text{HCO}_3^-$  increased in porewater (Siddique et al., 2014a). Also, the iron oxide minerals were reduced ( $\text{Fe}^{\text{III}}$  transformed into  $\text{Fe}^{\text{II}}$  minerals) and carbonate minerals were dissolved under methanogenic conditions (Siddique et al., 2014b). Over time, by increasing the FFT densification, the porewater is released that increases the volume of overlying cap water and leads to the lowering of the mudline level (water-tailings interface). With the densification of FFT and expression of porewater due to methanogenesis, there is a potential concern about the movement of the constituents of concern (including ions, trace metals, naphthenic acids, and residual hydrocarbons in FFT) from underlying FFT to overlying capwater during the FFT fine minerals dissolution and transformation, and transportation of gases. The results of the mesocosm study (Siddique et al., 2014a; Siddique et al., 2014b) using MFT amended with hydrolyzed canola meal to enhance methanogenesis showed higher concentrations of some trace metals (As, V, and Sr) in MFT porewater in comparison with unamended MFT (no active methanogenesis) (data not published). Based on this mesocosm study, a 5 L bioreactor study was designed and conducted by Kuznetsova et al., (data not published). The results of this study also indicated the increase of some ions ( $\text{Ca}^{2+}$ ,  $\text{Mg}^{2+}$ , and  $\text{HCO}_3^-$ ) and trace metals (As, Co, Mn, Ni, Sr and V) in the porewater of amended tailings after five weeks incubation under active methanogenic conditions. Also, the decrease in the concentrations of some other trace metals (Cu, Cd, and Zn) was observed in their findings. In other small-scale studies that were conducted on the amended Syncrude and CNRL MFTs with some *n*-alkanes, the increased concentrations of some trace metals (As, Mo, Sr, and Ba) were observed in the porewater of both CNRL and Syncrude MFTs under methanogenic conditions (Samdai et al, in preparation). Based on the results discussed above, it is concluded that methanogenesis might be involved in the partitioning of constituents of

concerns (COCs) and every factor which affects methanogenesis, can affect COCs mobility and transport as well. The availability of nutrients in MFT may affect biogenic gas production (methanogenesis) and in turn, can impact the mobilization and immobilization of COCs. Therefore, the current research project evaluates the effect of nutrients on the biogeochemical processes in FFT and ultimately the movement of COCs from FFT to cap water. The research is important to assess the role of methanogenesis in the partitioning of COCs in relation to surface water quality and the performance of EPLs as healthy aquatic ecosystem, a viable reclamation strategy.

### **1.3.1. Research objectives**

The main objective of this thesis research is to evaluate how nutrients impact methanogenesis which affects quality of cap water under EPL scenario. To accomplish the main objective, the following specific objectives were investigated:

- Determine the effect of nutrients (N and P) on methanogenesis and microbial community compositions and functions in FFT (Chapter 2)
- Investigation the effect of methanogenesis on the mineral transformations in solid phase of FFT, the chemical composition of FFT porewater, and the flux of inorganic ions and trace metals from FFT to capwater (Chapter 3)

#### 1.4. References

- Abu Laban, N., Dao, A., & Foght, J. (2015). DNA stable-isotope probing of oil sands tailings pond enrichment cultures reveals different key players for toluene degradation under methanogenic and sulfidogenic conditions. *FEMS Microbiology Ecology*, 91(5), fiv039. <https://doi.org/10.1093/femsec/fiv039>
- AEP. (2015a). Total area of the oil sands tailings ponds over time. Retrieved from <http://osip.alberta.ca/library/Dataset/Details/542>
- AEP. (2015b). Historical Water use per Barrel of Oil Produced. Retrieved from <http://osip.alberta.ca/library/Dataset/Details/117>
- Alberta Government. (2015). Alberta's Oil Sands – about the Resource. Retrieved from <http://oilsands.alberta.ca/resource.html>.
- Allen, E.W. (2008). Process water treatment in Canada's oil sands industry: I. Target pollutants and treatment objectives. *Journal of Environmental Engineering Science*, 7(2): 123-138.
- Anderson, J.C., Wiseman, S.B., Moustafa, A., Gamal El-Din, M., Liber, K., & Giesy, J.P. (2012). Effects of exposure to oil sands process-affected water from experimental reclamation ponds on *Chironomus dilutus*. *Water Research*, 46(6), 1662-1672.
- Arkell, N., Kuznetsov, P., Kuznetsova, A., Foght, J. M., & Siddique, T. (2015). Microbial metabolism alters pore water chemistry and increases consolidation of oil sands tailings. *Journal of Environment Quality*, 44(1), 145–153. doi:10.2134/jeq2014.04.0164
- BGC Engineering Inc. (2010). *Review of reclamation options for oil sands tailings substrates*. (No. OSRIN Report No. TR-2). BGC Engineering Inc., University of Alberta, Oil Sands Research and Information Network.
- CAPP. (2017). Crude Oil: Forecast, Markets, and Transportation. Canadian Association of Petroleum Producers. Retrieved from <https://www.capp.ca/publications-and-statistics/publications>
- Chalaturnyk, R. J., Scott, J., & Özü, B. (2002). Management of oil sands tailings. *Petroleum Science and Technology*, 20(9-10), 1025–1046. doi:10.1081/LFT 120003695
- Collins, V. C. E., Foght, J. M., & Siddique, T. (2016). Co-occurrence of methanogenesis and N<sub>2</sub> fixation in oil sands tailings. *The science of Total Environment*, 565, 306–312. doi:10.1016/j.scitotenv.2016.04.154

- COSIA. (2012). *Technical guide for fluid fine tailings management*. Edmonton, AB: Canadian Oil Sands Innovation Alliance.
- ERCB. (2009). *Directive 074 tailings performance criteria and requirements for oil sands mining schemes*. Calgary, Alberta: Energy Resources Conservation Board.
- Fedorak, P. M., Coy, D. L., Dudas, M. J., Simpson, M. J., Renneberg, J., & MacKinnon, M. D. (2003). Microbially-mediated fugitive gas production from oil sands tailings and increased tailings densification rates. *Journal of Environmental Engineering & Science*, 2, 199–211. doi:10.1139/S03-022
- Foght, J.M., Gieg, L.M., & Siddique, T. (2017). The microbiology of oil sands tailings: past, present, future. *FEMS Microbiology Ecology*, 93, fix034. doi: 10.1093/femsec/fix034
- Guo, C. (2009). Rapid Densification of the oil sands mature fine tailings (MFT) by microbial activity. PhD. Thesis, University of Alberta.
- He, Y., Patterson, S., Wang, N., Hecker, M., Martin, J.W., Gamal El-Din, M., Giesy, J.P., & Wiseman, S.B. (2012). Toxicity of untreated and ozone-treated oil sands process-affected water (OSPW) to early life stages of the fathead minnow (*Pimephales promelas*). *Water Resources*. 46, 6359-6368.
- Holowenko, F. M., MacKinnon, M. D., & Fedorak, P. M. (2000). Methanogens and sulfate reducing bacteria in oil sands fine tailings waste. *Canadian Journal of Microbiology*, 46(10), 927–937.
- Kavanagh, R. J., Frank, R.A., Oakes, K.D., Servos, M.R., Young, R.F., Fedorak, P.M., ... Van Der Kraak, G. (2011). Fathead minnow (*Pimephales promelas*) reproduction is impaired in aged oil sands process-affected waters. *Aquatic Toxicology*, 101, 214-220.
- Kasperski, K. L., & Mikula, R. J. (2011). Waste streams of mined oil sands: characteristics and remediation. *Elements*, 7(6), 387–392. doi:10.2113/gselements.7.6.387
- Leclair, L.A., MacDonald, G.Z., Phalen, L.J., Kollner, B., Hogan, N.S., & van den Heuvel, M.R. (2013). The immunological effects of oil sands surface waters and naphthenic acids on rainbow trout (*Oncorhynchus mykiss*). *Aquatic Toxicology*, 142-143, 185-194.
- Li, C. (2010). Methanogenesis in oil sands tailings: An analysis of the microbial community involved and its effects on tailings densification. M.Sc. Thesis, University of Alberta.

- Li, C., Fub, L., Stafford, J., Belosevic, M., & El-Din, M. G. (2017). The toxicity of oil sands process-affected water (OSPW): A critical review. *The science of the Total Environment*, 601-602, 1785-1802.
- Liang, Y., Van Nostrand, J.D., Deng, Y., He, Z., Wu, L., Zhang, X., Li, G., & Zhou, J. (2011). Functional gene diversity of soil microbial communities from five oil-contaminated fields in China. *The ISME Journal*, 5 (3), 403-413.
- Mahaffey, A., & Dube, M. (2016). Review of the composition and toxicity of oil sands process affected water. *Environ. Reviews*, 25(1), 97-114. <http://dx.doi.org/10.1139/er-2015-0060>.
- Mendelsohn, I.A., Andersen, G.L., Baltz, D.M., Caffey, R.H., Carman, K.R., Fleeger, J.W. ... Rozas, L.P. (2012). Oil impacts on coastal wetlands: implications for the Mississippi River delta ecosystem after the deepwater horizon oil spill. *Bioscience*, 62 (6), 562-574.
- McQueen, A.D., Kinley, C.M., Hendrikse, M., Gaspari, D.P., Calomeni, A.J., Iwinski, K.J. ...Rodgers, J.H. (2017). A risk-based approach for identifying constituents of concern in oil sands process-affected water from the Athabasca Oil Sands region. *Chemosphere*, 173, 340-350.
- MacKinnon, M. D. (1989). Development of the tailings pond at Syncrude's oil sands plant: 1978-1987. *AOSTRA Journal of Research*, 5(1), 109 – 133.
- MacKinnon, M. D., Matthews, J. G., Shaw, W. H., & Cuddy, R. G. (2010). Water Quality Issues Associated With Composite Tailings (CT) Technology for Managing Oil Sands Tailings.
- McNeill, J., & Lothian, N. (2017). *Review of directive 085 tailings management plans*. Retrieved from <http://www.pembina.org/reports/tailings-whitepaper-d85.pdf>.
- Mohamad Shahimin, M.F., Foght, J.M., & Siddique, T. (2016). Preferential methanogenic biodegradation of short-chain n-alkanes by microbial communities from two different oil sands tailings ponds. *Science of the Total Environment*, 553, 250–257
- Mohamad Shahimin, M.F., & Siddique, T. (2017a) .Methanogenic biodegradation of paraffinic solvent hydrocarbons in two different oil sands tailings. *Science of the Total Environment*. 583,115–122
- Mohamad Shahimin, M.F., & Siddique, T. (2017b). Sequential biodegradation of complex naphtha hydrocarbons under methanogenic conditions in two different oil sands tailings. *Environmental Pollution*, 221, 398–406

- Natural Resources Canada-Canmet, E. (2010). *Oil sands water toxicity: A critical review*. Devon AB: Natural Resources Canada-Canmet ENERGY.
- OSTC, & COSIA. (2012). *Technical guide for fluid fine tailings management*. Calgary, Alberta: Oil Sands Tailings Consortium and Canada's Oil Sands Innovation Alliance. Retrieved from <http://www.cosia.ca/uploads/documents/id7/TechGuideFluidTailingsMgmt>
- Penner, T. J., Foght, J. M. (2010). Mature fine tailings from oil sands processing harbor diverse methanogenic communities. *Canadian Journal of Microbiology*, *56*, 459–470. doi:10.1139/W10-029
- Puttaswamy, N., & Liber, K. (2012). Influence of inorganic anions on metals release from oil sands coke and on toxicity of nickel and vanadium to *Ceriodaphnia dubia*. *Chemosphere*, *86* (5), 521–529. <http://dx.doi.org/10.1016/j.chemosphere.2011.10.018>.
- Siddique, T., Fedorak, P.M., & Foght, J.M. (2006). Biodegradation of short-chain n-alkanes in oil sands tailings under methanogenic conditions, *Environmental Science and Technology*, *40*, 5459-5464.
- Siddique, T., Fedorak, P.M., MacKinnon, M.D., & Foght, J.M. (2007). Metabolism of BTEX and naphtha compounds to methane in oil sands tailings, *Environmental Science and Technology*, *41*, 2350-2356.
- Siddique, T., P. Kuznetsov, A. Kuznetsova, N. Arkell, R. Young, S. Guigard, & J.M. Foght. (2014a). Microbially accelerated consolidation of oil sands tailings. Pathway I: Changes in porewater chemistry. *Frontiers in Microbiology*, *5*,106. doi:10.3389/fmicb.2014.00106
- Siddique, T., Kuznetsov, P., Kuznetsova, A., Li, C., Young, R., Arocena, J.M., & Foght, J.M. (2014b). Microbially-accelerated consolidation of oil sands tailings. Pathway II: solid phase biogeochemistry. *Frontiers in Microbiology*, *5*,107. doi: 10.3389/fmicb.2014.00107
- Siddique, T., Mohamad Shahimin M.F., Zamir S., Semple, K., Li, C., & Foght, J.M. (2015). Long-term incubation reveals methanogenic biodegradation of C5 and C6 iso-alkanes in oil sands tailings. *Environmental and Science Technology*, *49*, 14732–14739
- Siddique, T., Penner, T., Klassen, J., Nesbo, C., & Foght, J.M. (2012). Microbial communities involved in methane production from hydrocarbons in oil sands tailings, *Environmental and Science Technology*, *46*, 9802-9810.

- Siddique, T., Penner, T., Semple, K., & Foght, J. M. (2011). Anaerobic biodegradation of longerchainn-alkanes coupled to methane production in oil sands tailings. *Environmental Science & Technology*, *45*(13), 5892–5899. Doi: 10.1021/es200649t
- Siddique, T., Stasik, S., Mohamad Shahimin, M. F., & Wendt-Potthoff, K. (2018). Microbial communities in oil sands tailings: Their implications in biogeochemical processes and tailings management. In T. J. McGenity (Ed.), *Microbial communities utilizing hydrocarbons and lipids: Members, metagenomics and ecophysiology* (pp. 1-33) Springer.
- Siles, J. A., Martín, M. A., Chica, A. F., & Martín, A. (2010). Anaerobic co-digestion of glycerol and wastewater derived from biodiesel manufacturing. *Bioresource Technology*, *101*, 6315-6321.
- Smith, E., Thavamani, P., Ramadass, K., Naidu, R., Srivastava, P., & Megharaj, M. (2015). Remediation trials for hydrocarbon-contaminated soils in arid environments: evaluation of bioslurry and biopiling techniques. *International Biodeterioration & Biodegradation*, *101*, 56–65. doi:10.1016/j.ibiod.2015.03.029
- Sobkowicz, J. (2012). *Oil sands tailings technology deployment roadmap*. (No. 2). Calgary, Alberta, Canada: Golder Associates Ltd.
- Tan, B., Semple, K., & Foght, J.M. (2015). Anaerobic alkane biodegradation by cultures enriched from oil sands tailings ponds involves multiple species capable of fumarate addition. *FEMS Microbiology Ecology*, *91*(5), fiv042. doi: 10.1093/femsec/fiv042.
- The government of Alberta. (2017). *Alberta oil sands industry quarterly update*. Edmonton, AB: The government of Alberta.
- Thompson, D.K., Motta F.L., & Soares J.B.P. (2017). Investigation on the flocculation of oil sands mature fine tailings with alkoxysilanes. *Minerals Engineering*, *111*, 90-99.
- Van den Heuvel, M.R., Hogan, N.S., Roloson, S.D., & Van Der Kraak, G.J. (2012). Reproductive development of yellow perch (*Perca flavescens*) exposed to oil sands–affected waters. *Environmental Toxicology and Chemistry*, *31*, 654–662. <http://dx.doi.org/10.1002/etc.1732>.
- Vidal, G., Carvalho, A., Méndez, R., & Lema, J. M. (2000). Influence of the content in fats and proteins on the anaerobic biodegradability of dairy wastewaters. *Bioresource Technology*, *74*, 231-239

- Widdel, F., Knittel, K., & Galushko, A. (2010). Anaerobic hydrocarbon-degrading microorganisms: An overview. *In Handbook of hydrocarbon and lipid microbiology* (pp.1997–2021). Berlin, Heidelberg: Springer. doi.org/10.1007/978-3-540-77587-4\_146
- Zhang, Z., & Lo, I. M. (2015). Biostimulation of petroleum-hydrocarbon- contaminated marine sediment with co-substrate: involved metabolic process and microbial community. *Applied Microbiology and Biotechnology*, 99, 5683–5696. doi: 10.1007/s00253-015-6420-9

## **2 Nutrients' impact on the methanogenesis in oil sand tailings under End Pit Lake scenario: I: co-occurrence of N cycling and methanogenesis**

### **2.1 Abstract**

Establishment of end pit lakes (EPLs) are a viable remediation option for reclaiming huge volumes of fluid fine tailings (FFT), where FFT is transferred to a mined-out pit and capped with fresh and oil sands process affected water (OSPW). EPLs have anaerobic conditions and active methanogenesis in FFT can potentially induce flux of constituents of concerns (COCs) from underlying FFT to cap water that could affect the quality and sustainability of EPLs. Therefore, the factors affecting the methanogenesis can affect the partitioning of COCs across mudline (cap water-FFT interface). The present study aimed at characterizing how availability of nutrients (nitrogen; N and phosphorus; P) affects methane (CH<sub>4</sub>) production (methanogenesis) and the composition of the methanogenic microbial community in FFT. For this study, 10 L columns were filled with FFT (7 L) and cap water (1.4L), sealed anaerobically and incubated at room temperature in the dark. Labile hydrocarbons (a mixture of *n*-alkanes, *iso*-alkanes and monoaromatics compound) endogenous to FFT and N and P at C: N: P ratio (100:10:1) were added to FFT. The results showed that the FFTs amended with hydrocarbon plus N (HCN) generated CH<sub>4</sub> to a higher concentration than the FFTs amended with a hydrocarbon (HC) and the lowest CH<sub>4</sub> production was observed in the amended FFTs with hydrocarbon plus N plus P (HCNP) during the experiment. FFT samples were collected during peak methanogenesis and subjected to molecular analyses. 16S rRNA gene sequencing showed the highest abundance of *Syntrophaceae* and *Peptococcaceae*; However, HCNP exhibited a lower abundance of these two bacterial taxa in comparison with HCN and HC. The CH<sub>4</sub> generation in all amended FFTs was associated with the growth of *Methanoregulaceae* and *Methanosaetaceae*, with the highest and lowest OTU count in HCN and HCNP samples, respectively. This study also provided an analysis of the distribution of N-cycling genes in unamended and amended FFTs. All NifH, NirS, NosZ, NrfA functional genes involved in N cycling were detected in all unamended and amended FFTs. This study highlights the significant effect of N and P on CH<sub>4</sub> emission and microbial activities in the FFT samples.

### **2.2 Introduction**

The rapid expansion of the oil sands industry in northern Alberta, Canada has been producing enormous volumes of oil sand tailings in recent years. Alberta Energy Regulator (AER, 2017) estimated the current inventory of FFT in tailings ponds exceeding more than 1 billion cubic

meters covering a total area of  $\sim 246 \text{ km}^2$  (<http://osip.alberta.ca/map/>); and this volume is expected to grow correspondingly with the increase of bitumen production by 2030 (Houlihan and Hale, 2011). Environmental and geotechnical issues are main challenges in the management and reclamation of FFT (COSIA, 2012). Cumulative Environmental Management Association (CEMA) offers EPLs as a solution for the management of FFT at a large scale for all future time (CEMA, 2012). In recent years, the construction of 30 EPLs have been proposed for the Athabasca oil sands region of Alberta, Canada with FFT covered by water in more than half of these EPLs (Prakash et al., 2011). EPLs are projected to develop into self-sustaining aquatic ecosystems. However, the evolution of EPLs will be influenced by the release of chemical constituents in the long-term (Dompierre et al., 2016). Recent studies showed that the activities of indigenous microorganisms in oil sands tailings could change the chemistry of porewater and solid phase and accelerate consolidation and dewatering of tailings under anaerobic conditions (Arkell et al., 2015; Siddique et al., 2014a, 2014b); thus, these findings intensify the concern about the flux of inorganic and organic constituents from FFT to capwater that could influence on the quality and sustainability of tailing ponds and EPLs (Siddique et al., 2014a, 2014b). A full-scale EPL (Base Mine Lake; BML) has been established for demonstration at Syncrude site and has been under investigation since 2013.

It is established that indigenous microbes under methanogenic conditions biodegrade residual hydrocarbons in the oil sands tailings ponds and produce  $\text{CH}_4$  and  $\text{CO}_2$  (Siddique et al. 2006; Siddique et al, 2007; Siddique et al. 2011; Siddique et al., 2015; Mohamad Shahimin et al., 2016; Mohamad Shahimin and Siddique 2017a and b). A number of research studies conducted at laboratory scale assessed the potential of individual microbial communities in MFTs collected from different tailings pond to degrade different groups of hydrocarbons. These studies revealed the microbial key players and their potential pathways for the biodegradation of *n*-alkanes ( $\text{C}_5$ - $\text{C}_{18}$ ) (Siddique et al. 2006; Siddique et al. 2011; Siddique et al. 2012; Mohamad Shahimin et al., 2016), monoaromatics (toluene and isomers of xylene) (Siddique et al., 2007; Siddique et al. 2012), and *iso*-alkanes and a few cycloalkanes ( $\text{C}_5$ - $\text{C}_9$ ) (Abu Laban et al., 2014; Siddique et al., 2015; Tan et al., 2015) and whole naphtha and paraffinic solvent (Mohammad Shahimin and Siddique 2017a and b). Siddique et al., (2008) estimated that Mildred Lake Settling Basin (MLSB) known as the oldest oil sands tailings pond was emitting  $\sim 43$  million  $\text{L CH}_4 \text{ day}^{-1}$  confirming metabolism of hydrocarbons into methane. However, assessing field environmental conditions (temperature,

pressure, nutrients and identification and quantification of microbial taxa in tailings ponds) will help in developing more accurate predictions so that practical strategies could be devised to manage tailings and mitigate their emissions.

Inorganic nutrients in particular N and P are essential for microbial metabolism. The depletion or poor availability of N or P in natural environments (as a recalcitrant fraction or bound to the solid phase) during hydrocarbon degradation may affect the development of hydrocarbon-degrading microbial communities and biogenic gas production (Elango et al., 2014). The enhanced growth and activity of indigenous microorganisms have been reported in various hydrocarbon-contaminated sites amended with appropriate inorganic nutrients (N and P) (Smith et al., 2015; Zhang and Lo, 2015). Hester et al. (2018) reported that the addition of N into wetland ecosystems changed the structure of microbial communities and N cycling dynamic and in turn enhanced biogenic gas production ( $\text{CH}_4$ ,  $\text{CO}_2$ , and  $\text{N}_2\text{O}$ ). A limited biological activities in biodiesel wastewater containing high amounts of oil and low concentrations of N and P was also reported (Vidal *et al.*, 2000; Siles *et al.*, 2010). Sharma and Sing (2001) reported that addition of P to a bioreactor containing anaerobic sludge improved  $\text{CH}_4$  production. However, Mancipe-Jiménez et al. (2017) reported the inhibitory effect of P on methanogenic activities where they conducted an experiment on the treatment of liquid waste under anaerobic conditions and in the presence of P. Based on these findings, it is important to assess the effect of nutrients (N and P) on the kinetics of hydrocarbon biodegradation and indigenous microbial community structure and function in FFT as previous lab studies on hydrocarbon biodegradation were performed using FFT supplemented with nutrient media (Siddique et al. 2006, 2007, 2011, 2015; Mohamad Shahimin and Siddique, 2017 a and b), so that  $\text{CH}_4$  production from tailings ponds and EPLs could be predicted accurately for assessing the sustainability of EPLs.

Nitrogen cycling is a central core in biogeochemical processes and is closely coupled to  $\text{CH}_4$  cycle. Specific prokaryotes carry the diverse redox reactions (assimilatory and dissimilatory pathways) in N Cycle that might enhance or reduce  $\text{CH}_4$  emissions (Bae et al., 2018); for instance, stimulated denitrifiers can reduce  $\text{CH}_4$  production by utilizing substrates for methanogens (Bodelier and Steenbergh, 2014). Previous studies also indicated the enhancement in  $\text{CH}_4$  production via the cooperation of nitrogen fixers with methanogens in N-deficient tailings and also in wetlands (Collins et al., 2017; Bae et al., 2018). To assess the role of nutrients in methanogenesis, we established laboratory experiment by collecting FFT and cap water from BML and placing them

in closed columns simulating EPL. The FFT was amended with labile hydrocarbons and supplemented with nutrients (N and P). Microbial community structure was determined by 16S rRNA gene sequence and N cycling was inferred from functional genes (*nirS*, *nosZ*, *nrfA*, and *nifH*) involved in N transformation. The results from this study provide fundamental information on how methanogenesis is affected in BML tailings in response to nutrients availability, and if there is any role of N cycling in methanogenesis.

## **2.3 Materials and methods**

### **2.3.1 Chemicals and materials**

The samples of methanogenic FFT were collected from Base Mine Lake at 11.2 m below the water surface at Syncrude Canada Ltd. (Syncrude), Alberta, Canada (July 2013). Water samples were collected from BML and Beaver Creek Reservoir (BCR) in July 2013 for capping columns filled with FFT. Chemical analyses of FFT and water samples were performed (Table 2.1 and 2.2) and samples were stored in the dark at 10°C before their use in the experiments. Hydrocarbons such as 2-methylpentane (C<sub>6</sub>H<sub>14</sub>, CAS no.107-83-5, > 99 % purity), methylcyclohexane (C<sub>7</sub>H<sub>14</sub>, CAS no. 108-87-2, ≥ 99.0 % purity), o-xylene (C<sub>8</sub>H<sub>10</sub>, CAS no. 95-47-6, ≥ 99.0 % purity), and *n*-octane (C<sub>8</sub>H<sub>18</sub> CAS no. 111-65-9, ≥ 99.0 % purity), ammonium chloride (NH<sub>4</sub>Cl, CAS no.12125-02-9, 99.99 % trace metals grade) and ammonium phosphate monobasic (NH<sub>4</sub>H<sub>2</sub>PO<sub>4</sub>; CAS no.7722-76-1, 99.99% trace metals grade), were purchased from Sigma Aldrich. Methanol (CAS no. 67-56-1, > 99% purity), toluene (C<sub>6</sub>H<sub>5</sub>CH<sub>3</sub>; CAS no. 108-88-3, 99.9 % purity), *n*-decane (C<sub>10</sub>H<sub>22</sub>; CAS no. 124-18-5, ≥ 99.0 % purity), were purchased from Fisher Scientific. Hydrocarbon 3-methylhexane (C<sub>6</sub>H<sub>13</sub>CH<sub>3</sub>, CAS no. 589-34-4, 99 % purity) was procured from ChemSamp Co, Inc. Cylindrical acrylic columns were constructed with 6.55cm outer diameter, 0.3cm wall thickness, and 81.5cm height. The columns were fitted with four SS-316 sampling ports, to enable collection of FFT and water samples from the columns (Fig 2.1). SS-316 sampling ports for obtaining FFT and water samples from the inner portion of columns were purchased from Sailuoke Fluid Equipment Inc. (China).

### **2.3.2 Experimental setup**

To study the partitioning of the contaminants of concerns (COCs) between FFTs and overlying capwater, eight 10 L acrylic columns were established in April 2016. Four sampling ports were inserted at various locations along the length of the columns for the withdrawal of cap water and FFTs samples. One port was inserted in the section of capwater, and the other three

(Top, Mid., and Bot) ports were inserted in the FFTs by ~ 6, 24, and 42 cm distance from the mudline (FFT-cap water interface), respectively (Fig 2.1). Each column was filled with 7 L of FFT and capped with 1.4 L of water from the mixture of BML and BCR water samples at a ratio of 1:1. A FFT: cap water ratio of 5:1 was used to simulate the ratio found in BML. To maintain anaerobic conditions and reduce the risk of exposure of FFT to air during the establishment of the columns, FFT was flushed with helium gas under the plastic curtain and stirred manually and gently before adding to each column. Six columns were initially amended with hydrocarbons: *n*-octane (500 ppm), *n*-decane (500 ppm), 2-methylpentane (500 ppm), 3-methylhexane (500 ppm), toluene (150 ppm) and *o*-xylene (150ppm). After 380 days incubation, columns were refeed with hydrocarbons including Heptane (800ppm), Octane (800ppm), 2-methylpentane (800 ppm), 3-methylhexane (800 ppm), and 2-methylheptane (800 ppm), to maintain methanogenesis in columns. To maintain optimum conditions for microbial activity and accelerate natural processes, four out of the six hydrocarbon-amended columns were further supplemented with N or N plus P at a C:N:P ratio of 100:10:1 (Mclean, 1995). Two columns were used as a baseline control (unamended and unsupplemented columns) to investigate the changes in the rate of methanogenesis, microbial diversities and partitioning of COCs linked to methanogenesis. Residual endogenous carbon, N, and P, if any, were the only available carbon and nutrient sources for microbial activities in the unamended columns. FFT was added in 3 steps to each column. In each step, 1/3 volume of calculated hydrocarbons and nutrients for each treatment were added and mixed well manually with FFTs. After filling the columns with FFT, the column's surface was covered with cap water and sealed with acrylic plates using Silicone. Finally, the headspace of all columns (amended and unamended) was flushed with helium, and the columns were incubated in the dark condition at room temperature. Duplicate columns were prepared for each treatment.

Acrylic plates were equipped with a septum on top of each cylinder for the withdrawal of headspace gas samples using insulin syringe for analysis of produced gases (CH<sub>4</sub> and CO<sub>2</sub>) and volatile hydrocarbons. The plates were also equipped with plastic tubing. The plastic tubing from each column was connected to two 1-liter plastic bottles. One of the bottles (bottle1) was filled with acidic brine (200 g of NaCl and 5g of citric acid per litre of tap water), and another one (bottle 2) was left empty. The pressure of produced biogas in the headspace of each column displaced the acidic brine from bottle one to bottle two during daily gas production (Fig 2.1). Biweekly monitoring of CH<sub>4</sub> and CO<sub>2</sub> production was performed for each column during the incubation

period (~600 days). The FFT and cap water were sampled at day 0) and day 190 d. Due to the constant production of methane, the microbial analysis wasn't performed at other sampling dates after 190d assuming the developed microbial community will not change afterwards. FFT samples were analyzed for 16S rRNA, NifH, NrfA, NosZ, NirS genes. In chapter 3, the solid and liquid chemical analysis of FFTs and cap water samples have been described. The chemical analysis was performed over incubation period at days 0, 190, 353, and 600.

### **2.3.3 Chemical analysis**

To determine the CH<sub>4</sub> and CO<sub>2</sub> production in the sealed columns, 0.1 ml of gas was removed from the headspace of each column using an insulin syringe and injected directly into a gas chromatograph equipped with a flame ionization detector (GC-FID; Hewlett Packard 5890; column: Poropak Type R; oven temperature: 30 °C and helium flow rate: 12.5 mL min<sup>-1</sup>) (Fedorak et al., 2003). The pressure of the gas in the headspace of each column was also measured using a digital pressure gauge (DPG1000B ±15.00PSIG-5, MOD-TRONIC Instruments Limited, Brampton, ON) fitted with luer-lock needle. This value was subjected to mass calculation of CH<sub>4</sub>. The theoretical maximum CH<sub>4</sub> production was calculated using stoichiometric equations derived from the modified Symons and Buswell equation (Symons and Buswell, 1933). In this calculation, it has been assumed that the hydrocarbons are completely metabolized to CH<sub>4</sub> and CO<sub>2</sub>.

To monitor biodegradation, the concentrations of hydrocarbons in all amended FFT (HC, HCN, and HCNP) were determined at days 0, 190, and 350 over incubation period. The FFT samples were taken from port 3 (P3) and port 4 (P4) of each column. One milliliter of removed FFT from each port extracted with 10ml methanol in a 20ml EPA vial. The vials were shaken for 30min at 20°C. The solid parts in the vials were allowed to settle. One milliliter of the supernatant was transferred to a 44ml EPA glass vial and completely filled with ultrapure water (Milli-Q Water System) and capped immediately. All prepared vials were analyzed using a gas chromatograph fitted with a flame ionization detector (GC-FID) (Hewlett Packard HP 6890) which was equipped with a purge and trap system as described with Mohamad Shahimin and Siddique, (2017a and b).

### **2.3.4 Characterization of the microbial community by 16S rRNA genes and its involvement in nitrogen cycling by NifH, NirS, NosZ, NrfA genes**

#### **2.3.4.1 DNA extraction**

Genomic DNA was extracted from FFT and cap water samples at initial (day 0) and day 190 when FFT was producing active biogenic gas, using bead-beating method (Foght et al., 2004).

Samples of FFT or cap water (300  $\mu$ L) was added to screw-cap microcentrifuge tubes containing 1 g of 2.5 mm and 0.1 mm zirconia-silica beads (1:1 w/w), phosphate buffer (100 mM NaH<sub>2</sub>PO<sub>4</sub>, pH 8.0), lysis buffer (100 mM NaCl, 500 mM Tris at pH 8.0, 10% sodium dodecyl sulfate), and chloroform-isoamyl alcohol (24:1). Tubes were shaken at 3400 rpm for 45s in PowerLyzer™24 Bench Top Bead-based Homogenizer (MO BIO Laboratories Inc., Carlsbad, CA) and centrifuged by a microfuge at maximum speed (15000 rpm) for 5 min. Each sample was in triplicate. The samples were centrifuged at 15,000 rpm for 5min to allow for collection of clear supernatant DNA recovery. The extraction steps mentioned above were repeated three times using the same sample to increase DNA yield. For precipitation of dissolved proteins, ammonium acetate (7M) was added to each supernatant to achieve a final concentration of 2.5M, and mixed gently and centrifuged 7 min to pellet the precipitated proteins. The supernatant was transferred to a new tube containing 0.6 volume of isopropanol incubated overnight at -4°C. The precipitated DNA was recovered by spinning at 15,000 rpm for 30 min. Following centrifugation, the isopropanol was decanted, and the DNA pellet was dried at room temperature for 1-2 hr. DNA was dissolved in 30  $\mu$ l of nuclease-free water (Integrated DNA technologies). Extracted DNA from the same samples were pooled together and stored at -20°C. DNA extraction was also applied to the negative control to determine the lack of contamination in reagents.

#### **2.3.4.2 Sequencing and analysis of genes**

16S rRNA genes of bacteria and archaea and NifH, NirS, NosZ and NrfA genes (involved in nitrogen cycling) in FFT and cap water were amplified and sequenced on the Illumina MiSeq platform (TAGC, Edmonton, AB, Canada). PCR amplification was performed in 25- $\mu$ l reaction volumes and three replications from each sample were used. The PCR reaction mixture contained 12.5  $\mu$ l Accustart™ II PCR toughmix 2X (Quanta Biosciences), 2.5  $\mu$ l (10 $\mu$ M) of forward and reverse gene-specific primers (include Illumina forward and reverse adaptor overhangs (Table 2.3), 1.25  $\mu$ l DMSO, BSA (0.2  $\mu$ l for 16S rRNA, NirS and NifH and 0.75  $\mu$ l for NosZ and NrfA), 1.1  $\mu$ l DNA template (~10 ng  $\mu$ l<sup>-1</sup>) and balance nuclease-free water. Various PCR reaction conditions were used in S1000™ Thermal Cycler (BIO RAD) for targeting the desired genes (Table 2.4). All replicates of each sample were pooled together after PCR amplification. To ensure PCR quality, the negative controls containing PCR reagents and nuclease-free water without DNA template were also included during PCR amplification of each set of samples. The quality and yield of PCR reaction products were examined using agarose gel electrophoresis and sent to

TAGC (Edmonton, AB, Canada) for sequencing with the Illumina MiSeq platform. Amplicon sequencing results were analyzed using the MetaAmp pipeline, and the amplicon reads were clustered into Operational Taxonomic Units (OTUs) at  $\geq 97\%$  similarity level. OTUs with the relative percentage abundance  $\geq 2\%$  were included in the results. For 16S rRNA genes, the percentages of bacterial and archaeal communities within each sample was determined. Basic Local Alignment Search Tool (BLAST) (blast.ncbi.nlm.nih.gov) was used to compare the sequence of each accepted OTUs from 16S rRNA and other functional genes with a reference sequence database in NCBI. The data were statistically analyzed using the package R. Statistical significance was detected using the independent samples t-test and analysis of variance at  $\alpha=0.05$ .

## **2.4 Results**

### **2.4.1 Biogas production in FFT amended with a mixture of hydrocarbons, with or without nutrients addition**

Cumulative CH<sub>4</sub> production in the headspace of each column was monitored biweekly during the incubation period (~600 days) (Fig 2.2). The results showed that CH<sub>4</sub> production in unamended columns (baseline controls) (U) was insignificant (~0.4 mmol). However, the CH<sub>4</sub> production in the columns amended with hydrocarbon (HC), hydrocarbon plus N (HCN), and hydrocarbon plus N plus P (HCNP) was observed after a lag phase of 50 days and CH<sub>4</sub> exponentially increased after ~60 days. CH<sub>4</sub> production steadily increased until day 190 up to 266.41±13.46, 299.93±1.49, and 211.02±5.34 mmol in HC, HCN, and HCNP, respectively. In continuous, until day 228, the only a small decrease was observed in all amended columns. CH<sub>4</sub> production reached a maximum of (285.25±7.14 mmol in the HC columns, and in HCNP (227.18±15.47 mmol). However, HCN columns exhibited significantly higher increase (345.7±12.02 mmol) than others by 578d. Afterward, a plateau level was reached in these columns. The cumulative CH<sub>4</sub> produced during the experiment period was significantly higher in HCN columns, than in the HC or HCNP columns. However, significantly lower amounts of CH<sub>4</sub> production were observed in HCNP columns. After 380 days of incubation, the columns were refeed again with hydrocarbon, N, and P to maintain methanogenesis activity. From day 400, small increase in CH<sub>4</sub> production was observed in all amended columns, particularly in HCN columns. However, the produced CH<sub>4</sub> was not impressive in all amended columns.

## 2.4.2 Biodegradation of the hydrocarbons in the FFT

Measurement of residual hydrocarbons in HC, HCN, and HCNP FFT revealed a similar pattern with different rate of biodegradation (Fig 2.3). The preferential biodegradation of hydrocarbons in sequence Toluene > O-xylene > 2MC<sub>5</sub> > Octane > 3MC<sub>6</sub> > Decane was observed in all amended FFT (Fig 2.3). Toluene and O-xylene were almost completely biodegraded after 190 d incubation in all amended FFT. Approximately, more than 60%, 80%, and 40% of 2MC<sub>5</sub> was depleted after 190 day from the initial concentrations, in HC, HCN, and HCNP FFT, respectively. Also, HC and HCN FFT exhibited ~50% and ~70% depletion of Octane and ~40% and ~60% of 3MC<sub>6</sub> after 190 d from the initial concentrations, respectively (Fig 2.3), while partial (~25%) depletion of Octane and partial (~20%) depletion of 3MC<sub>6</sub> were observed in HCNP FFT after 190d incubation. Approximately 40% of Decane was depleted after 190 d from the initial concentration, in HCN FFT while Decane was only slightly depleted after 190d incubation in HC and HCNP FFT (Fig 2.3). During the incubation of 350 d, 2MC<sub>5</sub>, 3MC<sub>6</sub>, and Octane were almost completely biodegraded in HC and HCN FFT. However, 3MC<sub>6</sub>, and Octane exhibited ~80-85% depletion from the initial concentrations, respectively in HCNP FFT (Fig 2.3). 2MC<sub>5</sub> completely depleted after 350d in HCNP FFT. After 350d of incubation, Decane exhibited only ~20% depletion from initial concentration in HCNP FFT whereas ~65% and ~85% of Decane was depleted in HC and HCN FFT, respectively.

## 2.4.3 Characterization of microbial community in FFTs and cap water

The bacterial and archaeal communities in the unamended, HC, HCN and HCNP columns were determined by targeting and sequencing the V6 region of the 16S rRNA gene using the Illumina MiSeq. Samples were taken at day 0 as initial samples (before manipulation) and day 190 when CH<sub>4</sub> production reached the highest level during exponential phase. The samples were taken from unamended and amended columns from all ports sampling ports: cap water port as well as Top, Mid and Bot ports for FFT below the mud line. After trimming primers and barcodes, a total of 2, 124, 231 merged reads with sequence length of 300bp were obtained. In initial FFTs, the archaeal DNA reads constituted ~28% of the total prokaryotic community DNA reads, and the rest proportion belonged to bacteria. On day 190, the archaeal DNA reads constituted ~25% of the total prokaryotic community DNA reads and the rest proportion belonged to bacteria. However, the archaeal community changed to 45, 60, and 38% of the total prokaryotic reads in HC, HCN, and HCNP FFTs while the remaining reads belonged to bacteria. In initial and final

unamended capwater samples, all reads were belonged to bacterial reads; however, in the capwater of all final amended column samples, the bacterial reads constituted 87-91% of the total prokaryotic reads while the remaining reads belonged to archaea. The amplicon reads were clustered into Operational Taxonomic Units (OTUs) based on  $\geq 97\%$  similarity.

#### 2.4.3.1 Microbial community composition and structure

Multiple samples' similarity tree and the relative abundance of dominant bacteria at phyla level are shown in Fig 2.4. Analysis of community composition in INT-FFT, UNA, HC, HCN, and HCNP samples indicated that more than 99% of all reads were classified into 12 phyla. In the Initial FFT, *Proteobacteria* made up 34% of total bacterial reads and was composed of 16% *Deltaproteobacteria* (8-9% *Desulfobacteraceae*) and 9% *Betaproteobacteria* (7-8% *Comamonadaceae*) of total bacterial reads. Also, 11% of total bacterial reads were belonged to *Chloroflexi* (32% *Anaerolineaceae*) in the initial FFT (Figs 2.4T, 2.5, and 2.6). Whereas, the FFTs retrieved from various depths of unamended columns (Top-UNA, Mid-UNA, and Bot-UNA) at 190 days showed a significant increase in the abundance of *Proteobacteria* (~55-65% of bacterial reads, with 44-68% *Betaproteobacteria* and 12-30% *Comamonadaceae*), and a decrease in the abundance of *Chloroflexi* (15-30% *Anaerolineaceae*). In FFT retrieved from various depths (Top-UNA, Mid-UNA, and Bot-UNA) of amended columns at 190 days, *Proteobacteria* made up 45% of total bacterial reads and was composed of 56% *Deltaproteobacteria* (~55% *Syntrophaceae*) of total bacterial reads in HC FFT. Also, *Firmicutes* made up 29% of total bacterial reads in this sample and was composed of ~4.5% *Clostridia* (~ 6% *Peptococcaceae*) (Fig 2.5 and 2.6). Higher abundances of these two families were observed in HCN FFT compared with HC and HCNP FFT at day 190. The abundance of *Deltaproteobacteria* was composed of 67% of total bacterial reads (~70% *Syntrophaceae*) in HCN FFT. Also, the abundance of *Clostridia* was composed of 6% (~ 10% *Peptococcaceae*) of total bacterial reads in this sample (Fig 2.5 and 2.6). However, these two families showed lower abundance in HCNP FFT compared with HC and HCN FFT. The abundance of *Deltaproteobacteria* was composed of 43% of total bacterial reads (~40% *Syntrophaceae*) in HCNP FFT. Also, the abundance of *Clostridia* was composed of ~4.5% (~ 7% *Peptococcaceae*) of total bacterial reads in this sample (Fig 2.5 and 2.6). Members of *Chloroflexi* (*Anaerolineaceae*) decreased to 10-15% in all the unamended, HC and HCNP columns. Compared to INT-FFT, the highest decrease (5-7%) in the phyla *Chloroflexi* appeared in the FFT from HCN columns. On the

other hand, *Dehalococcoidia* (from *Chloroflexi* phyla) showed increasing trend in the FFT of all the amended treatments (Fig 2.5 and Fig 2.6).

The relative abundance of the archaeal community at the family level is shown in Fig 2.4B. *Methanoregulaceae*, and *Methanosaetaceae* were the predominant families present in the INT-FFT at day 0, and in Unamended FFT (U), HC, HCN, and HCNP FFT samples at day 190. These two families accounted for more than 99% of all archaeal communities in the FFT samples from these columns. No significant differences among initial (day0), and unamended and amended treatments at day190 was observed for the archaeal communities in percentages; however, the OTU numbers in both families *Methanoregulaceae*, and *Methanosaetaceae* significantly increased in all amended FFTs (HC, HCN, and HCNP) at day 190 when compared to INT-FFT at day 0. In FFT Samples taken from various depths of the columns amended with hydrocarbon (Top-HC, Mid-HC, Bot-HC), *Methanoregulaceae* and *Methanosaetaceae*, represented 275-394 and 181-287 of OTUs numbers, respectively. HCN FFT samples taken from various depths of HCN columns indicated highest OTU numbers for *Methanoregulaceae* (275-495) and *Methanosaetaceae* (218-416) among all amended FFTs. While FFTs samples taken from various depths of HCNP columns showed the lowest numbers of OTUs in *Methanoregulaceae* (111-257) and *Methanosaetaceae* (83-241) in compare with HC and HCN FFTs at day 190. Unamended FFT also showed the increase of OTUs , in both families *Methanoregulaceae* (110-142) and *Methanosaetaceae* (104-126) in compare with INT-FFT (110 and 118, respectively) (Fig. 2.4B, Table 2.5).

The results of the bacterial community structure in cap water samples at the phyla level (Fig 2.4T) showed that *Proteobacteria* (~ 62-75%) was the most dominant phyla in INT-Cap (day0), Cap-UNA and all amended (Cap-HC, Cap-HCN, Cap-HCNP) cap water samples at day 190. *Gammaproteobacteria* (45% of *Proteobacteria*) had the highest relative abundance value in INT-Cap. A significant increase in the abundance of *Alphaproteobacteria* was observed in Cap-UNA (~ 27% of *Proteobacteria*), Cap-HC (~44% of *Proteobacteria*), and Cap-HCN (~49% of *Proteobacteria*) at day 190. However, compared to Cap-HCN and Cap-HC samples, *Betaproteobacteria* (~ 41% of *Proteobacteria*) was more dominant in Cap-HCNP samples (Fig. 2.5A). The cap water of all amended columns was also enriched with *Firmicutes* particularly in the class *Clostridia* (Fig 2.5B and Fig 2.6). In addition, Cap-HCN showed the highest abundance of *Erysipelotrichia* (~11%) (Fig 2.5B). The increasing trend in *Chloroflexi* phyla was observed in

Cap-UNA (~4%), Cap-HCN (~4%), and Cap-HCNP (~9%) samples at day 190 (Fig. 2.5C). Highest abundance of *Anaerolineaceae* (~3%) and *Dehalococcoidaceae* (~12%) was observed in Cap-HCN and Cap-HCNP samples, respectively. Archaea was not detected in Cap-INT and Cap-UNA (at day 190); however, *Methanoregulaceae*, *Methanosaetaceae*, and *Methanosarcinaceae* occupied Cap-HC, Cap-HCN, and Cap-HCNP samples at day 190. *Methanoregulaceae* (~36%; 26 OTUs), and *Methanosaetaceae* (47%; 34 OTUs) were the dominant families in the Cap-HC samples. While in Cap-HCN samples, *Methanoregulaceae* was approximately 63% (40 OTUs). However, the cap water of HCNP samples showed the highest abundance of *Methanosarcinaceae* (~42%; 24 OTUs) (Fig. 2.4B, Table 2.5).

#### 2.4.3.2 Genes involved in nitrogen cycling process

Identifying the presence of microorganisms responsible for N-cycle in the FFT and understanding the link between methanogenic communities and N-cycling in the FFT is essential to establishing the sustenance of methanogenesis. Key functional genes for nitrogen fixation (*nifH*), denitrification (nitrite reductase (*nirS*) and nitrous oxide reductase (*nosZ*), and dissimilatory nitrate reduction to ammonium (DNRA) (*nrfA*) were detected in all unamended and amended (HC, HCN, and HCNP) FFTs and cap water samples (Table 2.7). These intended functional genes were also detected in the initial FFT and initial cap water samples. The highest OTU numbers for genes involved in nitrogen fixation belonged to the archaea *Methanosaetaceae* (Fig 2.7). *Methanosaeta concili* (100% identity) was detected across all unamended and amended FFTs (Table 2.7). When compared to 16S data (Table 2.5), *Methanosaetaceae* increased in all unamended and amended FFTs at day 190 in comparison with initial FFT at day 0. This confirms the detection of *Methanosaeta concili* in unamended and all amended FFTs. However, the increase of *Methanosaetaceae* was higher in amended FFTs when compared with unamended one. Among amended FFTs, highest and lowest increase in the OTU number of *Methanosaetaceae* detected in HCN and HCNP FFT samples, respectively. Additionally, limited OTU number of bacterial genes related to nitrogen fixation within the phylum *Proteobacteria* detected in all amended and unamended FFTs (Table 2.7 and Fig 2.7). Similarly, the denitrification genes; *nirS* and *nosZ* were also detected in all unamended and amended FFT samples. Almost all of the *nirS* and *nosZ* sequences originated from the phyla *Proteobacteria* (Table 2.7). Also, the sequences involved in DNRA pathway, *nrfA* gene, was also detected in all unamended and amended FFT samples that was related to *Beta* and *Deltaproteobacteria* by 86% and 92% identity, respectively (Table 2.7).

## 2.5 Discussion

Movement of contaminant of concerns (COCs) from underlying FFT to the overlying cap water is one of the major potential indices in gauging the feasibility of EPL for tailings reclamation. Any process that influences biogeochemical processes ultimately affects the flux of COCs from FFT to cap water. Methanogenesis known as a predominant terminal catabolic process under anaerobic condition might be involved in the partitioning of COCs. Under methanogenic condition, indigenous microbes in FFT alter pore water chemistry due to production of CO<sub>2</sub>. Subsequently, dissolution of CO<sub>2</sub> decreases the pH of pore water and increases the solubility of carbonate minerals that induces the release of ions in pore water (Siddique et al., 2014). Electrons, under fermentation and methanogenic processes, are directly and indirectly transferred to Fe<sup>III</sup> minerals, producing Fe<sup>II</sup> minerals (Siddique et al., 2014) which can influence the mobility of metals, as well as organic and inorganic pollutants in the environment (Oren, 2014).

Physico-chemical conditions such as temperature, pH, moisture content, nutrient availability, terminal electron acceptor, etc. severely influence microbial metabolism (Sarkar et al., 2016). Nutrients (mainly N and P) are essential for microbial growth. Consequently, it can be hypothesized that the production of biogenic gases (CH<sub>4</sub> and CO<sub>2</sub>) might be enhanced in FFT when supplement with inorganic N and P and this would in turn affect COC mobilization and immobilization. From other aspect, there is still a gap between N and CH<sub>4</sub> cycling since the microbes that are involved in producing methane, can consume N fertilizers as N (assimilation, fixation) and energy source (NH<sub>4</sub><sup>+</sup> and NO<sub>3</sub><sup>-</sup>). In this chapter, the focus is on a) how nutrients (N and P) affect CH<sub>4</sub> emission and microbial community composition, and b) how CH<sub>4</sub> production might be influenced by nitrogen cycling. In chapter 3, the effect of methanogenesis on chemical and mineralogical processes and contaminant partitioning is discussed.

In HC, HCN, and HCNP amended FFTs, CH<sub>4</sub> production began after a lag phase of about 50 days. Similar lag phases (~85-100 days) in producing CH<sub>4</sub> were observed in the MFT from Syncrude MLSB (Siddique et al., 2007) and in Albian and CNRL MFTs as well (Shahimin and Siddique, 2017) during naphtha biodegradation. After the lag phase, biogenic CH<sub>4</sub> production increased in all three amended FFTs and major proportion of CH<sub>4</sub> was produced by ~190 d in all amended FFTs (Fig. 2.2) when most of the hydrocarbons were metabolized into CH<sub>4</sub>. The measured CH<sub>4</sub> in the headspace of amended columns yielded 30-40% of the calculated (predicted) theoretical maximum CH<sub>4</sub> production by day 190, which was much lower than the values reported by previous

studies (Siddique et al., 2006, 2007; Mohammad Shahimin and Siddique 2017b). The difference between the measured and predicted  $\text{CH}_4$  might be attributed to 1) the loss of hydrocarbons through releasing from the FFT to the cap water of all amended columns after ~70 days when methane production was actively started (Fig 2.8), 2) the production of recalcitrant metabolites through incomplete oxidation of complex substrate, and 3) the assimilation of carbon to biomass (Fowler et al., 2012; Tan et al., 2015; Mohamad Shahimin et al., 2016; Mohammad Shahimin and Siddique 2017b). Further incubation time was extended to 600d to observe any substantial  $\text{CH}_4$  production upon addition of another dose of hydrocarbons. The results showed only a slight increase in  $\text{CH}_4$  production afterwards due to lack of proper hydrocarbon mixing the FFT.

In the current study, mixtures of two alkyl-benzenes (toluene and *o*-xylenes), two iso-alkanes (2-MC<sub>5</sub>, and 3-MC<sub>6</sub>), and two n-alkanes (nC<sub>8</sub> and nC<sub>10</sub>) were incubated with HC, HCN, and HCNP FFT. Methanogenic biodegradation of alkyl-benzenes (toluene and *o*-xylenes) occurred rapidly in all amended FFT (after 190days of incubation) (Fig 2.3). It can be concluded indigenous microbial communities in the FFT can readily utilize certain fraction of hydrocarbon mixture to support methanogenesis (Siddique et al., 2007). Both iso-alkanes incubated were completely depleted in HC and HCN FFT during longer incubation (350d) and under stimulated methanogenesis; however, rate of iso-alkanes depletion decreased under the slowed methanogenesis in HCNP FFT. Also, the presence of both n-alkanes in HC and HCNP FFT (with higher percentage in HCNP FFT) and nC<sub>10</sub> in HCN (with lower percentage compared to HC and HCNP) were observed during longer incubation period (Fig 2.3). Because of slightly higher molecular weight of n-alkanes (nC<sub>8</sub> and nC<sub>10</sub>) than iso-alkanes (2-MC<sub>5</sub>, and 3-MC<sub>6</sub>), it can be expected n-alkanes to deplete in all amended FFT in longer incubation period. Also, from the results it can be concluded that the rate of methanogenic activities might influence on the biodegradation rate of iso and n-alkanes in FFT. Previous studies on naphtha biodegradation showed that during the short incubation period, short chain *n*-alkanes (C<sub>7</sub>-C<sub>10</sub>) and some alkyl-benzenes (toluene and *m*- and *o*-xylenes) were biodegraded under methanogenic condition with the production of copious amounts of  $\text{CH}_4$  (Siddique et al., 2007, Mohamad Shahimin and Siddique, 2017a and b). Longer incubations also revealed biodegradation of iso-alkanes to  $\text{CH}_4$  (Mohamad Shahimin and Siddique 2017a and b; Abu Laban et al., 2014)

Trends in  $\text{CH}_4$  production in HCN columns indicated that enhancement of methanogenesis was higher in FFTs containing mixture of hydrocarbons and N compared with FFTs amended with

only the hydrocarbons. It is due to the fact the N is needed for the metabolism of organic carbon compounds (Van Hamme et al., 2003; Östeberg et al., 2006 and Volke-Sepulveda et al. 2006). Adding nutrients (N and P) to oil contaminated soils and sediments can increase the indigenous microbial activity and enhance hydrocarbon biodegradation and CH<sub>4</sub> release in anaerobic conditions (Xu and Obbard, 2003, Devi et al., 2011). Therefore, lower rate of CH<sub>4</sub> production in HC columns when compared with HCN columns could be attributed to the poor availability of N sources. Sarkar et al. (2016), reported similar results for the slower rate of hydrocarbon biodegradation in various hydrocarbon enriched environments under inadequate condition of N availability. Comparing the rates of CH<sub>4</sub> production in HC and HCN, it can be concluded that microbes have the potential to degrade hydrocarbons even under the dearth of dissolved nutrients and then, nutrients play an important role in accelerating microbial activity (Edward et al. 2011). The findings of Leilei et al., (2017) suggested that increased amount of ammonium nitrogen depositions in a coastal wetlands system could increase the abundance of methanogens and in turn enhanced the CH<sub>4</sub> emissions. Our findings (Table 2.5 and Fig 2.2) also highlight the stimulation role of NH<sub>4</sub>-N in enhancing the relative abundance of methanogens and CH<sub>4</sub> production in HCN amended columns.

In contrast to synergistic effect of N on CH<sub>4</sub> production, the addition of phosphorous to FFTs treated with a mixture of hydrocarbons and N (C:N: P ratio 100:10:1), suppressed methanogenesis resulting in reduced production of CH<sub>4</sub> in HCNP in compare with HC and HCN during the long incubation time (~600d). Boonsawang et al. (2014) observed similar behavior. They reported that increasing phosphorous from C: P of 100:0 to 100:0.5 enhanced CH<sub>4</sub> production during treatment of biodiesel wastewater. However, increasing the C: P ratio to 100:1 produced low CH<sub>4</sub> content (Boonsawang et al., 2014). Mancipe-Jiménez et al., (2017) found that the increase of phosphorous from 3.3 mg P L<sup>-1</sup> to 33.3 mg P L<sup>-1</sup> caused the increased rate of Volatile Fatty Acid (VFA) production by acidogenic bacteria. Although VFA are essential substrates for methanogenesis, high concentrations of VFA could be toxic for methanogens and resulting in decrease in methanogens frequency and CH<sub>4</sub> production (Khanal, 2008, Boonsawang et al., 2014, and Mancipe-Jiménez et al., 2017). Similarly, in our study, the concentration of phosphorous increased from 0 in initial FFT to 24 mg P L<sup>-1</sup> in HCNP FFT samples. Although the VFT wasn't measured in our study, it might be possible that high VFA production could also have led to lower CH<sub>4</sub> production in HCNP FFT samples. The accumulation of VFA causes the pH values to

decrease and can lead to a toxic condition and a damage of methanogenesis (for example, inhibit the methanogens growth) that are known as the most vulnerable stage in anaerobic processes when pH is decreased (Franke-Whittle et al., 2014; Mancipe-Jiménez et al., 2017). Khanal (2008), reported that the optimum pH for the occurrence of acidogenesis and methanogens are 5.5-6.5 and 6.5-7.2, respectively. However, pH values didn't decrease significantly under the optimum pH condition in the porewater of HCNP columns, which is assumed to accumulate VFA, compared with HC and HCN columns. In all our amended columns the pH of FFT porewater decreased significantly from  $7.56 \pm 0.08$  (day 0) to  $6.76 \pm 0.12$  (day 190) under active methanogenesis and the pH values didn't varied significantly during experiment period. It would appear the high bicarbonate in the porewater of amended columns most likely make good buffering capacity in the system which results in the stability of pH. Thus, the pH may not be problematic in this study, and the type and concentration of VFAs can be considered reliable for the methanogenesis surpassing in HCNP columns. Different VFAs are produced in anaerobic digestion systems which result in different effects on bacteria and archaea (Franke-Whittle et al., 2014), however, some previous studies indicated butyric acid, valeric acid, propionic acid or the ratio of propionic: acetic acid could be an appropriate indicator for indicating the state of an anaerobic process (Boe, 2006). However, the level of each VFA should be determine in the considered system to indicate the stability or instability of an anaerobic process because different anaerobic systems have adopted to their own levels of VFAs (Franke-Whittle et al., 2014). Our results (Fig 2.2 and Table 2.5) indicated that adding P, inhibited hydrogenotrophic methanogens (*Methanomicrobiaceae* and *Methanoregulaceae*) in HCNP columns. In the environments with low P concentration, acetic acid is the main product of acid production but by supplying the system with higher amounts of N and P, the production of longer chain acid products (butyric acid, valeric acid and caproic acid) is increased and the produced hydrogen during fermentation processes is used to produce longer carbon chain acids (Sreethawong et al. 2010, Boonsawang et al., 2014). Therefore, the decrease in the hydrogen yield could influence the number of hydrogenotrophic methanogens and in turn can have effect on CH<sub>4</sub> emission.

Microbial community composition in all amended samples (HC, HCN, and HCNP) changed at day 190. Bacterial members of the genera *Smithella* and *Syntrophus* (*Syntrophaceae*) and *Desulfosporosinus* (*Peptococcaceae*) were enriched in all amended FFTs (HC, HCN, and HCNP) (Table 2.6 and Fig 2.6). Previous studies showed the enrichment of *Syntrophaceae* as key

oxidizers of various hydrocarbons in methanogenic cultures and/or environments (Mohamad Shahimin and Siddique, 2017a and b; Mohamad Shahimin et al., 2016; Tan et al., 2014; Cheng et al., 2013; Siddique et al., 2012, 2011; Gray et al., 2011; Ramos-Padrón et al., 2011). In most of these studies, *Smithella/Syntrophus* (*Syntrophaceae*) were reported to have direct involvement in degrading hydrocarbons to acetate and H<sub>2</sub> or formate for CH<sub>4</sub> production. In addition, some studies describing dominance of *Peptococcaceae* (*Firmicutes*) affiliated bacteria capable of biodegrading short chain (C<sub>5</sub>-C<sub>8</sub>) *n*- and *iso*-alkanes into CH<sub>4</sub> in Albian, CNRL and Syncrude MFTs have been reported (Mohamad Shahimin and Siddique, 2017a and b; Mohamad Shahimin et al., 2016; Siddique et al., 2015; Tan et al., 2015). In all of these previous studies, the increase in CH<sub>4</sub> production was linked to hydrocarbon biodegradation. Our findings also showed the abundance of *Syntrophaceae* and *Peptococcaceae* during hydrocarbon metabolism in HC columns and these taxa further increased with the availability of ammonium N in HCN columns. The results suggest that biostimulation by carbon and N increased the total number of syntrophic bacteria in amended columns particularly higher in HCN than HC and HCNP columns (Fig 2.6). Similar results have been reported by other researchers. Enrichment of hydrocarbon samples with N improved the microbial' growth rate and increased the hydrocarbon degradation under oxic conditions (Walworth et al., 2007). Leilei et al. (2017) reported the increased abundance of *Geobacillus* and *Clostridium* (*Firmicutes*) and CH<sub>4</sub> production in costal wetland ecosystem after fertilizing with ammonium nitrogen. They believed that hydrogenotrophic and acetoclastic methanogenic archaea could get acetate, H<sub>2</sub>, and electrons from syntrophic bacteria and produce methane. Similarly, we observed the enhancement of CH<sub>4</sub> production from NH<sub>4</sub>-N treated FFT due to higher number of syntrophic bacteria during hydrocarbon metabolism.

The results of archaeal sequences revealed that acetoclastic methanogens belonging to the family *Methanosaetaceae*, and hydrogenotrophic methanogens belonging to the family *Methanoregulaceae* occurred in relatively equal proportions (only with 5-10% higher abundance in *Methanoregulaceae*) and were dominant in all the amended FFTs (HC, HCN, and HCNP). The number of OTUs of both acetoclastic and hydrogenotrophic methanogens increased significantly in all the amended FFTs (Table 2.5). Interestingly, the enrichment of both *Syntrophaceae* and *Peptococcaceae* also revealed in all amended FFTs at 190d. During hydrocarbon degradation under methanogenic conditions, Syntrophic bacteria (*Syntrophaceae* and/or *Peptococcaceae*) produce acetate, hydrogen or formate that are favorable for acetoclastic and hydrogenotrophic

methanogens (Mohamad Shahimin and Siddique, 2017b; Mohamad Shahimin et al., 2016; Stackebrandt, 2014 Siddique et al., 2012). The production rate of syntrophic metabolisms byproducts could effect on the growth rate of methanogens (Mohamad Shahimin and Siddique, 2017b). Dolfing et al. (2008) reported the cooperation of methanogens in the removal of fermentation byproducts (acetate and H<sub>2</sub> or formate), which is the reason for the sustainability of bacterial syntrophy. It might be concluded that the co-occurrence of acetoclastic and hydrogenotrophic methanogenesis in all the amended FFTs at day 190 might be related to the increased abundance of *Syntrophaceae* and *Peptococcaceae* in these samples. Some previous studies reported the higher abundance of acetoclastic Methanosaetaceae during active biodegradation of *n*-alkanes in oil sand tailings under methanogenic conditions (Mohamad Shahimin and Siddique, 2017 a and b; Mohamad Shahimin et al., 2016; Siddique et al., 2012; Tan et al., 2015). Other studies reported hydrogenotrophic methanogenesis as the primary pathway in biodegradation of naphtha, long chain *n*-alkanes (C<sub>15</sub>–C<sub>20</sub>) (Zhou et al., 2012) and monoaromatics (BTEX) (Siddique et al., 2012). However, our results have been shown the co-occurrence of acetoclastic and hydrogenotrophic methanogenesis similar to the research findings for crude-oil degradation (Morris et al., 2012) and biodegradation of various hydrocarbons in MFTs (Siddique et al., 2011, 2012, 2015; Mohamad Shahimin and Siddique, 2017a and b).

To explore a linkage between CH<sub>4</sub> production and nitrogen cycling, the relevant genes for assimilatory or dissimilatory denitrification (*nirS*, *nosZ*, and *nrfA*) and N<sub>2</sub> fixation (*nifH*) were determined in the initial, unamended, and all amended FFTs (Fig 2.9). Higher proportion of *Methanosaeta concili* (*Methanosaetaceae*) in the *nifH* sequences was detected in all initial, unamended and amended FFTs compared to detected Proteobacteria carrying *nifH* gene in these samples (Fig 2.7). Previous studies highlighted that *Methanosaetaceae* played a role in acetoclastic methanogenesis in oil sand tailings (Mohamad Shahimin and Siddique, 2017 a and b; Mohamad Shahimin et al., 2016; Siddique et al., 2012; Tan et al., 2015). Moreover, sequences of *nifH* genes, which plays a role in biological reduction of N<sub>2</sub> gas to ammonium have been recovered from *Methanosaeta concili*, and some other methanogens in diverse environments including oceans, marine sediments, soils, and termite guts (Leigh et al, 2000; Zahr et al, 2003; Bae et al., 2018). Bae et al. (2018) suggested that all methanogens have the *nifH* genes; therefore, the methanogen *nifH* might be detected in diverse environment. As a result, it can be concluded that *acetoclastic methanogenesis* can play a role in N<sub>2</sub> fixation in our FFT samples in addition to their

involvement in CH<sub>4</sub> production. Our previous study showed the potential of N<sub>2</sub>-fixation in N deficient cultures during methanogenic biodegradation of organic substrate in oil sands tailings (Collins et al. 2016). In the current study, N<sub>2</sub>-fixation was not investigated thoroughly. The columns were also devoid of N<sub>2</sub> in the headspace, but N<sub>2</sub> could be produced during anammox process (Kuypers et al., 2003; Kalvelage et al., 2015). Nitrite and nitrate as byproducts of nitrification pathway could be used in denitrification, DNRA and anammox pathways. In our experiment, NH<sub>4</sub>-N sources were used for amending FFTs and nitrate and nitrite were never detected in our initial FFTs samples. However, small amounts of nitrate were detected in various incubation time in HCN. Our columns were incubated in strictly anaerobic condition. As a result, nitrate should not be produced via nitrification. Clement et al (2005) demonstrated NH<sub>4</sub> could be oxidized to nitrite under iron reducing anaerobic conditions. It might be expected that the same thermodynamically feasible reaction could also occur in our iron rich FFTs in the presence of NH<sub>4</sub> source. The detection of key functional genes involved in denitrification pathways (*nirS*, *nosZ*, and *nrfA*) in HCN could suggest the possibility of N<sub>2</sub> gas production through denitrification and anammox. However, unfortunately, the anammox genes was not assessed in this study. In denitrification pathway, some organisms from class alpha, beta and gamma-Proteobacteria, which harboring the targeted denitrification genes (*nirS* and *nosZ*), were detected in all initial, unamended and amended FFTs samples (Table 2.7). The combination of anaerobic nitrification with denitrification, DNRA, and anammox might be occurring in our amended FFT samples; however, further studies are needed to comprehend these processes through identifying the gene copy numbers along with transcriptional analyses. In short, biostimulation of indigenous microbial communities with nutrients aids in bioremediation of petroleum hydrocarbons and the presence of N transformation genes drive N metabolism (Sarkar et al., 2016).

## **2.6 Conclusion**

The current study revealed that the addition of N and P decreased the methanogenesis. However, the N (NH<sub>4</sub>) individually had a positive effect on biostimulation of microorganisms' growth and promoted CH<sub>4</sub> emission. Results suggested that the P supplements might be an effective agent for slowing CH<sub>4</sub> production in the FFT samples. The abundance of syntrophic bacteria and archaea increased after the application of ammonium nitrogen resulting in enhanced methanogenesis in FFT. The role of P in decreasing the methanogenesis is not clear at this time and needs further study. This study also explored the distribution of functional genes (*nifH*, *nirS*,

nosZ, and nrfA) involved in N transformation in the FFT. Methanogenic archaea were found as a key organism harboring nifH in FFT. The results suggest the possibility of CH<sub>4</sub> production coupled to N-cycling. These observations are essential for determining the sustenance of CH<sub>4</sub> production in tailings and its ultimate effect on the partitioning of constituents of concerns from FFTs to cap water in tailings ponds and end pit lakes. Thus, the implications of this study will be helpful in developing management strategies for future EPLs.

## 2.7 References

- Abu Laban, N., Dao, A., Semple, K., & Foght, J. M. (2014). Biodegradation of C7 and C8 isoalkanes under methanogenic conditions. *Environmental Microbiology*, 17 (12), 4898–4915. doi:10.1111/1462-2920.12643
- ARE. (2017). Tailings. Retrieved from <https://www.aer.ca/providing-information/by-topic/tailings>
- Arkell, N., Kuznetsov, P., Kuznetsova, A., Foght, J. M., & Siddique, T. (2015). Microbial metabolism alters pore water chemistry and increases consolidation of oil sands tailings. *Journal of Environment Quality*, 44(1), 145–153. doi:10.2134/jeq2014.04.0164
- Bae, H. S., Morrison, E., Chanton, J.P., & Ogram, A. (2018). Methanogens are major contributors to nitrogen fixation in soils of the Florida Everglades. *Applied and Environmental Microbiology*, 84(7):e02222-17. <https://doi.org/10.1128/AEM.02222-17>.
- Bodelier, P. L. E., & Steenbergh, A. K. (2014). Interactions between methane and the nitrogen cycle in light of climate change. *Current Opinion in Environmental Sustainability*, 9(10): 26–36.
- Boe, K. (2006). Online monitoring and control of the biogas process. PhD. Thesis. Technical University of Denmark.
- Boonsawang, P., Rerngnarong, A., Tongurai, C., & Chairapat, S. (2014). Effect of nitrogen and phosphorus on the performance of acidogenic and methanogenic reactors for treatment of biodiesel wastewater. *Songklanakarin Journal of Science and Technology*, 36(6), 643-649.
- Cumulative Environmental Management Association. (2012b). *End pit lakes guidance document*. (No. 37(12)). Fort McMurray, AB, Canada: CEMA.
- Cheng, L., Ding, C., Li, Q., He, Q., Dai, L.R., & Zhang, H. (2013). DNA-SIP reveals that *Syntrophaceae* play an important role in methanogenic hexadecane degradation. *Plos One*, 8(7), e66784. doi:10.1371/journal.pone.0066784
- Clement, J.C., Shrestha, J., Ehrenfeld, J. G., & Jaffé, P. R. (2005). Ammonium oxidation coupled to dissimilatory reduction of iron under anaerobic conditions in wetland soils. *Soil Biology and Biochemistry*, 37(12), 2323-2328. <https://doi.org/10.1016/j.soilbio.2005.03.027>
- Collins, V. C. E., Foght, J. M., & Siddique, T. (2016). Co-occurrence of methanogenesis and N<sub>2</sub> fixation in oil sands tailings. *Science of the Total Environment*, 565, 306–312. doi:10.1016/j.scitotenv.2016.04.154

- COSIA. (2012). *Technical guide for fluid fine tailings management*. Edmonton, AB: Canadian Oil Sands Innovation Alliance.
- Devi, M. P., Reddy, M. V., Juwarkar, A., Sarma, P. N. & Mohan, S. R. V. (2011). Effect of Co-culture and nutrients supplementation on bioremediation of crude petroleum sludge. *Clean Soil, Air, and Water*, 39 (10), 900–907.
- Dolfing, J., Larter, S.R., & Head, I.M. (2008). Thermodynamic constraints on methanogenic crude oil biodegradation. *ISME Journal*. 2(4), 442–452.
- Dompierre, K. A., Lindsay, M. B. J., Cruz-Hernández, P., & Halferdahl, G. M. (2016). Initial geochemical characteristics of fluid fine tailings in an oil sands end pit lake. *Science of the Total Environment*, 556, 157-177
- Edwards, B. R., Reddy, C. M., Camilli, R., Carmichael, C. A., Longnecker, K., & Van Mooy, B. A. S. (2011). Rapid microbial respiration of oil from the Deepwater Horizon spill in offshore surface waters of the Gulf of Mexico. *Environmental Resources Letter*, 6 (3), 035301. doi: 10.1088/1748-9326/6/3/035301
- Elango, V., Urbano, M., Lemelle, K. R., & Pardue, J. H. (2014). Biodegradation of MC252 oil in oil: sand aggregates in a coastal headland beach environment. *Frontiers in Microbiology*, 5(161). doi: 10.3389/fmicb.2014.00161
- Engelbrektson, A., Kunin, V., Wrighton, K. C., Zvenigorodsky, N., Chen, F., & Ochman, H. (2010). Experimental factors affecting PCR-based estimates of microbial species richness and evenness. *The ISME Journal*, 4(5), 642–647.
- Fedorak, P. M., Coy, D. L., Dudas, M. J., Simpson, M. J., Renneberg, J., & MacKinnon, M. D. (2003). Microbially-mediated fugitive gas production from oil sands tailings and increased tailings densification rates. *Journal of Environmental Engineering & Science*, 2, 199–211. doi:10.1139/S03-022
- Foght, J., Aislabie, J., Turner, S., Brown, C.E., Ryburn, J., Saul, D.J., & Lawson, W. (2004). Culturable bacteria in subglacial sediments and ice from two Southern Hemisphere glaciers. *Microbial Ecology*, 47(4), 329–340.
- Fowler, S. J., Dong, X., Sensen, C. W., Suflita, J. M., & Gieg, L. M. (2012). Methanogenic toluene metabolism: community structure and intermediates. *Environmental Microbiology*, 14(3), 754–764. doi:10.1111/j.1462-2920.2011.02631.x

- Franke-Whittle, I. H., Walter, A., Ebner, C., & Insam, H. (2014). Investigation into the effect of high concentrations of volatile fatty acids in anaerobic digestion on methanogenic communities. *Waste management*, 34(11), 2080-9.
- Gray, N. D., Sherry, S., Grant, R.J., Rowan, A.K., Hubert, C.R.J., Callbeck, C.M., ... Larter, S.R., Head, I.M. (2011). The quantitative significance of *Syntrophaceae* and syntrophic partnerships in methanogenic degradation of crude oil alkanes. *Environmental Microbiology*, 13(11): 2957–2975. doi: 10.1111/j.1462-2920.2011.02570.x
- Hester, E. R., Harpenslager, S. F., van Diggelen, J., Lamers, L. L., Jetten, M., Lüke, C., Lückner, S., & Welte, C. U. (2018). Linking Nitrogen Load to the Structure and Function of Wetland Soil and Rhizosphere Microbial Communities. *M Systems*, 3(1), e00214-17.
- Houlihan, R.H., & Hale, C.E. (2011). Alberta mine reclamation and abandonment requirements. Paper presented at the *Sixth International Conference on Mine Closure*, 13-22.
- Kalvelage, T., Lavik, G., Jensen, M. M., Revsbech, N.P., Löscher, C., Schunck, H.,... Kuypers, M. M. M. (2015). Aerobic microbial respiration in oceanic oxygen minimum zones. *Plos One*. 10:e0133526 DOI 10.1371/journal.pone.0133526.
- Khanal, S. K. (2008). *Anaerobic biotechnology for bioenergy production: Principles and applications*. Singapore: Wiley Blackwell, John Wiley & Sons, Inc.
- Kloos, K., Mergel, A., Rösch, C., & Bothe, H. (2001). Denitrification within the genus *Azospirillum* and other associative bacteria. *Australian Journal of Plant Physiology*, 28(9), 991–998.
- Kuypers, M. M. M., Sliemers, A. O., Lavik, G., Schmid, M., Jorgensen, B. B., Kuenen, J. G., ... Jetten, M. S. M. (2003). Anaerobic ammonium oxidation by anammox bacteria in the Black Sea. *Nature*, 422, 608-611. DOI 10.1038/nature01472.
- Leigh, J.A. (2000). Nitrogen fixation in methanogens: the archaeal perspective. *Current Issues in Molecular Biology*, 2(4), 125–131.
- Leilei, X., Baohua, X., Jinchao, L., Hongxia, Z., Guangxuan, H., Oumei, W., & Fanghua, L. (2017). Stimulation of long-term ammonium nitrogen deposition on methanogenesis by Methanocellaceae in a coastal wetland. *Science of the Total Environment*, 595, 337–343.

- Mancipe-Jiménez, D.C., Costa, C., Márquez, M. C. (2017). Methanogenesis inhibition by phosphorus in anaerobic liquid waste treatment. *Liquid Waste Recovery*, 2, 1–8. doi:10.1515/lwr-2017-0001
- McLean, K. M. (1995). High-rate anaerobic digestion: A review. In Kolarik, L.O. and Priestley, A.J. (Ed.), *Modern techniques in water and wastewater treatment* (pp. 133-140). Melbourne. CSIRO.
- Mohamad Shahimin, M.F., Foght, J.M., & Siddique, T. (2016). Preferential methanogenic biodegradation of short-chain n-alkanes by microbial communities from two different oil sands tailings ponds. *Science of the Total Environment*, 553, 250–257
- Mohamad Shahimin, M.F., & Siddique, T. (2017a) .Methanogenic biodegradation of paraffinic solvent hydrocarbons in two different oil sands tailings. *Science of the Total Environment*. 583,115–122
- Mohamad Shahimin, M.F., & Siddique, T. (2017b). Sequential biodegradation of complex naphtha hydrocarbons under methanogenic conditions in two different oil sands tailings. *Environmental Pollution*, 221, 398–406
- Morris, B. E. L., Herbst, F. A., Bastida, F., Seifert, J., von Bergen, M., Richnow, H. H., & Suflita, J. M. (2012). Microbial interactions during residual oil and *n*-fatty acid metabolism by a methanogenic consortium. *Environmental Microbiology Reports*, 4(3), 297–306. doi:10.1111/j.1758-2229.2012.00333.x
- Oren, A. (2014). The family Methanosarcinaceae. In Eugene Rosenberg, Edward F DeLong, Stephen Lory, Erko Stackebrandt & Fabiano Lopes Thompson (Eds.), *The prokaryotes : Other major lineages of bacteria and the archaea* (pp. 259-281) doi:10.1007/978-3-642-38954-2\_408
- Östeberg, T.L., Jonsson, A., & Lundström, U.S. (2006). Accelerated biodegradation of n-alkanes in aqueous solution by the addition of fermented whey. *International Biodeterioration & Biodegradation*, 57(3):190–194
- Petersen, D., Blazewicz, S., Firestone, M., Herman, D., Turetsky, M., & Waldrop, M. (2012). Abundance of microbial genes associated with nitrogen cycling as indices of biogeochemical process rates across a vegetation gradient in Alaska. *Environmental Microbiology*, 4(4):993-1008.

- Prakash, S., Vandenberg, J.A., & Buchak, E. The oil sands pit Lake Model sediment diagenesis module. Paper presented at the Retrieved from <http://mssanz.org.au/modsim2011>
- Ramos-Padrón, E., Bordenave, S., Lin, S., Bhaskar, I.M., Dong, X., Sensen, C.W., Fournier, J., Voordouw, G. & Gieg, L.M. (2011). Carbon and sulfur cycling by microbial communities in a gypsum-treated oil sands tailings pond. *Environmental Science & Technology*, 45(2):439-446.
- Rösch, C., Mergel, A. & Bothe, H. (2002). Biodiversity of denitrifying and dinitrogen-fixing bacteria in an acid forest soil. *Applied and Environmental Microbiology*, 68(8), 3818–3829.
- Sarkar, J., Kazy, S. K., Gupta, A., Dutta, A., Mohapatra, B., Roy, A., Bera, P., Mitra, A., & Sar, P. (2016). Biostimulation of Indigenous Microbial Community for Bioremediation of Petroleum Refinery Sludge. *Frontiers in Microbiology*. 7, 1407. doi: 10.3389/fmicb.2016.01407.
- Sharma, J., & Singh, R. (2001). Effect of nutrients supplementation on anaerobic sludge development and activity for treating distillery effluent. *Bioresource Technology*. 79(2), 203-206.
- Siddique, T., Fedorak, P.M., & Foght, J.M. (2006). Biodegradation of short-chain n-alkanes in oil sands tailings under methanogenic conditions, *Environmental Science and Technology*, 40, 5459-5464.
- Siddique, T., Fedorak, P.M., MacKinnon, M.D., & Foght, J.M. (2007). Metabolism of BTEX and naphtha compounds to methane in oil sands tailings, *Environmental Science and Technology*, 41, 2350-2356.
- Siddique, T., Gupta, R., Fedorak, P. M., MacKinnon, M. D., & Foght, J. M. (2008). A first approximation kinetic model to predict methane generation from an oil sands tailings settling basin. *Chemosphere*, 72(10), 1573–1580. doi:10.1016/j.chemosphere.04.036
- Siddique, T., P. Kuznetsov, A. Kuznetsova, N. Arkell, R. Young, S. Guigard, & J.M. Foght. (2014a). Microbially accelerated consolidation of oil sands tailings. Pathway I: Changes in porewater chemistry. *Frontiers in Microbiology*, 5,106. doi:10.3389/fmicb.2014.00106
- Siddique, T., Kuznetsov, P., Kuznetsova, A., Li, C., Young, R., Arocena, J.M., & Foght, J.M. (2014b). Microbially-accelerated consolidation of oil sands tailings. Pathway II: solid phase biogeochemistry. *Frontiers in Microbiology*, 5,107. doi: 10.3389/fmicb.2014.00107

- Siddique, T., Mohamad Shahimin M.F., Zamir S., Semple, K., Li, C., & Foght, J.M. (2015). Long-term incubation reveals methanogenic biodegradation of C5 and C6 iso-alkanes in oil sands tailings. *Environmental and Science Technology*, *49*, 14732–14739
- Siddique, T., Penner, T., Klassen, J., Nesbo, C., & Foght, J.M. (2012). Microbial communities involved in methane production from hydrocarbons in oil sands tailings, *Environmental and Science Technology*, *46*, 9802-9810.
- Siddique, T., Penner, T., Semple, K., & Foght, J. M. (2011). Anaerobic biodegradation of longerchainn-alkanes coupled to methane production in oil sands tailings. *Environmental Science & Technology*, *45*(13), 5892–5899. Doi: 10.1021/es200649t
- Siles, J. A., Martín, M. A., Chica, A. F., & Martín, A. (2010). Anaerobic co-digestion of glycerol and wastewater derived from biodiesel manufacturing. *Bioresource Technology*, *101*, 6315-6321.
- Smith, E., Thavamani, P., Ramadass, K., Naidu, R., Srivastava, P., & Megharaj, M. (2015). Remediation trials for hydrocarbon-contaminated soils in arid environments: evaluation of bioslurry and biopiling techniques. *International Biodeterioration & Biodegradation*, *101*, 56–65. doi:10.1016/j.ibiod.2015.03.029
- Sreethawong, T., Niyamapa. T., Neramitsuk, H., Rangsunvigitt, P., Leethochawalit, M., & Chavadej, S. (2010). Hydrogen production from glucose-containing wastewater using an anaerobic sequencing batch reactor: Effects of COD loading rate, nitrogen content, and organic acid composition. *Chemical Engineering Journal*, *160*, 322-332.
- Stackebrandt, E. (2014). The emended family peptococcaceae and description of the families' desulfitobacteriaceae, desulfotomaculaceae, and thermincolaceae. In Rosenberg, E., DeLong, E.F., Lory, S., Stackebrandt, E., Thompson, F. (Ed.), *The prokaryotes: Firmicutes and Tenericutes* (pp. 285-290) Retrieved from [http://dx.doi.org/ 10.1007/978-3-642-30120-9](http://dx.doi.org/10.1007/978-3-642-30120-9)
- Symons, G. E., & Buswell, A. M. (1933). The methane fermentation of carbohydrates. *Journal of the American Chemical Society*, *55*(5), 2028–2036. Doi.10.1021/ja01332a039
- Tan, B., Rozycki, T., & Foght, J.M. (2014). Draft genome sequences of three *Smithella* spp. obtained from a methanogenic alkane-degrading culture and oil field produced water. *Genome Announc*, *2*(5), [http://dx.doi.org/10.1128/ genomeA.01085-14](http://dx.doi.org/10.1128/genomeA.01085-14) e01085e14.

- Tan, B., Semple, K., & Foght, J.M. (2015). Anaerobic alkane biodegradation by cultures enriched from oil sands tailings ponds involves multiple species capable of fumarate addition. *FEMS Microbiology Ecology*, *91*(5), fiv042. doi: 10.1093/femsec/fiv042.
- Throback I. N., Enwall K., Jarvis A., & Hallin S. (2004). Reassessing PCR primers targeting *nirS*, *nirK* and *nosZ* genes for community surveys of denitrifying bacteria with DGGE. *FEMS Microbiology Ecology*, *49*, 401–417.
- Van Hamme, J. D., & Ward, O. P. (2003). Recent advances in petroleum microbiology. *Microbiology and Molecular Biology Reviews*, *67*(4): 503-549.
- Vidal, G., Carvalho, A., Méndez, R., & Lema, J. M. (2000). Influence of the content in fats and proteins on the anaerobic biodegradability of dairy wastewaters. *Bioresource Technology*, *74*, 231-239
- Volke-Sepúlveda, T., Gutiérrez-Rojas, M., & Favela-Torres, E. (2006). Biodegradation of high concentrations of hexadecane by *Aspergillus Niger* in a solid-state system: Kinetic analysis. *Bioresource Technology*, *94*(14), 1583–1591
- Walworth, J., Pond, A., Snape, I., Rayner, J., Ferguson, S., & Harvey, P. (2007). Nitrogen requirements for maximizing petroleum bioremediation in a sub-Antarctic soil. *Cold Reg. Science Technology*, *48*, 84–91.
- Welsh, A., Chee-Sanford, J., Connor, L., Löffler, F., & Sanford, R. (2014). Refined NrfA phylogeny improves PCR-based *nrfA* gene detection. *Applied and Environmental Microbiology*, *80*(7), 2110-2119. doi:10.1128/AEM.03443-13.
- Xu, R., & Obbard, J.P. (2003). Effect of Nutrient Amendments on Indigenous Hydrocarbon Biodegradation in Oil Contaminated Beach Sediments. *Journal of Environmental Quality*, *32*(4):1234-43.
- Zahr, J. P., Jenkins, B. D., Short, S. M., & Steward, G. F. (2003). Nitrogenase gene diversity and microbial community structure: a cross-system comparison. *Environmental Microbiology*, *5*, 539 –554. <https://doi.org/10.1046/j.1462-2920.2003.00451.x>.

- Zhang, Z., & Lo, I. M. (2015). Biostimulation of petroleum-hydrocarbon- contaminated marine sediment with co-substrate: involved metabolic process and microbial community. *Applied Microbiology and Biotechnology*, *99*, 5683–5696.doi: 10.1007/s00253-015-6420-9
- Zhou, L., Li, K. P., Mbadinga, S. M., Yang, S. Z., Gu, J. D., & Mu, B. Z. (2012). Analyses of n-alkanes degrading community dynamics of a high-temperature methanogenic consortium enriched from production water of a petroleum reservoir by a combination of molecular techniques. *Ecotoxicology*, *21*, 1680–1691. <http://dx.doi.org/10.1007/s10646-012-0949-5>.

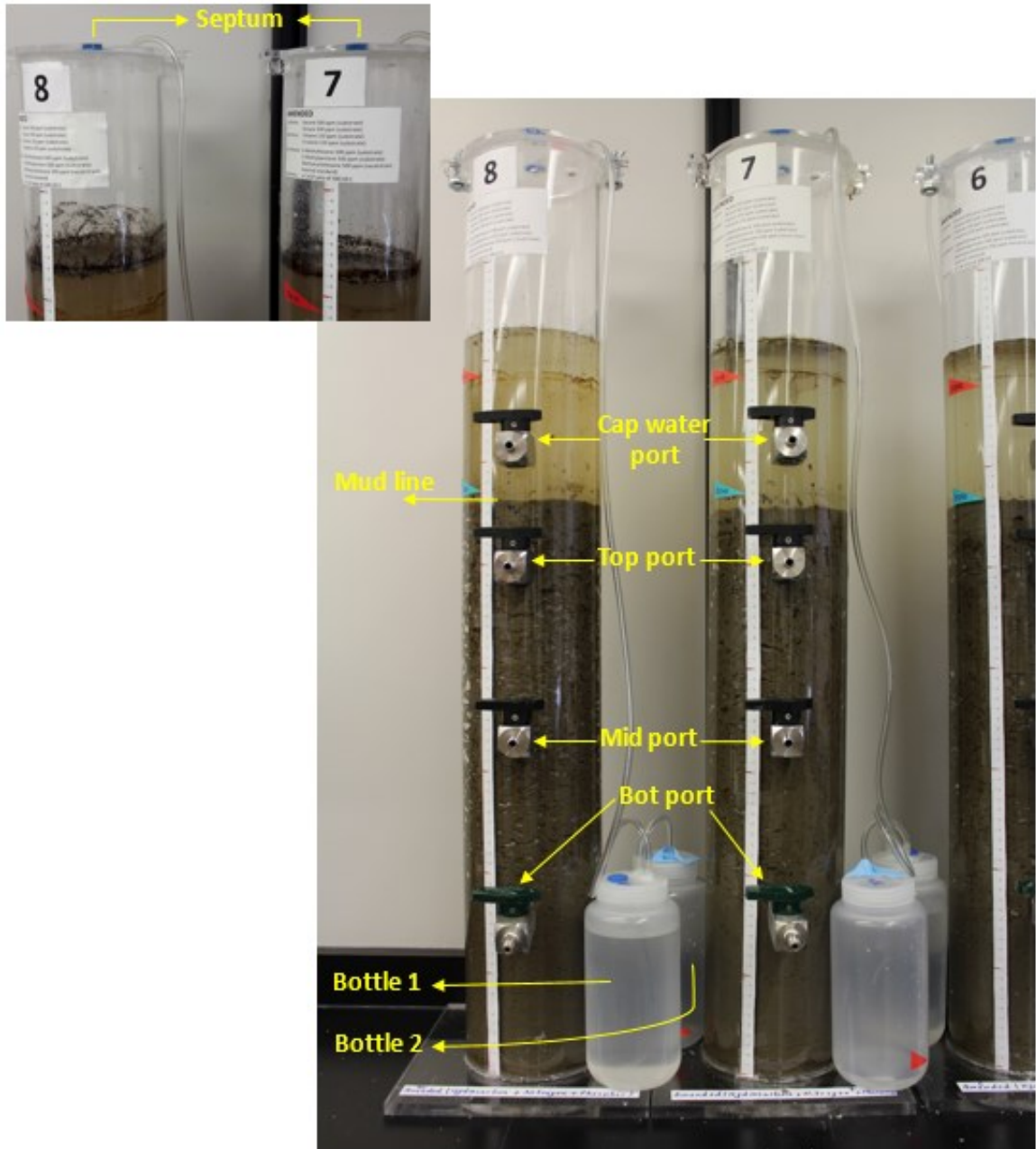


Figure 0-1. Experimental 10L columns used for measuring biogenic gas emission, microbial communities, and the COCs in the capwater, liquid and solid phases of FFT. Septum for measuring CH<sub>4</sub> and CO<sub>2</sub> gas. Four sampling ports for collecting capwater and FFT (cap water, Top, Mid, and Bot ports). Bottles 1 and 2 for monitoring pressure buildup in the columns and reducing the risk of columns ‘explosion. In some parts of second chapter, cap water, Top, Mid, and Bot ports respectively defined as P1, P2, P3, and P4.

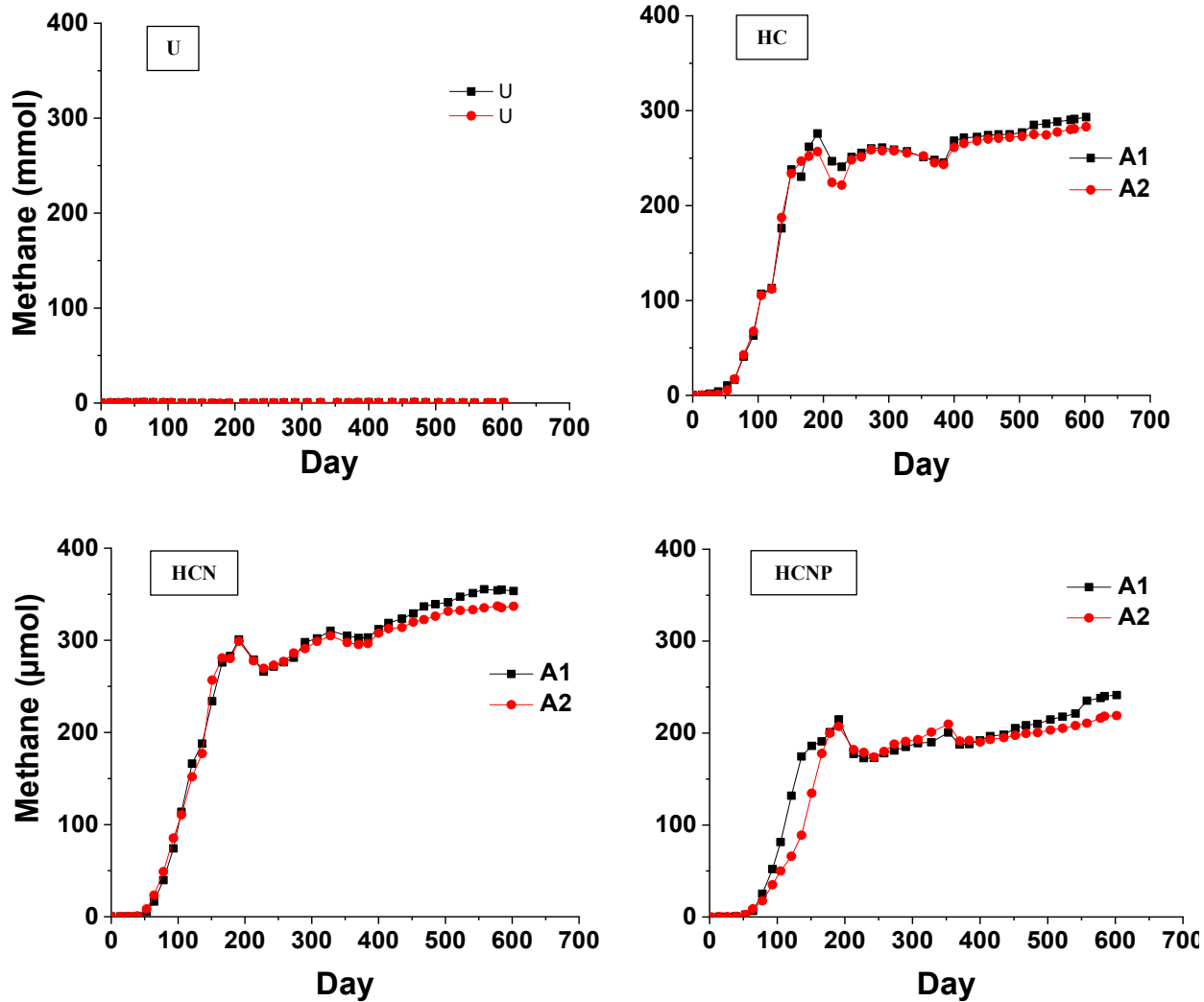
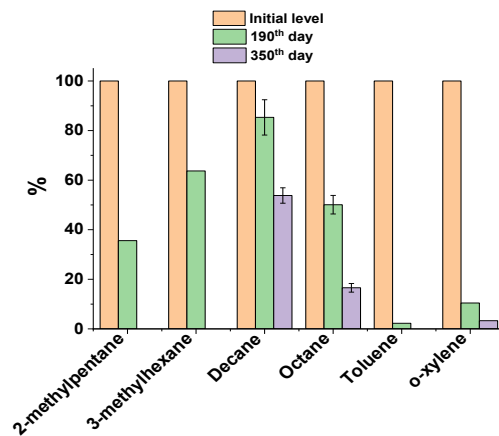
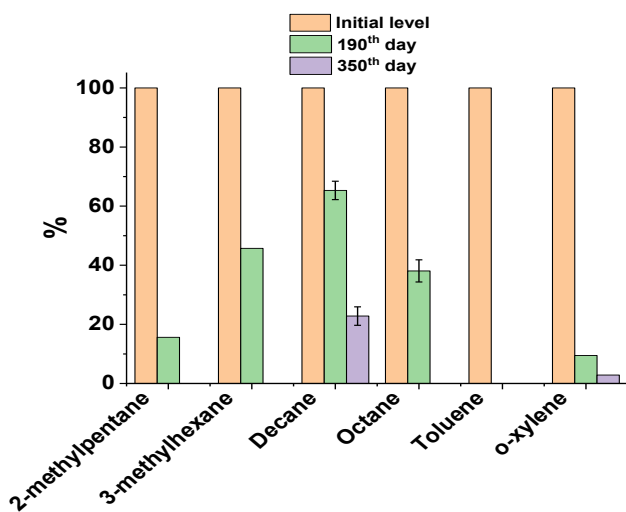


Figure 0-2. Cumulative emitted Methane ( $\text{CH}_4$ ) measured in the headspace of methanogenic unamended and amended columns (2 columns per each treatment); U: unamended columns; HC: columns amended with hydrocarbon mixture; HCN: columns amended with hydrocarbon plus nitrogen; HCNP: columns amended with hydrocarbon plus nitrogen plus phosphorus

HC



HCN



HCNP

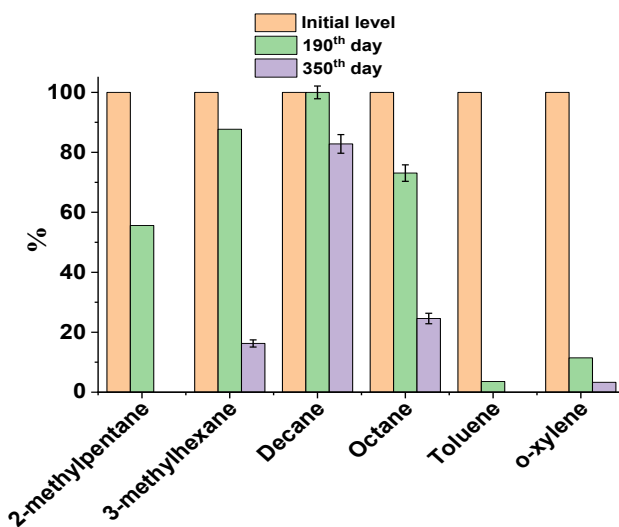


Figure 0-3. Percent degradation of hydrocarbons in initial FFT at day 0 and unamended and amended (HC, HCN, HCNP) FFT at days 190 and 350. Bars represent the mean from analysis of two FFT samples taken from Mid and Bot ports (see Fig 2.1) of each columns ( $\pm 1$  standard deviation).

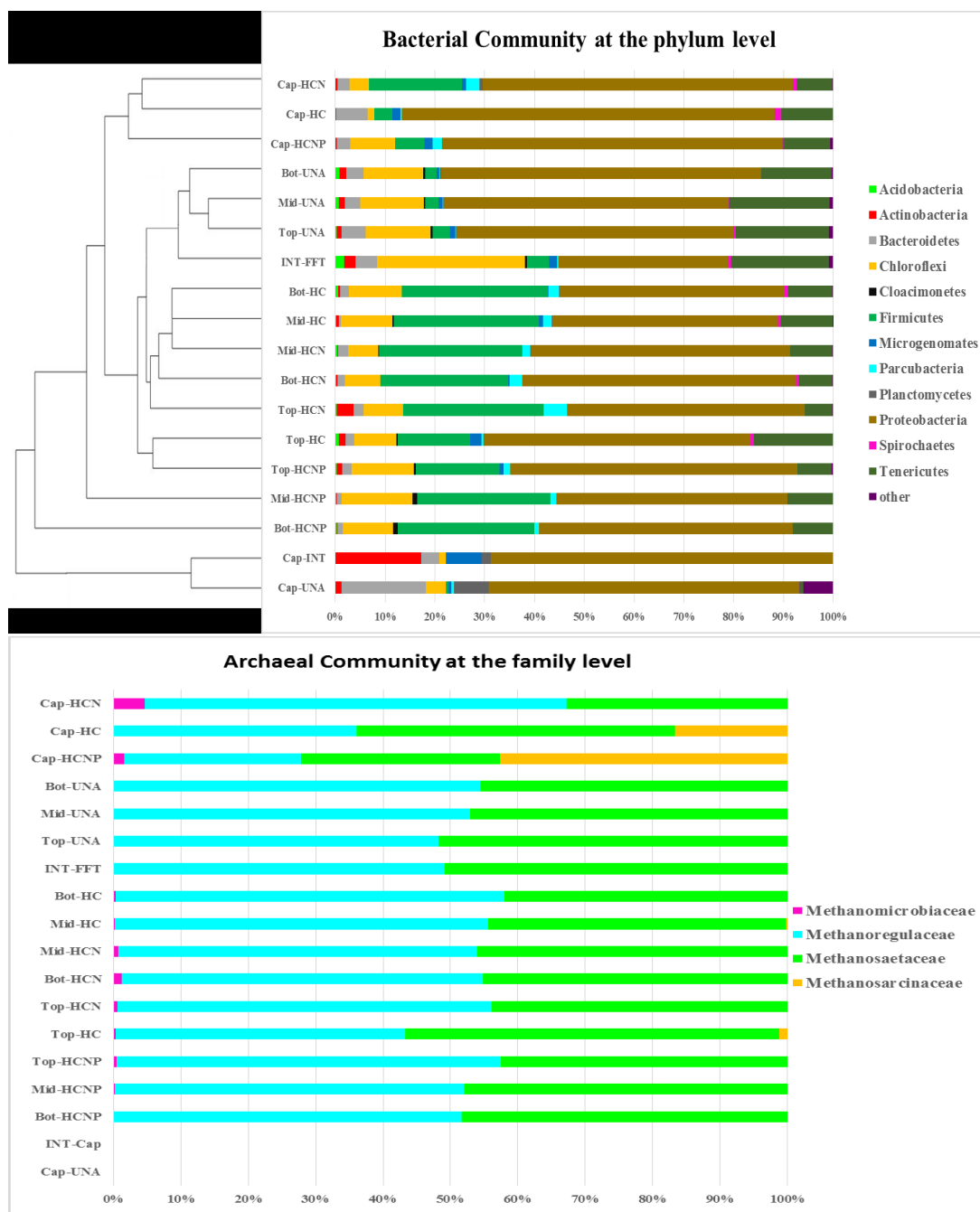
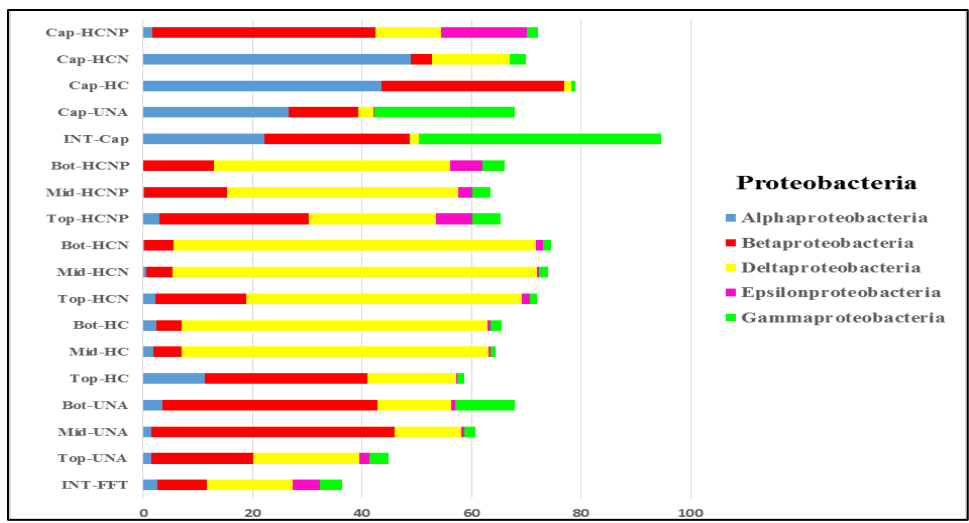
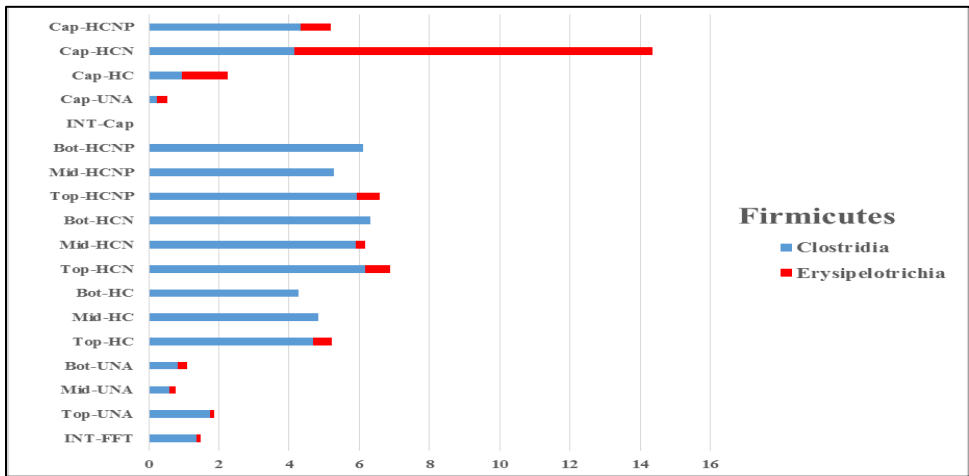


Figure 0-4. Taxonomic composition of the Bacterial (Top figure (T)) and Archaeal (Bottom Figure (B)) community in the FFT and capwater at each treatment, organized at the phylum level. INT: initial FFT at day 0; U: unamended columns; HC: columns amended with hydrocarbon mixture; HCN: columns amended with hydrocarbon plus nitrogen; HCNP: columns amended with hydrocarbon plus nitrogen plus phosphorus. [Cap: capwater; Top, Mid and Bot: respectively, Top, Middle, and Bottom ports in each column, see Fig 2.1].

A



B



C

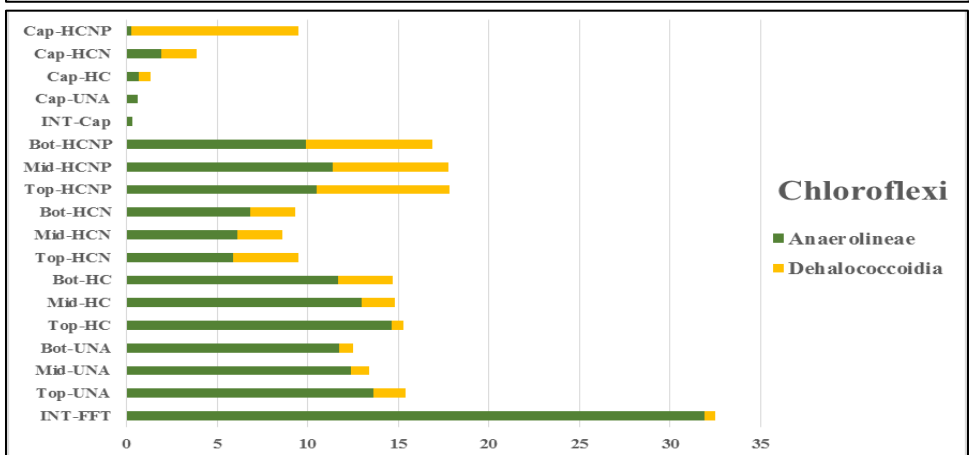


Figure 0-5. Taxonomic composition of the Bacterial community in the FFT and capwater at each treatment, organized at the Class level. INT. initial FFT at day 0; U: unamended columns; HC: columns amended with hydrocarbon mixture; HCN: columns amended with hydrocarbon plus nitrogen; HCNP: columns amended with hydrocarbon plus nitrogen plus phosphorus. [Cap: capwater; Top, Mid and Bot: respectively, Top, Middle, and Bottom ports in each column, see Fig 2.1].

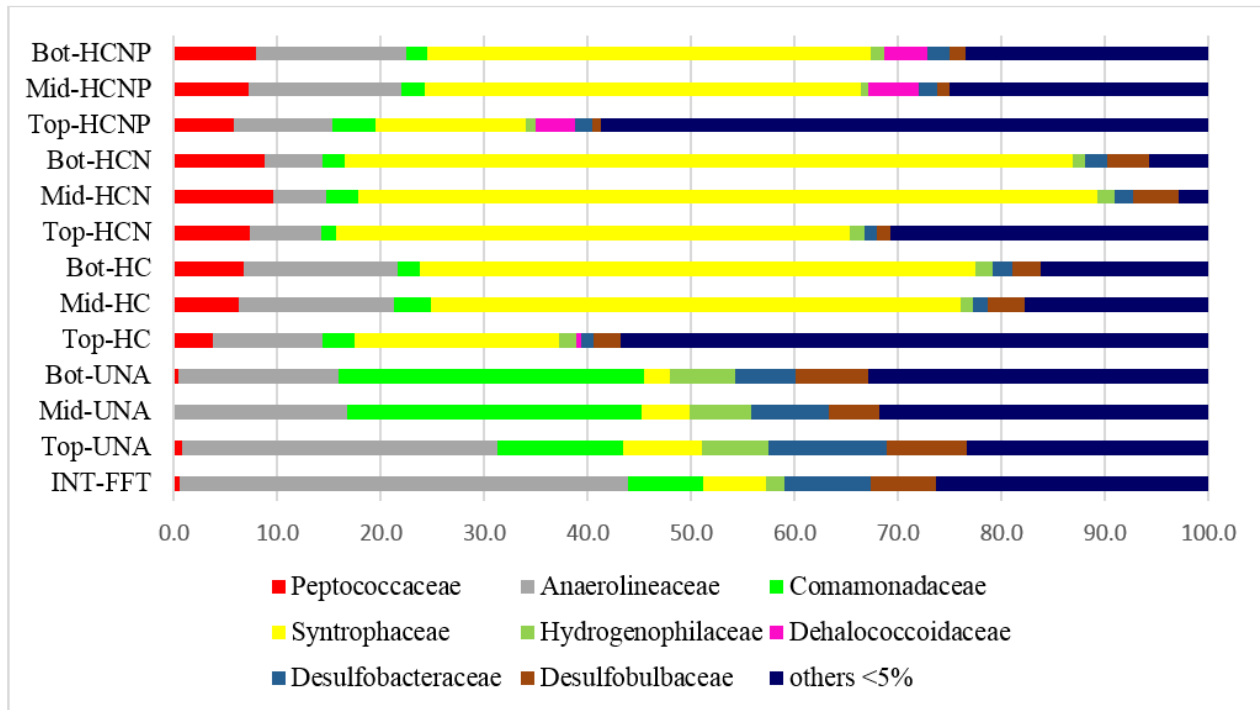


Figure 0-6. Taxonomic composition of the Bacterial community in the FFT at each treatment, organized at the family level. INT. initial FFT at day 0; U: unamended columns; HC: columns amended with hydrocarbon mixture; HCN: columns amended with hydrocarbon plus nitrogen; HCNP: columns amended with hydrocarbon plus nitrogen plus phosphorus. [Top, Mid and Bot: respectively, Top, Middle, and Bottom ports in each column, see Fig 2.1].

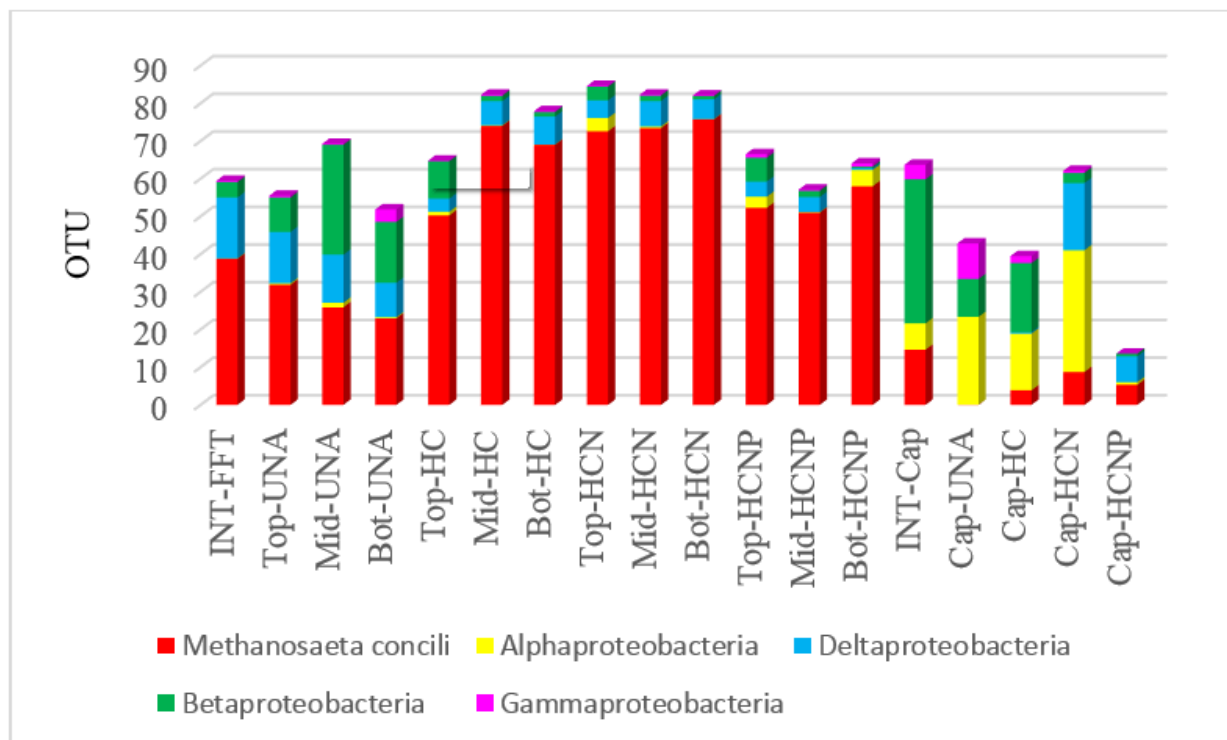


Figure 0-7. Taxonomic distribution of nifH-generated OTUs in the FFT and capwater at each treatment. INT. initial FFT at day 0; U: unamended columns; HC: columns amended with hydrocarbon mixture; HCN: columns amended with hydrocarbon plus nitrogen; HCNP: columns amended with hydrocarbon plus nitrogen plus phosphorus. [Cap: capwater; Top, Mid and Bot: respectively, Top, Middle, and Bottom ports in each column, see Fig 2.1].



Figure 0-8. The release of hydrocarbons from FFT to the capwater in amended column by day 70 (center photo), when the methane production was actively started, and by day 100 (right photo) in compared with day 0 (left photo), the day of experiment set up.

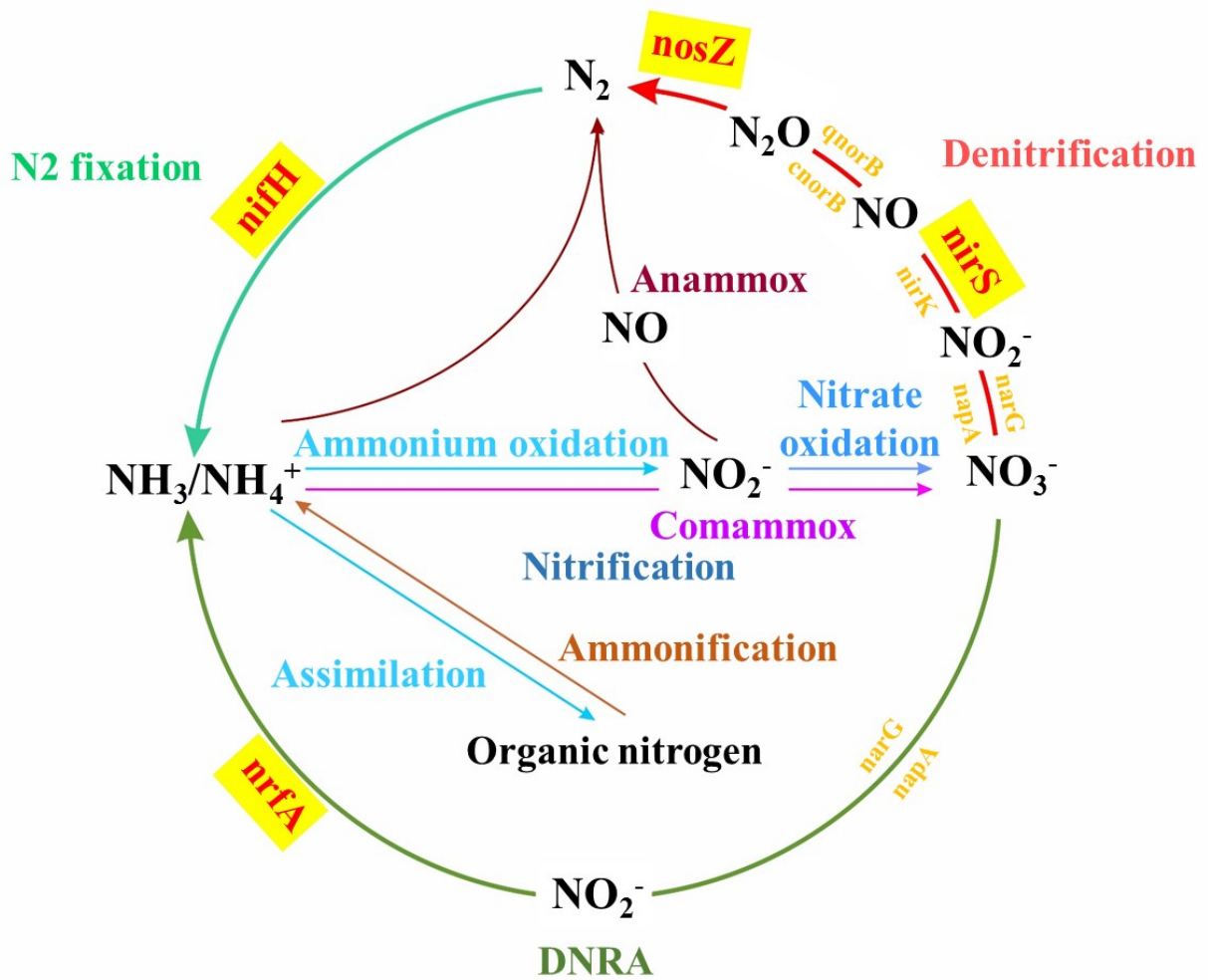


Figure 0-9. Diagram of the anaerobic microbial nitrogen cycle, with the key functional genes studied in the current study highlighted in yellow.

Table 0-1: Chemical characteristics of initial fluid fine tailings used in 10-L column experiment before amendment and incubation. Values are presented as means  $\pm$  standard deviation

Analysis(units); the number of replicates	Value
Texture(wt%), n=1	
Clay <2 $\mu$ m	37.5
Silt 2-50 $\mu$ m	38.5
Fine Sand 50-500 $\mu$ m	24
Bulk pH; n=3	7.57 $\pm$ 0.02
EC(ms/cm); n=3	1.96 $\pm$ 0.01
Eh (mV); n=3	-86.66 $\pm$ 2.89
Soluble Cations (mg L <sup>-1</sup> porewater)	
Ca <sup>2+</sup> ; n=3	17.99 $\pm$ 1.87
Mg <sup>2+</sup> ; n=3	11.13 $\pm$ 0.13
K <sup>+</sup> ; n=3	21.54 $\pm$ 1.39
Na <sup>+</sup> ; n=3	834.49 $\pm$ 42.67
Soluble Anions (mg L <sup>-1</sup> porewater)	
SO <sub>4</sub> <sup>2-</sup> ; n=2	37 $\pm$ 1.23
HCO <sub>3</sub> <sup>-</sup> ; n=2	1369.56 $\pm$ 37.28
CO <sub>3</sub> <sup>2-</sup> ; n=2	114.81 $\pm$ 15.23
PO <sub>4</sub> <sup>3-</sup> ; n=2	BDL*
NO <sub>3</sub> <sup>-</sup> ; n=2	BDL
NH <sub>4</sub> <sup>+</sup> ; n=2	BDL
Cl <sup>-</sup> ; n=2	703.9 $\pm$ 32.82

BDL\*: Below Detection Limit

Table 0-2. Chemical characteristics of initially collected water samples from BML and BCR before capping the 10-L column experiment. Values are presented as means± standard deviation

Analysis(units); the number of replicates	Value
Bulk pH; n=3	7.24±0.03
EC(ms/cm); n=3	1.23±0.01
Eh (mV); n=3	200.67±5.51
Soluble Cations (mg L <sup>-1</sup> porewater)	
Ca <sup>2+</sup> ; n=3	21.88±1.20
Mg <sup>2+</sup> ; n=3	13.34±0.02
K <sup>+</sup> ; n=3	7.80±0.18
Na <sup>+</sup> ; n=3	363.61±23.31
Soluble Anions (mg L <sup>-1</sup> porewater)	
SO <sub>4</sub> <sup>2-</sup> ; n=2	59.7±3.61
HCO <sub>3</sub> <sup>-</sup> ; n=2	455.51±12.21
CO <sub>3</sub> <sup>2-</sup> ; n=2	42.27±6.24
PO <sub>4</sub> <sup>3-</sup> ; n=2	BDL*
NO <sub>3</sub> <sup>-</sup> ; n=2	BDL
NH <sub>4</sub> <sup>+</sup> ; n=2	BDL
Cl <sup>-</sup> ; n=2	232.41±18.32

BDL\*: Below Detection Limit

Table 0-3. Primers used in PCR analysis

Gene target	Primer, sequence (5'-3')	Reference
16S rRNA	926F, 5'-AAACTYAAAKGAATTGRCGG -3' 1392R, 5'- ACGGGCGGTGTGTRC -3'	Engelbrektson et al., 2010
NirS	cd3aF, 5'-GT(C/G) AAC GT(C/G) AAG GA(A/G) AC(C/G) GG-3' R3cd, 5'- GA(C/G) TTC GG(A/G) TG(C/G) GTC TTG A-3'	Petersen et al., 2012
NifH	NifHF, 5'AAAGGYGGWATCGGYAARTCCACCAC-3' NifH-R, 5'TTGTTSGCSGCRTACATSGCCATCAT-3'	Rösch et al., 2002
NrfA	nrfAF2aw, 5'- CARTGYCAYGTBGARTA-3' nrfAR1, 5'- TWNGGCATRTGRCARTC-3'	Welsh et al., 2014
NosZ	nosZ-F, 5'- CGYTGTTTCMTCGACAGCCAG-3' nosZ1622R, 5'- CGSACCTTSTTGCCSTYGCG-3'	Kloos <i>et al.</i> , 2001; Throback <i>et al.</i> , 2004

Table 0-4. PCR reaction conditions for various gene

Gene target	Step	Temperature(°C)	Time	
<b>16S rRNA</b>	initialization	95	15min*	
	35Cycles	Denaturation	95	30sec**
		Annealing	54	45sec
		Elongation	72	30sec
	Final elongation	72	5min	
<b>Nirs</b>	initialization	95	5min	
	35Cycles	Denaturation	95	30sec
		Annealing	59	45sec
		Elongation	72	30sec
	Final elongation	72	5min	
<b>NifH</b>	initialization	95	5min	
	35Cycles	Denaturation	95	30sec
		Annealing	57	30sec
		Elongation	72	30sec
	Final elongation	72	5min	
<b>NosZ</b>	initialization	95	3min	
	35Cycles	Denaturation	95	30sec
		Annealing	58	1min
		Elongation	72	1min
	Final elongation	72	5min	
<b>NrfA</b>	initialization	95	3min	
	35Cycles	Denaturation	95	30sec
		Annealing	49	1min
		Elongation	72	1min
	Final elongation	72	5min	

\*min=minute, \*\*Sec=second

Table 0-5. Archaeal community in the FFT and capwater at each treatment, organized at the family level.

<b>Methanogens</b>	INT-FFT	Cap-INT	Cap-UNA	Top-UNA	Mid-UNA	Bot-UNA	Cap-HC	Top-HC	Mid-HC	Bot-HC	Cap-HCN	Top-HCN	Mid-HCN	Bot-HCN	Cap-HCNP	Top-HCNP	Mid-HCNP	Bot-HCNP
<b>Family</b>																		
Methanomicrobiaceae	0.0	0.0	0.0	0.0	0.0	0.0	0.0	1.0	1.0	2.0	3.0	3.0	6.0	11	1.0	1.0	1.0	0.0
Methanoregulaceae	114	0.0	0.0	110	142	124	26	140	313	394	40	275	444	495	16	111	243	257
Methanosactaceae	118	0.0	0.0	118	126	104	34	181	250	287	21	218	384	416	18	83	223	241
Methanosarcinaceae	0.0	0.0	0.0	0.0	0.0	0.0	12	4.0	1.0	0.0	0.0	0.0	0.0	0.0	26	0.0	0	0.0

Table 0-6. Distribution of the 27 most abundant genera (%) in the FFT and capwater at each treatment.

Taxon	INT-FFT	Cap-INT	Cap-UNA	Top-UNA	Mid-UNA	Bot-UNA	Cap-HC	Top-HC	Mid-HC	Bot-HC	Cap-HCN	Top-HCN	Mid-HCN	Bot-HCN	Cap-HCNP	Top-HCNP	Mid-HCNP	Bot-HCNP
<b>Methanogens</b>																		
Methanolinea	6.61	0.0	0.0	7.8	10.2	6.0	11.5	3.6	6.9	8.5	26.1	10.2	10.5	5.4	19.0	12.0	12.5	0.0
Methanoregula	40.5	0.0	0.0	52.7	46.0	55.7	14.7	32.5	55.0	45.3	35.4	45.0	47.6	45.4	16.2	39.0	47.6	50.0
Methanosacta	48.7	0.0	0.0	34.0	38.5	35.8	29.5	46.7	37.5	45.2	32.3	43.9	41.0	47.8	46.0	47.3	39.5	50.0
<b>Hydrocarbon degradation-associated bacteria</b>																		
Smithella	4.2	0.0	0.5	8.8	7.3	6.5	3.5	26.0	61.3	62.5	7.2	55.2	73.9	74.3	2.7	16.7	43.1	47.3
Syntrophus	2.7	0.0	0.0	1.9	2.3	0.9	0.7	1.6	4.8	4.4	2.0	4.7	5.6	5.7	0.2	1.9	4.1	4.5
Pelotomaculum	0.5	0.0	0.0	0.5	0.0	0.5	0.0	0.2	0.0	0.3	0.0	0.0	0.0	0.0	0.0	0.0	0.0	0.0
Extensimonas	0.0	0.0	1.7	0.0	0.3	0.0	0.0	0.0	0.0	0.3	0.3	0.0	0.0	0.0	23.3	12.2	6.0	4.8
Leptolinea	20.3	0.0	0.0	1.93	8.3	3.2	0.1	2.1	6.2	4.8	0.3	1.6	3.0	2.7	0.0	1.5	4.25	3.8
Pelolinea	1.9	0.4	0.6	2.4	1.3	0.9	0.0	0.5	0.92	1.0	0.7	0.51	0.4	0.0	0.0	0.4	2.0	2.3
<b>Iron Cycling Bacteria</b>																		
Albidiferax*	9.0	3.4	9.6	10.6	30.8	29.1	7.9	6.2	1.9	1.6	4.9	15.1	1.9	3.0	2.1	15.3	13.7	12.82
Thiobacillus**	3.3	0.0	0.0	9.0	13.4	29.5	0.0	1.9	1.4	1.9	0.0	4.2	1.9	1.3	0.8	1.5	5.9	5.2
<b>Nitrogen cycling Bacteria</b>																		
Defluviimonas	1.9	0.0	3.6	1.1	2.0	5.3	14.8	3.0	1.0	1.0	11.7	1.0	0.4	0.0	0.0	0.8	0.1	0.0
Pseudomonas	0.9	8.5	0.1	0.8	0.3	0.8	0.0	0.8	0.4	0.3	0.0	0.0	0.7	0.3	0.2	1.5	0.8	0.67
Magnetospirillum***	0.0	0.0	2.3	0.0	0.0	0.0	32.9	11.0	1.0	0.0	35.5	0.0	0.0	0.0	0.8	0.0	0.0	0.0
Dechloromonas***	0.1	0.0	0.0	0.0	0.0	0.0	0.0	0.0	0.0	0.0	0.0	0.0	0.0	0.0	0.0	0.2	1.5	1.34
Thauera***	0.2	0.0	0.0	0.0	0.3	0.5	0.2	0.0	0.7	0.0	0.0	0.0	0.0	0.0	0.0	0.8	1.5	1.21
Azospirillum	0.0	0.0	3.7	0.0	0.0	0.0	0.1	0.0	0.0	0.0	17.6	1.0	0.0	0.0	0.0	0.0	0.0	0.0
<b>Sulfur cycling Bacteria</b>																		
Desulfosporosinus	0.0	0.0	0.0	0.0	0.0	0.0	0.3	1.7	1.9	3.5	4.2	5.2	3.4	6.0	1.0	4.6	3.0	3.3
Desulfatirhabdium	0.1	0.0	0.0	0.0	0.5	0.0	0.5	0.1	0.2	0.0	0.0	0.0	0.0	0.0	0.0	0.0	0.4	0.3
Desulfurivibrio	0.5	0.5	0.0	0.0	0.9	0.8	2.7	0.1	0.2	0.0	0.3	0.7	1.9	0.8	0.0	0.4	0.0	0.0
Desulfomicrobium	0.7	0.0	0.0	0.0	0.0	0.3	0.5	0.1	0.7	0.0	0.0	0.0	0.0	0.0	0.3	7.0	0.0	0.0
Sulfurovum	14.6	0.0	0.3	4.0	2.0	1.4	0.0	0.2	0.5	0.6	0.0	2.1	0.4	1.3	5.6	10.3	3.9	4.2
Desulfuromonas	0.3	0.0	0.0	0.0	0.0	1.0	0.7	0.0	0.7	0.0	0.0	0.0	1.6	0.0	0.0	1.0	0.4	0.26
Desulfocapsa	9.4	0.0	0.0	6.9	7.1	4.6	0.1	1.9	2.9	1.9	0.0	1.6	2.6	1.7	0.2	4.2	3.1	2.8
Desulfobulbus	1.4	0.0	0.0	2.1	3.0	2.7	0.0	0.7	1.4	0.6	0.0	0.5	0.7	0.3	0.0	1.5	2.0	1.8
<b>Organohalid respiring Bacteria</b>																		
Dehalococcoides	0.0	0	0	0	0	0	0.1	0.47	0	0	0.3	0	0	0	11.9	1.91	0.51	0.48
<b>Methanotroph Bacteria</b>																		
Methylocaldum	0.9	0	0	0.3	0.8	0.2	0	0	0.5	0	0.3	0	0	0	0	0.38	1.96	2.23

Table 0-7. Composition of nifH, nrfA, nirS, and nosZ transcripts in the FFT and capwater of unamended and amended samples. Symbols + and - represents presence and absence of each gene in each sample, respectively.

Key Functional Genes	Coverage	Identity	nifH																			
			INT-FFT	Cap-INT	Cap-UNA	Top-UNA	Mid-UNA	Bot-UNA	Cap-HC	Top-HC	Mid-HC	Bot-HC	Cap-HCN	Top-HCN	Mid-HCN	Bot-HCN	Cap-HCNP	Top-HCNP	Mid-HCNP	Bot-HCNP		
<b>Euryarchaeota</b>	99	100	+	-	-	+	+	+	+	+	+	+	+	+	+	+	+	+	+	+		
Methanosaeta concili																						
<b>Alphaproteobacteria</b>	99	98	-	+	+	-	-	-	+	+	-	-	+	+	-	-	-	-	-	-		
Methylocystis	99	98																				
Rhodobacter	99	98																				
Rhodovulum	99	98																				
Nitrospirillum	99	98																				
amazonense	99	98																				
Bradyrhizobium	99	98																				
Methylocystis	99	98																				
Niveispirillum	99	98																				
Defluviimonas	99	98																				
Magnetospirillum	99	98																				
<b>Betaproteobacteria</b>	99	100	+	+	+	+	+	+	+	+	+	+	+	+	+	+	+	+	+	+	+	
Cupriavidus	99	100																				
Curvibacter	99	100																				
Variovorax	99	100																				
Paraburkholderia nodosa	99	100																				
Burkholderia	99	100																				
Paraburkholderia mimosarum	99	100																				
Pelomonas	99	100																				
Rhodoferax Fermentans	99	100																				
Hydrogenophaga taeniospiralisi	99	99																				
Methyloversatilis	99	99																				
Methyloversatilis	99	99																				
Polaromonas naphthalenivorans	99	99																				
Leptothrix cholodnii	99	100																				
Paraburkholderia phymatum	99	100																				
Pelomonas saccharophila	99	100																				
Variovorax taiwanesis	99	100																				
<b>Deltaproteobacteria</b>	99	98	+	-	-	+	+	+	-	+	+	+	+	+	+	+	+	+	+	+	+	
Desulfobulbus	99	98																				
Geobacter	99	98																				
Geobacter thiogenes	99	100																				
Geobacter lovleyi	99	100																				

<b>nrfA</b>																			
<b>Betaproteobacteria</b>	99	86	+	+	+	+	+	+	+	+	+	+	+	+	+	+	+	+	+
Propionivibrio	99	86																	
<b>Deltaproteobacteria</b>	99	92	-	+	-	+	+	+	+	+	+	+	+	+	+	+	+	+	+
Desulfovibrio	99	92			99	98													
Desulfocurvus	99	92																	
Desulfobacula	99	92																	
<b>nirS</b>																			
<b>Betaproteobacteria</b>	99	100	+	-	+	+	+	+	+	+	+	+	+	+	+	+	+	+	+
Thauera	99	100																	
Dechloromonas	99	98																	
<b>Gammaproteobacteria</b>	99	100	+	-	+	+	+	+	+	+	+	+	+	+	+	+	+	+	+
Pseudomonas	99	100																	
<b>nosZ</b>																			
<b>Alphaproteobacteria</b>	99	100	+	+	+	+	+	+	+	+	+	+	+	+	+	+	+	+	+
Porphyrobacter	99	100																	
Caulobacter	99	100																	
Erythrobacter	99	100																	
Defluviimonas alba	99	100																	
Magnetospirillum	99	100																	
<b>Betaproteobacteria</b>	99	100	+	+	+	+	+	+	+	+	+	+	+	+	+	+	+	+	+
Thauera	99	100																	
Acidovorax	99	100																	
Polaromonas	99	100																	
Alicyclophilus	99	100																	
Caenimonas	99	100																	
<b>Gammaproteobacteria</b>	99	100	+	-	-	+	+	+	+	+	+	+	-	+	+	+	+	+	+
Pseudomonas	99	100																	

### 3 Nutrients' impact on the methanogenesis in oil sand tailings under End Pit Lake scenario: II. Flux of constituents of concern

#### 3.1 Abstract

Partitioning of inorganic constituents (including ions, and trace metals) from underlying FFT to overlying cap water is a potential concern for the quality and sustainability of end pit lakes (EPLs) in Alberta, Canada. Active methanogenesis altered the composition of fluid fine tailings (FFTs) and transformed FFT minerals. This process enhanced FFT dewatering and porewater water migration to the surface of EPL. However, the factors that affect methanogenesis and biogeochemical transformation of FFT minerals affecting mobilization or immobilization of inorganic constituents have not been studied before. In previous chapter, we showed that amending the FFT with nutrients (nitrogen, N and phosphorus, P) and a mixture of easily to slowly degradable hydrocarbons affected methanogenesis: N stimulated whereas N plus P decreased methanogenesis. Here, we show that microorganisms indigenous to FFT stimulated with hydrocarbons and N (HCN) significantly changed the porewater chemistry, and enhanced FFT mineral transformation and the flux of inorganic constituents from FFT to cap water. However, the rate of these processes decreased in the FFT amended with hydrocarbons, nitrogen, and phosphorus (HCNP). Microbial metabolisms in FFT amended with HCN produced significantly higher methane ( $\text{CH}_4$ ) and carbon dioxide ( $\text{CO}_2$ ) than FFT amended with hydrocarbons (HC) or HCNP. Dissolution of biogenic  $\text{CO}_2$  lowered the pH of all the amended FFT (HC, HCN, and HCNP) to pH 6.7 versus unamended FFT (pH 7.6). Decreased pH in all the amended FFTs dissolved carbonate minerals which lead to the release of cations such as calcium ( $\text{Ca}^{2+}$ ), magnesium ( $\text{Mg}^{2+}$ ), and potassium ( $\text{K}^+$ ), and bicarbonate ( $\text{HCO}_3^-$ ) in porewater that were ultimately transported to cap water during porewater expression. The higher concentrations of ions increased the ionic strength of porewater in all amended columns. The transformation of  $\text{Fe}^{\text{III}}$  to amorphous  $\text{Fe}^{\text{II}}$  minerals during the methanogenic metabolisms was also observed in all amended FFTs. Concentrations of total strontium (Sr) and barium (Ba) increased in the porewater and cap water of all amended columns (HC, HCN, HCNP). However, the release of total As, Sb, Mo, V, and Cr to the pore water was decreased under active methanogenesis in all amended columns. Also, all amended columns particularly HCN achieved a higher removal of NAs in pore and capwater compared to unamended columns under active methanogenesis. Our findings suggest that unrecovered hydrocarbons and the presence of ammonium-N in FFT stimulate

methanogenesis in EPL leading to the release and partitioning of ions and Sr and Ba from porewater to cap water and the decrease of NAs concentrations in pore water and cap water in EPL. These results provide critical information for the flux of constituents of concern for the sustainable management of EPLs.

### **3.2 Introduction**

End pit lakes (EPLs) are open-pit mines that are located around the world. In various mining operations such as metals and coal mining, EPLs have been defined as part of their mine closure plans. Based on the experience of the surface mining of these industries, the EPLs have also been developed for the closure of oil sands mine pits (CEMA, 2012a). The oil sands reserves in the northern Alberta are the third largest oil reserves in the world, which produce 1.9 million barrels of bitumen per day. Oil sands ore is comprised of sand, clay, water, and a type of heavy oil called bitumen. Before upgrading the bitumen into the crude oil and other petroleum products, bitumen must be extracted from the oil sands ore. Two methods, surface mining and in situ drilling are employed for the extraction of bitumen. When deposited at shallow depths (<70 m) from the surface, the oil sands are excavated through surface mining. Bitumen from deeper oil sands ore is extracted through in-situ techniques (Alberta Government, 2015) described in Chapter 1 and 2. Athabasca oil sands region (AOSR), north of Fort McMurray, Alberta is a largest area of the surface mining operation in Canada. Enormous volumes of Fluid Fine Tailings (FFT) (currently >1billion m<sup>3</sup>) (<http://osip.alberta.ca/map/>) are produced during bitumen extraction from surface-mined oil sands ores and it is expected that this volume will increase with the development of new and future mining operations (Siddique et al., 2018). Tailings are byproducts of surface mining extraction containing waste rock (sand and clay), oil sands process affected water (OSPW), residual bitumen and naphtha and elevated concentrations of salts (Allen, 2008; Kavanagh et al., 2011). Alberta Energy Regulator (AER) regulates the management of these tailings (<https://www.aer.ca/providing-information/by-topic/tailings/tailings-management>).

The development of EPLs is one of closure plan, which has been developed by all surface mining operators for the management of tailings (Kabwe et al., 2018). An oil sands EPL is an engineered water body containing FFT covered by an overlying fresh water and OSPW which is projected to develop into a self-sustaining aquatic ecosystem (CEMA 2012b). EPLs must meet the water quality in short, medium and long term to support fish populations, wildlife, and migratory or seasonal waterfowl and could be used for human use following the recreational water quality

guidelines (CEMA 2012b; Kabwe et al., 2018). EPLs are proposed as reclamation strategy that can act as a permanent containment for keeping mature fine tailings or fluid fine tailings under a fresh water cap. Base mine lake (BML) is a first EPL at a surface mining project in north of Fort McMurray and the construction of more than thirty EPLs have been proposed in AOSR. This demonstration has been approved for many oils sands mine, but there are several issues with EPLs that must be resolved to reach a successful use of EPLs as a reclamation strategy (Westcott, 2007). This chapter concentrate on the surface water quality issue affected by the underlying FFT.

The FFT solids composition varies with the properties of the original oil sands ore (Osacky et al., 2013); however, the quartz and clay minerals generally comprise the solids (Kasperski and Mikula, 2011). The kaolinite and illite with small portions of chlorite and smectite were determined to be predominant clay minerals in FFT (Kasperski and Mikula, 2011). In a study on the assessment of geochemical properties of FFT in BML, the information about FFT mineralogy and the characteristics of FFT porewater was provided by Dompierre et al. (2016). The collected information about the FFT porewater from BML were comparable with collected OSPW from other tailings impoundments (Allen, 2008; Stasik and Wendt-Potthoff, 2014). The major dissolved ions determined in the porewater were sodium (Na), chloride (Cl), calcium (Ca), magnesium (Mg), potassium (K), and ammonia (NH<sub>3</sub>). The near neutral pH and anoxic conditions were also observed in the FFT. The location and the depth of sampling, showed the variation in the measured parameters. It also showed the potential of biogeochemical reactions in BML (Dompierre et al., 2016). The decreased pH in the porewater below the FFT water interface was referred to the dissolution of biogenic gas such as carbon dioxide (CO<sub>2</sub>) produced during methanogenesis (Siddique et al., 2006, 2007, 2011) resulted from biodegradation of residual bitumen and naphtha presented in FFT (Fedorak et al., 2003; Siddique et al., 2006, 2007, 2011; Stasik et al., 2014; Stasik and Wendt-Potthoff, 2014). In a laboratory experiment conducted by Siddique et al. (2014a), they reported that decreased pH in the porewater of FFT increased the carbonate mineral dissolution and consequently increased the concentrations of Ca and Mg in the pore water. The higher concentration of ions increases the ionic strength of pore water and in turn reduces the surface charge potential of the clay particles and in turn decreases the thickness of diffuse double layer associated with clay particles that induce the stimulation of FFT settlement (Siddique et al., 2014a). Previous studies reported the evidences of microbial reduction of iron (Fe) and sulfate (SO<sub>4</sub>) near the FFT water interface in BML (Dompierre et al., 2016; Ramos-Padrón et al., 2011; Stasik et al.,

2014; Stasik and Wendt-Potthoff, 2014). The formation of iron sulfide has also been reported in the FFT (Chen et al., 2013; Siddique et al., 2014; Stasik et al., 2014) which Siddique et al., (2014b) suggested these iron sulfide minerals could mask the electronegative charge of clay surfaces in stimulated FFT and therefore enhance the FFT settlement. The increased settlement enhanced FFT dewatering which could generate vertical pore water flux that could contribute to the transport of COCs to the capwater (Dompiere et al., 2016). Besides inorganic constituents, the toxicity of naphthenic acid (as an organic constituent) in BML surface water was reported by White (2017). In a laboratory study was conducted by Clothier and Gieg (2016), a variety of NAs were biodegraded under anaerobic conditions in the presence of nitrate, sulfate, iron and methane as electron acceptors. However, the studies about anaerobic biodegradation of NAs are still very limited and there are concerns about the production of more toxic mobile NAs in anaerobic conditions through incomplete oxidation and/or co-metabolism of hydrocarbons (Foght et al., 2017). Therefore, active biogeochemical reactions occurring in BML may influence FFT settling and porewater release and in turn influence the movement of organic and inorganic contaminants from the underlying FFT to overlying cap water. Recent studies showed that the active methanogenesis in the FFT produce biogenic gas including CH<sub>4</sub> and CO<sub>2</sub> (Penner and Foght, 2010; Siddique et al., 2006, 2007, 2011). Through ebullition, the gas bubble formation, the bubbles can migrate through the FFT until are released to overlying cap water (Scandella et al., 2011). Therefore, an additional form of the transport of constituents of concerns over the FFT water interface may occur. Therefore, as described above, methanogenesis can be linked to water quality of EPLs. Every factor which affects methanogenic activities can affect partitioning of COCs as well. In previous chapter, we investigated the influence of nutrients (N and P) on methanogenesis and in this chapter, the porewater and solid phase sample as well as cap water samples retrieved during 600 days incubation were analyzed to understand the contaminant release and partitioning between FFT and cap water by the influence of nutrients on the biogeochemical processes. The results of this study can help oil sands industry predict the performance and environmental sustainability of EPLs.

### **3.3 Materials and methods**

#### **3.3.1 Experimental setup and sampling scheme**

The experiment was conducted using 10 L anaerobic columns prepared as described previously in chapter 2 (Fig.1). Briefly, each column was filled with 7 L FFT (collected from

BML) and capped with 1.4 L water from BML and BCR (1:1 ratio) and sealed with a headspace of helium to maintain anaerobic conditions. A mixture of slow to fast degradable hydrocarbons (*n*-octane, 500ppm; *n*-decane, 500ppm; 2-methylpentane, 500ppm; methylhexane, 500ppm; toluene, 150ppm and *o*-xylene, 150ppm) was used as carbon source in six out of eight established columns. One pair of columns contained FFT amended only with hydrocarbon (HC). In the second and third pairs of columns, FFT was amended with hydrocarbon plus N (HCN) and hydrocarbon plus nitrogen plus P (HCNP), by a C:N ratio of 100:10 and C:N:P ratio of 100:10:1, respectively. The purpose of adding hydrocarbon and nutrients (N and P) was used to stimulate indigenous microbial activities to promote methanogenesis. The last pair of columns contained unamended (U) FFT and represented baseline controls. In this treatment, endogenous carbon, N, and P were the only available carbon and nutrient sources to support microbial activities. The columns were incubated in the dark at room temperature for 600 days. Biweekly monitoring of CH<sub>4</sub> and CO<sub>2</sub> production was performed for each column during incubation period (~600 day). The FFT and Cap water were sampled using syringe from the sampling ports at four sampling times: day 0 (when incubation started after hydrocarbon amendment), day190 (after significant methane was produced in amended columns), day 350 and day 600 (final sampling day). Experimental approach and analytical procedures for determining biogenic gas production, the characterization of microbial communities by 16S rRNA gene and the detection of functional genes (NifH, NirS, NosZ, and NrfA) involved in nitrogen cycling have been described in Chapter 2. In this chapter, the analytical procedures related to in situ pH, soluble cations and anions, carbonate minerals, fractionation of iron and sulfides, total metals concentration, and metals sequential extraction are described.

### 3.3.2 Porewater recovery as cap water and FFT consolidation

To measure the consolidation and porewater recovery during the consolidation, the volumes of capwater and FFT including solids plus porewater plus gas below the mudline (the interface between cap water and FFT) were determined via measuring the height of capwater level above the mudline and the height of the mudline in each column. The measured heights were converted to volumes using column diameter.

Then, water recovery (WR) defined as the volume of capwater above the mudline and calculated as the initial volume of pore water in FFT.

$$WR = (V_{cw}/V_{in}) \times 100 \quad (1)$$

Where, WR is water recovery (%),  $V_{cw}$  is the measured volume of cap water, and  $V_{in}$  is the initial volume of FFT porewater.

The consolidation of FFT defined as the volume of FFT below the mudline and calculated as a percentage of the initial volume of FFT.

$$\text{Consolidation (\%)} = [(V_{in} - V_{FFT})/V_{in}] 100 \quad (2)$$

Where,  $V_{MFT}$  is the measured volume of MFT, and  $V_{in}$  is the initial volume of FFT.

### 3.3.3 Chemical analyses of the Cap water and FFT porewater

The pH of FFT pore water and cap water was determined in situ biweekly during incubation period (600d). The pH meter (Hach H170multi), fitted with an ISFET pH stainless steel micro probe (PHW17-SS), was inserted through side ports at different depths of column to measure pH. The pH was also measured in initial FFT porewater and cap water samples at initial day. To collect the pore water of sampled FFT from various ports of each column, the FFT was centrifuged using a Sorvall RC 5B super speed centrifuge at 5000 g for half an hour. The cap water was directly sampled from the ports located in the cap water zone. Soluble cations such as calcium ( $Ca^{2+}$ ), magnesium ( $Mg^{2+}$ ), sodium ( $Na^+$ ), and potassium ( $K^+$ ) were analyzed in filtered (0.45 $\mu$ m) and diluted (with 1%  $HNO_3$ , trace metal grade) porewater and cap water using inductively coupled plasma optical emission spectrometry (ICP-OES). Soluble Sulfate concentration in the porewater and capwater was determined using an ion chromatograph equipped with a 4mm analytical column (AS9-HC). The methyl orange indicator method (US EPA, 1974) was used for determining dissolved carbonate ( $CO_3^{2-}$ ) and bicarbonate ( $HCO_3^-$ ). Appropriate internal and external standards were used during the above analysis. The collected pore water samples from centrifuged FFTs and the cap water samples were filtered (0.45 $\mu$ m) and diluted with 1%  $HNO_3$  (trace metal grade) and analyzed using ICP-MS (PerkinElmer SCIEX ELAN 9000). Ionic strength of the FFT pore and capwater was calculated using following formula (Essington, 2004):

$$I = 1/2 \sum (C_i Z_i^2) \quad (1)$$

Where “I” represents ionic strength, “ $C_i$ ” represents the concentration of individual charged species ( $molL^{-1}$ ) and “ $Z_i$ ” is the valence of individual ions in porewater and “ $\sum$ ” is the summation of all species measured in the porewater and capwater.

Naphthenic acids were measured in the FFT and capwater samples by using standard method based on Fourier-transform infrared spectroscopy technique (Jivraj et al., 1995; Scott et al., 2008). Three replicates were run for each sample and the results were compared with a calibration plot of Merichem NAs standards.

### **3.3.4 Chemical analyses of the FFT**

#### **3.3.4.1 Carbonate minerals**

The acid digestion method was used to determine the total carbonates in the solid phase of FFT (Pansu and Gautheyrou, 2006). Before starting analysis, 10 ml of FFTs samples was washed with 30 ml methanol and centrifuged to remove soluble  $\text{HCO}_3^-$  from FFT and separate solid phase from liquid phase (repeated twice). Two grams of FFT solid phase was transferred to a serum bottle capped with a butyl rubber stopper. The headspace of bottle was flushed under a stream of  $\text{N}_2$  gas. To dissolve the carbonate minerals, 20 ml of 1M HCl was added to the bottle using syringe and the bottle was shaken gently for 2 h. The released  $\text{CO}_2$  in the headspace of the bottle was measured using GC-FID (Hewlett Packard 5890). The Ca and Mg concentration were also analyzed in the residual contents of the bottle using ICP-OES. The above concentrations were used to calculate  $\text{CaCO}_3$  and  $\text{Ca Mg}(\text{CO}_3)_2$  in the FFT.

#### **3.3.4.2 Phosphate minerals**

For determining the contents of phosphates in the FFT, 1 g of FFT was placed in a centrifuge tube and treated with a 50 ml of 0.1 M NaOH /1M NaCl solution. The mixture was shaken for 16 h and then centrifuged at 3057 g for 1 h to separate supernatant. Ascorbic acid method and a UV/VIS spectrophotometer (Optizen POP) at the wavelength of 880nm was used to determine the concentration of phosphorous in the supernatant (Kuo, 1996; Siddique et al., 2014).

#### **3.3.4.3 Total metals**

Microwave acid digestion method (US EPA, 2007) was used to treat FFT samples. One gram of FFT was placed in Teflon digestion vessels and 5 ml nanopure water and 10 ml concentrated nitric acid were added. Vessels were transferred to microwave (ETHOS SEL High Performance Extraction System) for 20 min digestion at 180°C. The digested samples were filtered (0.45 $\mu\text{m}$ ) and diluted with 1%  $\text{HNO}_3$  (trace metal grade) and analyzed using ICP-MS (PerkinElmer SCIEX ELAN 9000). Results were reported on dry weight basis.

#### **3.3.4.4 Sulfide minerals**

The free hydrogen sulfide ( $\text{H}_2\text{S}$  gas), the most labile fraction defined as acid volatile sulfides (AVS) that include amorphous and poorly crystalline monosulfides (Morse et al., 1987), and the chromium reducible sulfide (CRS) representing pyrite and elemental sulfur (Huerta-Diaz et al., 1993; Bollinger et al., 2001) were determined in the FFT samples. Free  $\text{H}_2\text{S}$  was determined by placing 3 g FFT sample in a pre-weighed vacuum flask under flushing with  $\text{N}_2$ . The flask was connected to an Erlenmeyer flask contain 30 ml zinc acetate as  $\text{H}_2\text{S}$  trapping solution. The sample was continuously flushed with  $\text{N}_2$  gas and stirred for 1 h. The iodometric titration method with starch as an indicator was used to determine the concentration of  $\text{H}_2\text{S}$  in the trapping solution. The sulfur content was calculated and reported based on dry mass. The AVS was determined by injecting 20 ml 6 N HCl to solid residue after  $\text{H}_2\text{S}$  extraction (in the same rubber- stopped digestion flask) and continuously flushed with  $\text{N}_2$  gas and stirred for 2 h. The digestion flask was connected to a separated Erlenmeyer flask contain 30 ml zinc acetate to trap digested AVS. The trapping solution was titrated with standard iodine solution in the presence of starch indicator to the permanent blue end point (Ahern, et al., 1998; Pansu and Gautheyrou, 2006). The CRS fractions was extracted from 3 g FFT placed in a tared round- bottom three-neck flask containing 2 g Cr powder. The 60 ml 5.65 M HCl was injected to the sample flask and the sample was digested at  $150^\circ\text{C}$  for 1 h. The  $\text{H}_2\text{S}$  was trapped in the same manner as explained in detail for AVS and then titrated with the iodometric titration method to a blue end- point. The amounts of sulfur content were calculated and reported on a dry mass basis (Ahern, et al., 1998; Pansu and Gautheyrou, 2006).

#### **3.3.4.5 Iron (Fe) minerals**

The concentration of total Fe in the acid digested FFT was determined using ICP-MS (method's detail has been described in section 3.3.3.3). Available  $\text{Fe}^{\text{II}}$  was determined using Ferrozine method (Sorensen, 1982; Lovely and Phillips, 1986). For this, 0.1 g FFT was added to 5 ml of 0.1 % ferrozine in a 0.05 M HEPES buffer solution in anaerobic chamber. The mixture of FFT and ferrozine solution was shaken or 15 min and then centrifuged. The concentration of  $\text{Fe}^{\text{II}}$  in separated supernatant was analyzed using an UV/VIS spectrophotometer (Optizen POP) at a wavelength of 562 nm. The Dithionite-citrate-bicarbonate (DCB) method (Pansu and Gautheyrou, 2006) was used to determine the both crystalline and amorphous forms of total Fe oxides and hydroxides in the FFT. Two grams of FFT was placed in a 100-ml tube contains 45 ml of citrate-

bicarbonate buffer (pH=7) and incubated in a water bath at 75°C. The samples were stirred continuously. After the mixture reached 75°C, 1 g of sodium dithionite (Na<sub>2</sub>S<sub>2</sub>O<sub>4</sub>) was added to sample and additional 1 g proportion of Na<sub>2</sub>S<sub>2</sub>O<sub>4</sub> was added after 5 min. The mixture was centrifuged after the 15 min extraction period and the supernatant was transferred to a 250-ml volumetric flask. The sample was treated again for the second extraction as described above. Both pooled supernatants from two extractions were made to volume (250ml) with deionized water and analyzed for Fe using Atomic Absorption Spectroscopy (AAS). The ammonium oxalate (AO) extraction method (Pansu and Gautheyrou, 2006) was also used to determine the amorphous and poorly crystalline Fe oxides and hydroxides in the FFTs. In previous method (DCB method), pyrite and siderite could not be dissolved, however, AO buffer can also dissolve these minerals (Siddique et al., 2014). In AO method, 1 g of FFT was placed in a 50 ml centrifuge tube and 50 ml AO (pH~3) was added. The mixture was shaken in the dark environment. After the 4 h incubation period, the sample was centrifuged at 3075 g for 1 h and the concentration of Fe was analyzed in the separated supernatant using AAS. The Fe associated with amorphous sulfides, pyrite, carbonate, and phosphates were calculated using the molar ratio of Fe: S (1.7:1), Fe: S<sub>2</sub> (1:1.1), Fe: CO<sub>3</sub> (1:1.07), and Fe: P (2.7: 1), respectively (Siddique et al., 2014).

The different fractions of Fe in the FFT was calculated using the below equations (Siddique et al., 2014):

$$\text{Fe (total)}^* = \text{Fe (accessory minerals)} + \text{Fe (Fe of phyllosilicates)} \quad (2)$$

\* Total Fe was determined using acid digestion method as described above and is the summation of accessory minerals (such as hematite, magnetite, ferrihydrite, goethite, magnetite, lepidocrocite, siderite, amorphous sulfides, green rust etc.) and Fe bound to silicate minerals. In this study total metals has defined as the total concentration of easily released Fe to the environment because during acid digestion, only all compounds that are easily release Fe to the environment are dissolved not all the matrices (Siddique et al., 2014).

$$\text{Fe}^{\text{III}} = \text{Fe}_{\text{DCB}} - \text{Fe}^{\text{II}}_{\text{ferrozine}} \quad (3)$$

In the above equation, DCB indicates dithionite-citrate-bicarbonate extracting total Fe oxy/hydroxides from both crystalline and amorphous minerals and ferrozine extracts available Fe<sup>II</sup> in the FFTs.

$$\text{Amorphous Fe}^{\text{III}} = \text{Fe}_{\text{AOD}}^* - \text{Fe}_{\text{siderite}}^{\text{II}} - \text{Fe}_{\text{AVS}}^{\text{II}*} - \text{Fe}_{\text{ferrozine}}^{\text{II}} \quad (4)$$

The  $^*\text{Fe}_{\text{AOD}}$  and  $^{**}\text{Fe}_{\text{AVS}}^{\text{II}}$  respectively refers to the total Fe extracted from Fe amorphous compounds using AOD (Ammonium Oxalate in the dark) and amorphous Fe sulfide minerals (Pansu and Gautheyrou, 2006; Siddique et al., 2014).

$$\text{Crystalline Fe}^{\text{III}} = \text{Fe}^{\text{III}} - \text{Amorphous Fe}^{\text{III}} \quad (5)$$

$$\text{Fe}^{\text{II}} = \text{Fe}(\text{total}) - \text{Fe}^{\text{III}} \quad (6)$$

$$\text{Crystalline Fe}^{\text{II}} = \text{Fe}_{\text{pyrite}}^{\text{II}*} + \text{Fe}_{\text{vivianite}}^{\text{II}*} + \text{Fe}_{\text{siderite}}^{\text{II}} \quad (7)$$

The  $\text{Fe}_{\text{pyrite}}^{\text{II}*}$  and  $\text{Fe}_{\text{vivianite}}^{\text{II}*}$  respectively refers to the Fe associated to pyrite and phosphate, respectively.

$$\text{Amorphous Fe}^{\text{II}} = \text{Fe}^{\text{II}} - \text{Crystalline Fe}^{\text{II}} \quad (8)$$

### 3.3.4.6 Metal sequential extraction (BCR method)

The optimized three step sequential extraction procedure (Rauret et al., 1999) was used for the analysis of metals associated with different solid phase fractions of FFT. The extractable contents of Sr, Ba, As, V, Mo, and Cr were determined in the FFT as described below. In the first step, 1 g of FFT was placed in a 100 ml tube and 40 ml acetic acid solution (0.11 M) was added. The mixture was shaken overnight (16 h) at room temperature ( $22 \pm 5$  °C) and then centrifuged at 3000 g for 1 hr. The supernatant was separated and stored in the fridge at 4°C prior to analysis using ICP-MS. To wash the residual acetic acid from the FFT, 20 ml of nanopure water was added to the residue and shaken for 15 min and then centrifuged for 30 min at 3000 g. The supernatant was decanted and discarded. Acetic acid solution was used to recover the mobile fraction of metals (soluble in water and weak acid, carbonate bound) from the FFT. In the second step, 40 ml of hydroxyl ammonium chloride solution was added to the same 100 ml tube containing the residues from the step 1 and shaken for 16 h at room temperature. The extract was separated by centrifugation at 3000 g for 1 hr and stored at 4°C for analysis using ICP-MS. The residue was washed as described previously in step 1. The fraction of metals associated with iron and manganese oxides were recovered at this step. Third step was performed using hydrogen peroxide followed by ammonium acetate to recover the metals' fraction bound to organic matter and sulfides. The addition of 10 ml hydrogen peroxide (30%) to the residues from step 2 was applied

in small aliquots to avoid the violent reaction and sample loss. The tubes were capped loosely, incubated at room temperature for 1 h, and occasionally shaken by hand. The digestion continued for 1 h at  $85\pm 2^{\circ}\text{C}$  by incubating in water bath. Then, further heating of the uncovered tubes was used to reduce the volume of mixture to less than 3 ml. Second aliquot of 10 ml hydrogen peroxide was added to the residues and the incubation followed as described above until reaching 1 ml of liquid in the mixture. After cooling the residues, 50 ml of 0.1M ammonium acetate was added and shaken overnight at room temperature. The extract was separated by centrifugation and decantation as in previous steps and retained as before for the analysis by ICP-MS and the residue was washed as described previously. Then, the residue was transferred to the Teflon digestion vessels using nanopure water. The vessel was placed to the oven at  $50^{\circ}\text{C}$  until complete evaporation of the water. After residue was dried, 4 ml concentrated nitric acid, 3 ml hydrofluoric acid, and 3 ml hydrogen peroxide were added and the vessel was transferred to microwave and incubated for 20 min at  $180^{\circ}\text{C}$ . The digested samples were filtered and diluted before analysis by ICP-MS as described previously for the analysis of total metals. The microwave acid digestion method was used to recover the fraction of residual metals in the FFT.

The data were statistically analyzed using the package STATISTICA 10 (StatSoft, 2011). Statistical significance was detected using the independent-samples t-test and analysis of variance at  $\alpha=0.05$ .

### **3.4 Results**

#### **3.4.1 Biogenic gas production and changes in the porewater and cap water chemistry**

As described in chapter 2, the addition of hydrocarbons alone or in a combination with other nutrients (N and P) to FFTs resulted in a significant increase in the methane ( $\text{CH}_4$ ) in the headspace of HC, HCN, and HCNP columns during the experimental period. Meanwhile, minor methane production was observed in the unamended (U) columns. The cumulative  $\text{CH}_4$  and  $\text{CO}_2$  production in the FFTs treated with hydrocarbons and nitrogen (HCN) was significantly higher than FFTs treated with hydrocarbons only (HC) or hydrocarbon plus nitrogen plus phosphorous (HCNP). From day 60 onwards, the  $\text{CH}_4$  and  $\text{CO}_2$  emission was exponentially increased in all amended columns (HC, HCN, and HCNP). This pattern continued until 190 d and then  $\text{CO}_2$  production became plateaued during the remaining part of the experiment in all amended columns.

However, small increase in the CH<sub>4</sub> emission was observed in HC, HCN, and HCNP columns from day 190 to day 570. Afterward, a plateau level was reached in these columns. Compared within amendments, the cumulative CH<sub>4</sub> production was 9.5-11.5 times higher than cumulative CO<sub>2</sub> production during the entire experiment (Fig 3.1). After significant biogenic gas production till day 190, we were not able to sustain it though we added hydrocarbons to further sustain the methanogenesis.

The effect of methanogenic activities on FFT consolidation is shown in Fig 3.2. The results revealed that stimulated methanogenesis induced the rapid consolidation of FFT and dewatering in all amended columns as compared to unamended FFT. Interestingly, the greater porewater recovery and solids consolidation was observed in HCN FFT as compared to HC and HCNP FFTs. Slowed methanogenesis in HCNP FFT, also resulted in significantly lower porewater recovery and solid consolidation among amended FFTs (Fig 3.2).

The pH significantly decreased from  $7.56 \pm 0.08$  to  $6.76 \pm 0.12$  in the porewater and from  $7.24 \pm 0.1$  to  $6.65 \pm 0.03$  in the cap water of all columns amended with hydrocarbons and nutrient sources by day 190. However, from day 190 until the end of experiment, further significant changes in pH were not observed in the porewater and cap water of these amended columns. Also, no significant differences in the pH of the porewater and cap water were observed within the unamended columns. In U columns, pH changed slightly from  $7.56 \pm 0.08$  and  $7.24 \pm 0.1$  at day 0 to  $7.42 \pm 0.03$  and  $7.51 \pm 0.01$  by day 600, in the porewater and cap water samples, respectively. It can be concluded that pH remained unchanged in U columns during entire experiment (Fig 3.3). The carbonate minerals' solubility was significantly increased with decreasing pH in amended FFTs (Fig 3.4). In HCN FFT, the carbonate mineral content (5%wt) was significantly lower than HC (5.43%wt), HCNP (5.68%wt), and U (5.91%wt) FFTs at 600d.

Soluble Ca<sup>+2</sup> and Mg<sup>+2</sup> concentration in the porewater and cap water of amended columns (HC, HCN, and HCNP) significantly increased by day 190 compared with U columns (Fig 3.5). From 190 to the end of the experiment, small but insignificant increase was observed in the concentration of Ca<sup>+2</sup> and Mg<sup>+2</sup> in the porewater and cap water of amended columns because no further active methanogenesis occurred after day 190. Within amended columns, HCN columns yielded significantly higher concentration of Ca<sup>+2</sup> and Mg<sup>+2</sup> in the porewater (~71 and ~35 mgL<sup>-1</sup>, respectively) and cap water (~69 and ~28 mgL<sup>-1</sup>, respectively) compared with HC (porewater: ~37

and  $\sim 16 \text{ mgL}^{-1}$ , respectively and cap water:  $\sim 35$  and  $\sim 13 \text{ mgL}^{-1}$ , respectively) and HCNP (porewater:  $\sim 34$  and  $\sim 17 \text{ mgL}^{-1}$ , respectively and cap water:  $\sim 33$  and  $\sim 13 \text{ mgL}^{-1}$ , respectively). Soluble  $\text{K}^+$  also increased in porewater and cap water of all amended columns whereas the concentration of soluble  $\text{Ca}^{+2}$ ,  $\text{Mg}^{+2}$ , and  $\text{K}^+$  remained unchanged in U columns during the experiment. The results showed that the addition of phosphorous to HCNP columns resulted in a significant decrease in base cations ( $\text{Ca}^{+2}$ ,  $\text{Mg}^{+2}$ , and  $\text{K}^+$ ) concentrations in the porewater and cap water compared with HC and HCN columns which corresponded well to the trend observed in the active methanogenesis in these treatments.

Amended FFTs (HC, HCN, and HCNP) showed higher porewater and cap water concentrations of soluble  $\text{HCO}_3^-$  ( $\sim 1300$ - $2000 \text{ mgL}^{-1}$ ) than unamended FFT ( $\sim 1100$ - $1200 \text{ mgL}^{-1}$ ) by day 600 (Fig 3.5). In HCN columns, the concentration of  $\text{HCO}_3^-$  increased from  $\sim 460 \text{ mgL}^{-1}$  to  $1800 \text{ mgL}^{-1}$  in porewater and from  $\sim 1400 \text{ mgL}^{-1}$  to  $2000 \text{ mgL}^{-1}$  in cap water, respectively at day 0 and day 600. The concentrations of  $\text{HCO}_3^-$  in the porewater ( $\sim 1300 \text{ mgL}^{-1}$ ) and cap water ( $\sim 1400 \text{ mgL}^{-1}$ ) of HCNP samples were significantly lower than other amended columns by the day 600. Sulfate concentrations were depleted in the pore water of all amended columns by day 190 and only very low concentration of  $\text{SO}_4^{2-}$  ( $< 3 \text{ mgL}^{-1}$ ) were detected in the cap water of amended columns by 600 (Fig 3.6).

### 3.4.2 Changes in trace metals mobility during methanogenesis

Concentrations of strontium (Sr), barium (Ba), arsenic (As), antimony (Sb), molybdenum (Mo), vanadium (V), and chromium (Cr) in the porewater and cap water samples taken from the unamended and amended (HC, HCN, and HCNP) columns varied during incubation period. Figures 3.7, 3.8, and 3.9 show the total concentration of each trace metal in the cap water and porewater samples taken from different ports of each column (P1-P4) at days 0, 190, 353, and 600. Amended columns showed the higher concentrations of Sr and Ba in the porewater and cap water by day 190 during incubation compared with day 0 (Fig 3.7). A very slight increase in Sr and Ba concentrations observed afterwards until the end of experiment (day 600). However, the Sr and Ba concentrations in the porewater and cap water of unamended columns remained unchanged throughout the incubation. The HCN columns showed the highest increase in the concentration of Sr and Ba in the porewater and cap water samples among amended columns. Amount of Sr increased from  $676.7$  and  $446.5 \mu\text{g L}^{-1}$  at day 0 to  $\sim 2270$  and  $\sim 2200 \mu\text{g L}^{-1}$  at day 600, and

concentration of Ba increased from 601.7 and 224.4  $\mu\text{g L}^{-1}$  at day 0 to  $\sim 1880$  and  $\sim 2200$   $\mu\text{g L}^{-1}$  at day 600 in the porewater and cap water of HCN columns, respectively. HCNP columns yielded a lowest increase in the concentrations of Sr, from 676.7 and 446.5  $\mu\text{g L}^{-1}$  at day 0 to  $\sim 1056$  and  $\sim 1180$   $\mu\text{g L}^{-1}$  at day 600, and Ba, from 601.7 and 224.4  $\mu\text{g L}^{-1}$  at day 0 to  $\sim 1052$  and  $\sim 1300$   $\mu\text{g L}^{-1}$  at day 600, in the pore and cap water samples, respectively (Fig 3.7). The concentrations of As, Sb, Mo, V, and Cr in the porewater and cap water samples showed the highest values at day 0 and these concentrations decreased with time in all unamended and amended columns. However, the amendment addition reduced the availability of these trace metals greater in porewater and capwater samples of amended columns than unamended one (Fig 3.8 and 3.9). The highest decrease in As concentrations were from 13.03 and 1.94  $\mu\text{g L}^{-1}$  at day 0 to 0.44 and 0  $\mu\text{g L}^{-1}$  at day 600 in porewater and cap water samples in HCN columns, respectively (Fig 3.8). In addition, the availability of V and Cr also decreased with time in the porewater and cap water of HCN columns more than other amended columns (Fig 3.9). Both HC and HCNP columns showed the larger impact on the reduction of Sb availability in porewater and cap water samples with time than HCN column. The concentrations of Sb greatly decreased from 24.1 and 5.6  $\mu\text{g L}^{-1}$  at day 0 to  $\sim 1.65$  and  $\sim 0.29$   $\mu\text{g L}^{-1}$  at day 600 in porewater and cap water samples in HCNP columns, respectively (Fig 3.8). Greater reduction in the availability of Mo, from 62 and 32.6  $\mu\text{g L}^{-1}$  at day 0 to  $\sim 3.8$  and  $\sim 1.4$   $\mu\text{g L}^{-1}$  at day 600, was also observed in the porewater and cap water samples in HCNP columns than HC and HCN columns, respectively (Fig 3.9).

### **3.4.3 Transformation of Iron in Unamended and amended FFT as influenced by amendments**

Results of iron (Fe) fractionation in unamended and all amended FFT samples at day 0 and 600 of incubation is summarized in Table 3.1 and Fig. 3.10. Almost equal concentrations of  $\text{Fe}^{\text{II}}$  and  $\text{Fe}^{\text{III}}$  in crystalline forms were observed in unamended FFTs after 600 days of incubation. However, the  $\text{Fe}^{\text{III}}$  minerals, in crystalline form, transformed to  $\text{Fe}^{\text{II}}$  minerals, in the FFTs of all amended under methanogenic conditions by day 600. Highest and lowest transformation of  $\text{Fe}^{\text{III}}$  to  $\text{Fe}^{\text{II}}$  minerals were observed in HCN and HCNP FFTs, respectively (Fig 3.10). The content of amorphous FeS significantly increased in all amended FFTs with the highest and lowest increase in HCN and HCNP FFT samples at day 600, respectively (Fig 3.11). Chemical analysis showed the major sources of crystalline  $\text{Fe}^{\text{III}}$  minerals were iron oxyhydroxides whereas pyrite ( $\text{FeS}_2$ ), siderite ( $\text{FeCO}_3$ ), and vivianite ( $\text{Fe}_3(\text{PO}_4)_2 \cdot 8\text{H}_2\text{O}$ ) represented crystalline  $\text{Fe}^{\text{II}}$  minerals in FFT

samples. No change in pyrite contents was observed in unamended and amended FFTs during incubation period (Table 3.1). Siderite showed decreasing trend in all amended FFTs with the highest and lowest contents in HCNP and HCN FFT samples after 600 days, respectively; however, vivianite with very low contents in FFT was slightly increased in all amended FFT samples (HCNP>HC>HCN) (Fig 3.11).

#### **3.4.4 Influence of amendments on the fractionation of trace metals in FFT**

The Sequential extraction analysis provided insight into the contents of Sr, Ba, As, Sb, Mo, V, and Cr in different fractions (F1: soluble, weak acid soluble, carbonate bound; F2: Fe and Mn bound, F3: organic matter and sulfide bound; F4: residual) of initial, unamended (U), and amended FFT (HC, HCN, and HCNP) solid phases (Table 3.2 and Fig 3.12, 3.13, and 3.14). Strontium was more abundant in F1 (54-64% of total elemental mass) and F2 (21-30% of total elemental mass) fractions than other fractions in all initial, U, HC, HCN, and HCNP samples (Fig12). High contents of Ba was detected in the fraction bound to iron and manganese (39-48%) and in F1 fraction (33-39%) in all initial, U, HC, HCN, and HCNP samples. The contents of Sr and Ba in the residual fractions (F4) represented a small portion of the total contents in all initial, U, HC, HCN, and HCNP samples. The residual fraction was the main host of As (47-53% of the total As), V (~70%), and Cr (~84%) in all initial, U, HC, HCN, and HCNP samples and the secondary host for As, V, and Cr was detected in the fraction bound to organic and sulfide with an average at ~28%, ~19%, and ~11%, respectively. Antimony dominated in F2 and F3 fractions. The contents of Sb in the fraction bound to iron and manganese oxides (F2) and in the organic and sulfides fraction (F3) were with an average of 40 and 44% among all initial, U, HC, HCN, and HCNP samples, respectively. Molybdenum dominated in the organic and sulfides bound (F3) fractions, where its contribution in relation to the sum of all fractions was with an average of ~44% and the secondary host for Mo (36% of the total Mo) was detected in residual fraction among all initial, U, HC, HCN, and HCNP samples. The contents of all elements of interest in different fractions did not show significant changes with the time compared to initial samples (day zero) which reflected no significant change between the unamended (U) and amended (HC, HCN, and HCNP) FFT samples (Table 3.2; Fig. 3.13, and 3.14).

#### **3.4.5 Changes in NAs concentration in FFT and cap water after amendment**

The Merichem NAs concentration in the initial FFT pore water and cap water samples (day0) were  $38.45 \pm 2.56$ , and  $22.17 \pm 3.25$  mg Merichem  $\text{NAL}^{-1}$ , respectively (Fig 3.15). NAs

concentration remaining after 190-day incubation in the pore water and cap water of amended columns (HC, HCN, and HCNP) were significantly lower than U columns (Fig 3.15). Within amended columns, HCN columns showed significantly lower concentration of NAs in the porewater ( $\sim 28.56 \pm 1.42 \text{ mgL}^{-1}$ ) and cap water ( $17.21 \pm 0.09 \text{ mgL}^{-1}$ ) compared with HC (porewater:  $34.65 \pm 0.43 \text{ mgL}^{-1}$  and cap water:  $19.35 \pm 0.78 \text{ mgL}^{-1}$ ) and HCNP (porewater:  $33.79 \pm 1.67 \text{ mgL}^{-1}$ , and cap water:  $18.23 \pm 1.45 \text{ mgL}^{-1}$ ).

### 3.5 Discussion

The transportation of the contaminants of concerns (COCs), from FFT to overlying cap water might be a concern for the sustenance of EPLs. A variety of microbial and physico-chemical processes (e.g., microbial activity, pH, redox condition, mineral transformation), may enhance the flux of COCs from FFT to the overlying cap water and threaten the quality of surface water in end pit lakes. Therefore, any factor that stimulated the biogeochemical processes can affect the movement of COCs to cap water. In the chapter 2, it was described how N stimulated and P inhibited the methanogenic activity, as a controlling factor in COCs partitioning. In this chapter, we have focused on how stimulated and prohibited microbial activities alter pore water chemistry, transform the minerals, influence the distribution of ions ( $\text{CO}_3^{2-}$ ,  $\text{HCO}_3^-$ ,  $\text{SO}_4^{2-}$ ,  $\text{Ca}^{2+}$ ,  $\text{Mg}^{2+}$ ,  $\text{K}^+$ ), soluble metals (Sr, Ba, As, Sb, Mo, V, and Cr), and in turn affect the quality of surface water.

As described in chapter 2, amendment of hydrocarbons and inorganic nutrient (N) resulted in enhanced growth and activity of indigenous anaerobic microorganisms with higher rates of biogenic  $\text{CH}_4$  and  $\text{CO}_2$  production (Fig 3.1). Nitrogen in the form of  $\text{NH}_4^+$  and enough labile organic compounds (a mixture of hydrocarbons) proved an efficient biostimulation approach (HCN) allowing higher anaerobes growth and activity and higher production of  $\text{CH}_4$  and  $\text{CO}_2$  than HC and HCNP FFTs (Fig 3.1). The stimulated activity of anaerobes was also observed in previous studies where mature fine tailings (MFT) was amended with labile hydrocarbons (Siddique et al. 2006, 2007, 2011, 2015; Mohammad Shahimin and Siddique, 2017 a and b), organic acid such as acetate (Fedorak et al., 2003; Arkell et al., 2015) and agricultural waste (canola meal) (Siddique et al., 2014 a and b), and nutrient deficient hydrocarbon rich sludge amended with nutrients (N and/or P) (Devi et al., 2011; Sarkar et al., 2016). The biogenic gases produced during active methanogenesis in the FFTs of all amended columns (HC, HCN, and HCNP) escaped from the pressurized porewater through the created transient channels and moved to the cap water above

mudline. Because of the poor solubility of CH<sub>4</sub> in the water, it was observed that the migrated gas bubbles contained higher concentration of CH<sub>4</sub> than CO<sub>2</sub> (Fig 1). All of these observations are consistent with other reports (Voordouw, 2013; Siddique et al., 2014; Arkell et al., 2015). As reported in previous studies (Siddique et al., 2014; Arkell et al., 2015), the current study also revealed that the methanogenesis (production of CO<sub>2</sub> and CH<sub>4</sub>) affected the chemical properties of the FFT in all amended columns. In the initial stages of methanogenesis, the pH increased slightly probably due to acetate production and CO<sub>2</sub> consumption (Fotidis et al., 2013), but dissolution of trapped CO<sub>2</sub> in FFT porewater decreased the pH and increased the HCO<sub>3</sub><sup>-</sup> in the porewater and cap water of all amended columns (Fig 3.3, and 3.5). Similar findings were reported by Siddique, et al. (2014) and Arkell et al. (2015) who observed lower pH and higher soluble HCO<sub>3</sub><sup>-</sup> and carbonate minerals dissolution during the microbial acceleration of MFT consolidation under methanogenic conditions. Study of Wersin et al. (2011) on the biogeochemical processes involved in clay formation in situ also supported our results where carbonate dissolution, high pCO<sub>2</sub> and alkalinity (HCO<sub>3</sub><sup>-</sup> and CO<sub>3</sub><sup>2-</sup>), and a decrease in pH from 7.7 to 6.8 were associated with anaerobic degradation of an organic substrate under sulfate reducing and methanogenic condition. During the carbonate minerals dissolution, the solubility of calcite (CaCO<sub>3</sub>) are followed by dolomite (CaMg (CO<sub>3</sub>)<sub>2</sub>), and siderite (FeCO<sub>3</sub>) as pH decreases (Chou et al., 1989). This would explain the enhanced carbonate minerals (Calcite and Dolomite; Fig 3.4), and Siderite (Fig 3.11) dissolution and increased cations (Ca<sup>2+</sup> and Mg<sup>2+</sup>) release into porewater and cap water of all amended columns (Fig 3.5), as pH reduced in all amended FFTs. Similar results were also reported on the carbonate mineral dissolution in marine sediments due to benthic bacterial activity (Moulin et al., 1985) and increased atmospheric CO<sub>2</sub> pressure (Morse et al., 2007). The highest and lowest concentrations of Ca<sup>2+</sup>, Mg<sup>2+</sup>, and HCO<sub>3</sub><sup>-</sup> were observed in porewater and cap water of HCN and HCNP columns, respectively (Fig 3.5). In addition, highest and lowest dissolution of carbonate minerals were also observed in HCN and HCNP columns (Fig 3.4) which was consistent with the highest and lowest production of biogenic CO<sub>2</sub> in HCN and HCNP columns (Fig 3.1).

The results of iron fractionation in initial FFT at day zero and in unamended and amended FFT samples after 600 days indicated that microbial metabolisms reduced Fe<sup>III</sup> minerals and more amorphous Fe<sup>II</sup> minerals were formed in amended FFT (Fig 3.10 and Table 3.1). Interestingly, the stimulated FFT by hydrocarbons and N (HCN) showed higher methanogenic activity and higher rate of Fe<sup>III</sup> reduction as compared with HC and HCNP FFTs (Fig 3.10). In addition, higher

formation of amorphous FeS was observed in HCN FFT compared with initial, U, HC, and HCNP FFTs. In the studies conducted by Arkell et al., (2015) and Siddique et al, (2014b), the MFTs were amended with sodium acetate and canola meal, respectively to stimulate the methanogenesis. Similar results were reported from these two studies where transformation of Fe<sup>III</sup> to Fe<sup>II</sup> minerals occurred under stimulated methanogenic activities. Those studies proposed that Fe<sup>III</sup> minerals such as goethite and ferrihydrite as main iron oxide minerals in MFT were transformed into green rust (a mixture of Fe<sup>II</sup> and Fe<sup>III</sup> minerals) that was further transformed into Fe<sup>II</sup> minerals such as sulfides, siderite and vivianite (Siddique et al. 2014b). The microbial reduction of Fe<sup>III</sup> minerals and SO<sub>4</sub><sup>2-</sup> in anoxic FFT, and presence of CO<sub>3</sub><sup>2-</sup>, and PO<sub>4</sub><sup>3-</sup> in the pore water led to the sulfides, siderite and vivianite (Siddique et al., 2014b).

The results of consolidation and water recovery in unamended and amended FFT samples during 600 days incubation indicated that stimulated methanogenesis enhanced solids settlement and the recovery of the pore water in amended FFT, particularly in HCN FFT (Fig 3.2). As described in previous paragraph, the higher concentration of soluble ions (Ca<sup>2+</sup>, Mg<sup>2+</sup>, and HCO<sub>3</sub><sup>-</sup> in amended FFT significantly (p<0.05) (Fig 3.5) increased the ionic strength of the pore water, (Fig 3.16) that would reduce the surface charge potential of clay particles and in turn reduce the diffuse double layer (DDL) of clay particles and enhance the consolidation of amended FFT (Siddique et al., 2014a; Arkel et al., 2015). Therefore, significantly greater pore water was expressed from the amended FFT, particularly in HCN FFT, compared to unamended FFT (Fig 3.2). Reduced pH in the pore water of amended FFT also would decrease the net negative charges on the surface of clay minerals which their charges are highly pH dependent (such as Kaolinite which is dominant in FFT) and in turn decrease the thickness of DDL and increase the consolidation and dewatering of amended FFT (Siddique et al., 2014a). As described in previous paragraph, enhanced methanogenesis in amended FFT, enhanced the transformation of Fe<sup>III</sup> to Fe<sup>II</sup> minerals (Fig 3.10), and increased the formation of newly formed iron minerals such as amorphous iron sulfides (FeS) (Fig 3.11). The formation of new minerals can entrapped and masked electronegative clay surfaces and result in reducing the surface charges of clay particles and in turn increasing the clays aggregation and pores network formation (Siddique et al., 2014b). These processes increases the consolidation of amended FFT and enhance the porewater expression from FFT to cap water (Fig 3.2).

In addition to the effect of methanogenic activities on the chemistry of pore water of all amended columns and the transformation of iron minerals, the partitioning of Sr, Ba, As, Sb, Mo, V, and Cr was also affected by stimulated microbial activities. Regarding trace metals of interest, higher concentrations of Sr and Ba in the porewater and cap water of all amended FFTs were observed as compared to unamended FFT. Porewater and capwater of amended columns detecting strontium at close or even above levels the agency's health reference level ( $1.5 \text{ mgL}^{-1}$ ) (EPA, 2014). Among the amended FFTs, the highest and lowest concentrations of Sr and Ba were found in HCN and HCNP columns, respectively (Fig. 3a and b). Sequential extraction of metals from FFT (Fig 3.7) revealed that the major fraction of Sr (54-64%) was associated with soluble and weak acid soluble solid phase including carbonates. Therefore, it is suggested that the major portion of Sr in porewater was released during dissolution of carbonate minerals. This proposition is supported by the other chemical data in all amended columns where higher biogenic  $\text{CO}_2$  was produced that lowered pH and increased dissolution of carbonate minerals yielding higher concentrations of associated cations such as  $\text{Ca}^{2+}$ ,  $\text{Mg}^{2+}$ ,  $\text{Sr}^{2+}$  etc., in the porewater and cap water of amended columns. The solubility of Sr carbonate is gradually increased as  $\text{CO}_2$  pressure is increased and  $\text{CO}_2$  is dissolved in pore water (De Andrade et al., 2018). The metal fractionation results also showed the some Sr is associated with Fe and Mn oxides. If Sr is adsorbed on oxides, it forms outer sphere complexes with the solid matrix (Thorpe et al., 2012; Wallace et al., 2012). As pH decreases, the competition between strontium and hydronium ions for the adsorption on solid phases increases and Sr adsorption decreases (Wallace et al., 2012) that can lead to the higher concentrations of Sr in the porewater and cap water samples. Also, the increased concentrations of other ions ( $\text{Ca}^{2+}$ ,  $\text{Mg}^{2+}$ , and  $\text{HCO}_3^-$ ) in the porewater and cap water of amended columns was in line with the increased release of strontium in the in the porewater and cap water samples. The presence of higher soluble ions ( $\text{Ca}^{2+}$ ,  $\text{Mg}^{2+}$ , and  $\text{HCO}_3^-$ ) in FFT of HCN columns (Fig 3.5) significantly increased the ionic strength of pore water (Fig 3.16) that can lead to higher concentration of Sr in the porewater and cap water of HCN columns. Wallace et al., (2012) studied the sorption behavior of Sr in sediment-water system at a UK Sellafield unclear site. They observed that the presence of increasing concentrations of competing ions ( $\text{Na}^+$  and  $\text{Ca}^{2+}$ ) in the  $\text{HCO}_3^-$  buffered groundwater system induced higher ionic strength in this solution and resulted in much lower sorption of Sr. In another study conducted by Hull and Schafer (2008), the distribution of Sr among the layers of geologic strata was simulated and their simulation results also suggested the

accelerated release of Sr through the competition with high  $\text{Na}^+$  concentration in the liquid phase and high concentrations of  $\text{Ca}^{2+}$  released through calcite dissolution. As indicated in Figure 3.12, the Sr fraction bound in Mn and iron oxide minerals could be considered as another source of Sr release to the porewater. As observed in Fig 3.10 and 3.11, the  $\text{Fe}^{\text{III}}$  minerals were transformed to  $\text{Fe}^{\text{II}}$  minerals under methanogenic conditions in amended FFTs. Therefore, it might be presumed that  $\text{Sr}^{2+}$  desorbs during the reduction of  $\text{Fe}^{\text{III}}$  minerals where it is sorbed to iron oxide minerals (Langley et al., 2009). Langley et al., (2009) reported that in the groundwater discharge zones where the deposition of biogenic iron oxides (BIOS) were higher, the partitioning of Sr was lower; however, the significant amounts of Sr was remobilized and desorbed under BIOS reduction. Therefore, it could be concluded that the Fe oxidation state would also govern the partitioning of Sr bound to Fe minerals in our amended FFT and the higher release of Sr is expected from HCN samples with the higher extent of  $\text{Fe}^{\text{III}}$  to  $\text{Fe}^{\text{II}}$  transformation.

Similar to Sr, Ba was also released in significant amounts in the porewater and cap water of all amended FFTs (Fig 3.7). Metal fractionation in solid phase revealed that Ba, like Sr, was associated with carbonates and Fe and Mn oxide minerals (Fig 3.12). That was the reason that the solubility of  $\text{Ba}^{2+}$  increased when the pH decreased in amended FFTs (Fig 3.3) due to biogenic  $\text{CO}_2$  production in all amended columns, particularly in HCN columns, which increased the dissolution of carbonate minerals and increase Ba concentrations in amended FFTs. The other major Ba host phase was oxide minerals of Fe and Mn (co-precipitated and or adsorbed Ba) in FFT, and it could be presumed that Ba could be released in higher amount in the porewater of amended FFTs, particularly HCN FFT, through Fe and Mn oxide reduction under stimulated methanogenesis. Although, Ba does not have redox chemistry but a part of the elevated Ba concentrations in the porewater of amended FFTs could be explained by the redox transformation of Mn (Charette and Sholkovitz, 2006). In a study on the flux trace elements from submarine groundwater discharge to the coastal ocean, the findings indicated that Ba was absorbed onto the Mn oxides, released to the pore water by dissolution of Mn oxides minerals under reducing conditions; however, the Fe reduction did not influence the mobility of Ba (Charette and Sholkovitz, 2006), because Ba has high affinity for Mn oxide than Fe oxide minerals (Tonkin et al., 2004). Other soluble ions, such as  $\text{Ca}^{2+}$ ,  $\text{Mg}^{2+}$ ,  $\text{Na}^+$ ,  $\text{HCO}_3^-$ , and  $\text{Cl}^-$  may enhance the mobility of Ba in the porewater (Robins et al. 2012; Ebrahimi and Vilcaez 2018). In addition, under reducing conditions, low pH and low level of sulfate concentration, anaerobic bacteria such as *Desulfovibrio*

(sulfate-reducing bacteria) metabolize barite ( $\text{BaSO}_4$ ) and release Ba into porewater (Baladi et al., 1996). *Desulfovibrio* with higher abundance in HCN FFT was also detected in all initial, unamended, and amended FFTs (Chapter 2, Table 2.7); therefore, Ba might have also released from this minerals in the amended FFTs under our experiment situation.

Arsenic (As) is a metalloid observed in the oil sands process water where the Canadian Council of Ministers of the Environment water quality guidelines (Li et al., 2014; Zhang, 2016). The initial concentrations of As were  $13 \mu\text{g L}^{-1}$  in the FFT porewater and  $5 \mu\text{g L}^{-1}$  in the cap water (Fig 3.8) which were very close to the maximum acceptable concentration ( $5 \mu\text{g L}^{-1}$  in fresh water;  $12.5 \mu\text{g L}^{-1}$  in marine, and  $10 \mu\text{g L}^{-1}$  in drinking water) recommended by CCME (1997). As in the form of  $\text{As}^{\text{V}}$  (arsenate) tends to be adsorbed on the inorganic minerals surfaces especially  $\text{Fe}^{\text{III}}$  (hydr) oxides under oxic conditions and get immobilized through sorbing on solid phase; however,  $\text{As}^{\text{III}}$  is prevalent under anoxic conditions and more mobile than  $\text{As}^{\text{V}}$ . Because  $\text{As}^{\text{III}}$  has lower sorption affinity to  $\text{Fe}^{\text{III}}$  (hydr) oxides, the mobility of  $\text{As}^{\text{III}}$  increases under reducing conditions and through microbial reduction of  $\text{As}^{\text{V}}$  to  $\text{As}^{\text{III}}$  (Hu et al., 2015). Our findings indicated that in the anaerobic amended FFTs, the reduction of  $\text{Fe}^{\text{III}}$  (hydr) oxides led to the formation of higher amounts of amorphous  $\text{Fe}^{\text{II}}$  minerals (Fig 3.10 and 3.11; Table 3.1). Therefore, the release of total As adsorbed on the surface of  $\text{Fe}^{\text{III}}$  (hydr) oxides (Oremland and Stolz, 2005) to the porewater and subsequently to the cap water of all amended columns was expected. However, the concentration of total As decreased in the porewater of unamended and all amended columns (Fig 3.8). Sulfate ( $\text{SO}_4^{2-}$ ) concentrations showed a decreasing trend in the porewater and cap water of unamended and amended columns whereas  $\text{SO}_4^{2-}$  reduction enhanced in amended FFT (Fig 3.6). Reduction of  $\text{SO}_4^{2-}$  under anaerobic conditions may lead the formation of arsenic sulfide and removes dissolved arsenic from the porewater and capwater of columns (O'Day et al., 2004). Interesting results regarding As speciation were also observed where we found higher concentrations of  $\text{As}^{\text{V}}$  species than  $\text{As}^{\text{III}}$  under anaerobic conditions in the porewater and cap water of all columns during experiment period (Fig 3.17). These anomalous findings are supported by the findings of Finneran et al., (2003) who indicated *Albidiferax ferrireducens* (formerly known as *Rhodofeferax ferrireducens*) as an iron reducing bacteria was also capable of oxidizing  $\text{As}^{\text{III}}$ . The evidence of *Albidiferax* was also observed in our FFT samples (Chapter 2, Table 2.7). Other studies reported that denitrifying bacteria could use nitrate as electron acceptor to oxidize  $\text{As}^{\text{III}}$  to  $\text{As}^{\text{V}}$  under anaerobic conditions (Sun et al., 2008; Hu et al., 2015). Although, nitrate was not detected in our

FFT samples but small amounts of nitrate were detected in various incubation time in HCN column that might be produced through the  $\text{NH}_4^+$  oxidation coupled with iron reduction. Furthermore, significant removal of As from the pore and cap water of HCN columns compare with HC and HCNP columns might be explained by the promoting  $\text{As}^{\text{III}}$  oxidation by the activity of denitrifying bacteria. In addition to biotic processes discussed above, the adsorbed  $\text{As}^{\text{III}}$  on the surface of carbonate green rust could partially be oxidized by carbonate green rust (Su and Puls, 2004).

Like As, antimony (Sb) and its compounds are a hazardous pollutant by a greater toxicity than As. The concentration of Sb initially was  $\sim 25 \mu\text{g L}^{-1}$  in the FFT porewater and  $>5 \mu\text{g L}^{-1}$  in the cap water used for our experiment (Fig 3.8) which were very close to the maximum acceptable concentration recommended by EPA ( $6 \mu\text{g L}^{-1}$  in drinking water) (EPA, 1999) and even higher than recommendation value of Council of the European Communities (CEC) ( $5 \mu\text{g L}^{-1}$  in drinking water) (CEC, 1998). Similar to As, the concentrations of Sb decreased in the porewater and cap water of columns during experiment period. Mitsunobu et al. (2008) conducted an experiment on the abiotic reduction of Sb by green rust. Antimony can be precipitated with sulfide biotically or strongly adsorbed on the Fe minerals (such as goethite) (Polack et al., 2009; Leuz et al., 2006; Wang et al. 2013). Therefore, based on the results of decreased sulfate in the porewater and cap water particularly of amended columns (Fig 3.6) and the results of sequential extraction (Fig 3.13) which indicated Fe-Mn oxides and organic-sulfide bound fractions as a main hosts of Sb in FFT, it could be concluded that in amended FFT, abiotic and biotic processes accelerated the precipitation of Sb and decreased the concentration of Sb in the porewater and cap water of amended columns through bounding to the surface of iron hydr (oxides) or precipitation of Sb with sulfide.

The concentrations of Mo decreased in the cap water and porewater of unamended and amended columns. However, the Mo removal process was accelerated in amended columns (Fig 3.9). Under anaerobic conditions, Mo could be released from the dissolution of Fe and/or Mn oxides and again immobilize through precipitation and/or sorption to the newly formed metal sulfides (Smedley and Kinniburgh, 2017), including FeS (Helz et al., 2004), pyrite (Vorlicek et al., 2004). This findings are similar to our results where Fe reduced under methanogenic conditions particularly in HCN FFT and new forms of iron, FeS, was produced (Fig 3.11). In the presence of sulfide in the solution, the accumulation of Mo increase several times (McManus et al. 2006).

Although, the porewater and cap water of columns contained low concentration of sulfate (Fig 3.6) and the precipitation of Mo with sulfide could be concluded as a Mo removal process in FFT.

Although, the concentration of Cr was initially  $>0.2 \mu\text{gL}^{-1}$  and  $>0.8 \mu\text{gL}^{-1}$  in the porewater and cap water of columns, respectively (Fig 3.9). In unamended, HC, HCN, and HCNP columns, the concentration of Cr decreased in the porewater and cap water. However, the difference in the decreased Cr concentrations in unamended and amended columns was negligible (Fig 3.9). Our sequential extraction results indicated that, main host of Cr is residual fractions (Fig 3.14). The initial concentration of V was  $>11.8 \mu\text{gL}^{-1}$  in the porewater and  $>1.8 \mu\text{gL}^{-1}$  in the cap water in our experiment (Fig 3.9). As observed in Fig 3.9, the concentrations of V in the porewater and cap water of unamended columns indicated no significant differences during the experiment period. However, V removal was detected in the amended columns particularly in HCN columns (Fig 3.9). The fractionation of V also showed that main source of V in FFT is residual fraction that is no longer easily available part (Fig 3.14). Some researchers (Anderson et al., 2004; Marwijk et al., 2009) have reported the bioreduction of V by bacteria and archaea are capable to reduce  $\text{V}^{\text{V}}$  (soluble) to  $\text{V}^{\text{IV}}$  (insoluble). Yelton et al., (2013) conducted an experiment to decrease the aqueous concentration of  $\text{V}^{\text{V}}$  via contaminated sediments biostimulation. Their findings indicated that the bioreduction of  $\text{V}^{\text{V}}$  occurred through the electron transfer during microbial  $\text{V}^{\text{V}}$  respiration and precipitation of  $\text{V}^{\text{IV}}$ . These two processes might also have happened in our FFT samples and accelerate the microbial reduction of  $\text{V}^{\text{V}}$  in amended columns particularly HCN columns. Interestingly, relatively higher V removal was also observed in the pore water of HCNP columns compared with the porewater of HC columns which could be attributed to precipitation of sincosite  $[\text{CaV}_2(\text{PO}_4)_2(\text{OH})_4 \cdot 3\text{H}_2\text{O}]$  (Anderson et al., 2004; Zhang et al., 2014).

The concentrations of NAs in the cap water and porewater of unamended column at day 190 didn't change significantly compared with initial cap water and pore water samples at day 0. However, the concentrations of NAs decreased in the cap water and pore water of amended columns by day 190 (Fig 3.15). The decrease in NAs concentrations in amended columns might be attributed to some NAs biodegradation. Under anaerobic conditions, indigenous microbial communities in oil sands tailings can use simplest forms of NAs as carbon sources and stimulate methanogenesis (Clothier and Gieg, 2016). In the study on the methanogenic cultures from sewage sludge and tailings ponds, the findings indicated that the presence of surrogate NAs such as CHPA and CHCA in the cultures can stimulate methanogenesis (Holowenko et al., 2001; Clothier and

Gieg, 2016). Clothier and Gieg (2016) have indicated that biodegradation of NAs (CHCA) in methanogenic cultures is a function of the cooperation of syntrophs (*Clostridium*, *Syntrophus*) and acetate- and H<sub>2</sub>-utilizing methanogens, particularly *Methanosaeta*. Similar microbial community results were also observed in all of our amended columns (HC, HCN, HCNP) during the active methanogenesis with the higher and lower abundances of both bacteria and archaea in HCN and HCNP FFTs, respectively compared with HC FFTs (Chapter 2, Fig 2.4). It can be concluded that anaerobic biodegradation of NAs might be a function of the presence and the abundance of specific types of microbial communities. Interesting results were also observed where we found significantly highest decrease of NAs in cap water and porewater of HCN FFT samples under active methanogenesis (Fig 3.15). Herman et al. (1994) indicated that NAs biodegradation was a function of nitrogen and phosphorous availability. However, in the simulated wetlands microcosms contain oil sands process that was conducted by Toor et al., (2013), nitrogen and phosphorous addition didn't improve the biodegradation of NAs. Similarly, the addition of phosphorous in this study didn't significantly reduce the concentrations of NAs in either cap water or porewater of HCNP columns, likely the concentration of phosphorous was greater than what was required to enhance NAs degradation or the metabolic byproducts was accumulated in this closed system (Lai, 1996).

### 3.6 Conclusion

Due to stimulated methanogenesis in the presence of N source, higher biogenic gas (CH<sub>4</sub> and CO<sub>2</sub>) was produced in HCN FFT than HC and HCNP FFT. Consequently, higher contents of carbonate minerals were dissolved that led to the significantly enhanced concentration of cations (Ca and Mg) and anion (HCO<sub>3</sub><sup>-</sup>) in the porewater and cap water of HCN. This resulted in increased ionic strength of the pore water which in turn reduced the electrical double layer associated with clay particles and enhanced significantly consolidation and dewatering of HCN FFT. Also, higher transformation of Fe<sup>III</sup> minerals to amorphous Fe<sup>II</sup> minerals and the formation of amorphous iron sulfides in HCN FFT reduced the surface charges of clay particles and increased the aggregation of clays and pores' network and in turn increased the release of pore water from HCN FFT. Therefore, the transformation (dissolution and precipitation) of minerals under stimulated methanogenesis enhanced the porewater release and increased the remobilization of trace metals such as Sr. The total Sr and Ba concentrations in the pore water of HCN suggested enhanced partitioning under stimulated methanogenesis. The reductive dissolution of Fe (hydr) oxides was

also more obvious in HCN than HC and HCNP FFT. The concentration of the other trace metals of interest including As, Sb, Mo, V, and Cr was decreased in the pore and cap water of all amended FFT. Although, the accelerated removal of As, V, and Cr from pore water was observed in HCN FFT. The concentrations of NAs were also decreased in the porewater and cap water of all amended columns. This understanding might be used in remediation strategies in contaminated sites. The inorganic constituent's fluxes indicated that upward movement of these ions and trace metals at FFT water interface significantly depended to the promoted bacterial activity. The enhanced mobility of inorganic constituents is a concern as increased mobilization generally lead to elevated concentrations in surface water of EPLs and pose a potential risk to aquatic life, human, and other organisms. Still more detail and longer monitoring would be important for the better understand of the source and the fate of inorganic constituents, particularly trace metals in this complex system.

### 3.7 References

- Ahern, C.R., McElnea, A.E., & Sullivan, L.A. (1998). *Acid sulfate soils laboratory methods guidelines*. Wollongbar, NSW: Acid Sulfate Soil Management Advisory Committee.
- Alberta Government. (2015). Alberta's Oil Sands – about the Resource. Retrieved from <http://oilsands.alberta.ca/resource.html>.
- Allen, E.W. (2008). Process water treatment in Canada's oil sands industry: I. Target pollutants and treatment objectives. *Journal of Environmental Engineering Science*, 7(2): 123-138.
- Anderson, O.R.T., Vrionis, H.A., Lovley, D.R. (2004). Vanadium respiration by *Geobacter metallireducens*: novel strategy for in situ removal of vanadium from groundwater. *Applied Environmental Microbiology*, 70, 3091-3095.
- Arkell, N., Kuznetsov, P., Kuznetsova, A., Foght, J. M., & Siddique, T. (2015). Microbial metabolism alters pore water chemistry and increases consolidation of oil sands tailings. *Journal of Environment Quality*, 44(1), 145–153. doi:10.2134/jeq2014.04.0164
- Arshad, M., Khosa, M. A., Siddique, T., & Ullah, A. (2016). Modified biopolymers as sorbents for the removal of naphthenic acids from oil sands process affected water (OSPW). *Chemosphere*, 163, 334-341.
- Bolliger, C., Schroth, M. H., Bernasconi, S. M., Kleikemper, J. & Zeyer, J. (2001). Sulfur isotope fractionation during microbial reduction by toluene-degrading bacteria. *Geochimica et Cosmochimica Acta*, 65 (19), 3289–3298.
- Canadian Council of Ministers of the Environment. (1997). *Canadian water quality guidelines: Arsenic, bromacil, carbaryl, chlorpyrifos, deltamethin, and glycols*. Winnipeg: Canadian Council of Ministers of the Environment.
- CEC. (1998). *The quality of water intended for human consumption*. Brussels, Belgium: Council of the European Communities.
- Cumulative Environmental Management Association. (2012a). *Experiences from non-oil sands pit lakes*. Fort McMurray, AB, Canada: CEMA.
- Cumulative Environmental Management Association. (2012b). *End pit lakes guidance document*. (No. 37(12)). Fort McMurray, AB, Canada: CEMA.
- Charette, M.A., & Sholkovitz, E.R. (2006). Trace element cycling in a subterranean estuary: Part 2. Geochemistry of the pore water. *Geochimica et Cosmochimica Acta*, 70, 811–826.

- Chen, M., Walshe, G., Chi Fru, E., Ciborowski, J.J.H. & Weisener, C.G. (2013). Microcosm assessment of the biogeochemical development of sulfur and oxygen in oil sands fluid fine tailings. *Applied Geochemistry*, 37, 1-11.
- Chou, L., R.M. Garrels, & R. Wollast. (1989). Comparative study of the kinetics and mechanisms of dissolution of carbonate minerals. *Chemical Geology*. 78(3-4), 269–282. doi: 10.1016/0009-2541(89)90063-6
- Clothier, L.N., & Gieg, L.M. (2016). Anaerobic biodegradation of surrogate naphthenic acids. *Water Resources*. 90, 156–166.
- Devi, M. P., Reddy, M. V., Juwarkar, A., Sarma, P. N. & Mohan, S. R. V. (2011). Effect of Co-culture and nutrients supplementation on bioremediation of crude petroleum sludge. *Clean Soil, Air, and Water*, 39 (10), 900–907.
- Dompierre, K. A., Lindsay, M. B. J., Cruz-Hernández, P., & Halferdahl, G. M. (2016). Initial geochemical characteristics of fluid fine tailings in an oil sands end pit lake. *Science of the Total Environment*, 556, 157-177
- Ebrahimi, P., & Vilcaez, J. (2018). Petroleum produced water disposal: Mobility and transport of barium in sandstone and dolomite rocks. *Science of the Total Environment*. 1(634), 1054-1063. doi:10.1016/j.scitotenv.2018.04.067.
- EPA. (1999). *National primary drinking water standards*. Washington, DC: US EPA Office of Water.
- EPA. (2014). *Announcement of preliminary regulatory determinations for contaminants*. (No. 79 (202)). Third Drinking Water Contaminant Candidate List.
- Essington, M. E. (2004). *Soil and water chemistry: An integrative approach*. Boca Raton, FL: CRC.
- Fedorak, P. M., Coy, D. L., Dudas, M. J., Simpson, M. J., Renneberg, J., & MacKinnon, M. D. (2003). Microbially-mediated fugitive gas production from oil sands tailings and increased tailings densification rates. *Journal of Environmental Engineering & Science*, 2, 199–211. doi:10.1139/S03-022
- Finneran, K. T., Johnsen, C. V. & Lovley, D. R. (2003). *Rhodoferrax ferrireducens* sp. nov., a psychrotolerant, facultative anaerobic bacterium that oxidizes acetate with the reduction of Fe (III). *International Journal of Systematic and Evolutionary Microbiology*, 53, 669–673.

- Fotidis, I. A., Karkashev, D., Kotsopounlos, T.A., Martzopoulos, G. G., & Angleildaki, I. (2013). Effect of ammonium and acetate on methanogenic pathway and methanogenic community composition. *FEMS Microbiology Ecology*, 83, 38-48.
- Helz, G.R., Vorlicek, T.P., & Kahn, M.D. (2004). Molybdenum scavenging by iron monosulfides. *Environmental Science & Technology*, 38, 4263-4268.
- Herman, D.C., Fedorak, P.M., MacKinnon, M.D., & Costerton, J.W. (1994). Biodegradation of naphthenic acids by microbial populations indigenous to oil sands tailings. *Canadian Journal of Microbiology*, 40, 467-477.
- Holowenko, F.M., Mackinnon, M.D., & Fedorak, P.M. (2001). Naphthenic acids and surrogate naphthenic acids in methanogenic microcosms. *Water Resources*. 35(2), 595-606.
- Hu, M., Li, F., Liu, C., & Wu, W. (2015). The diversity and abundance of As (III) oxidizers on root iron plaque is critical for arsenic bioavailability to rice. *Scientific Reports*, 5, 13611. doi: 10.1038/srep13611
- Huerta-Diaz, M. A., Carignan, R., & Tessier, A. (1993). Measurement of trace metals associated with acid volatile sulfides and pyrite in organic freshwater sediments. *Environmental Science & Technology*, 27, 2367-2372.
- Hull, L.C., & Schafer, A.L. (2008). Accelerated transport of Sr-90 following a release of high ionic strength solution in vadose zone sediments. *Journal of Contaminant Hydrology*, 97, 135-157.
- Jivraj, M., MacKinnon, M., & Fung, B.(1995). Naphthenic acid extraction and quantitative analysis with FT-IR spectroscopy. *Syncrude analytical manuals*. Edmonton, AB: Syncrude Canada Ltd.
- Kabwe, L.K., Scott, J.D., Beier, N.A., Wilson, G.W., & Jeeravipoolvarn, S. (2018). Environmental implications of end pit lakes at oil sand mines in Alberta, Canada. *Environmental Geotechnics*, 1-8. <https://doi.org/10.1680/jenge.17.00110>
- Kasperski, K. L., & Mikula, R. J. (2011). Waste streams of mined oil sands: characteristics and remediation. *Elements*, 7(6), 387-392. doi:10.2113/gselements.7.6.387
- Kavanagh, R. J., Frank, R.A., Oakes, K.D., Servos, M.R., Young, R.F., Fedorak, P.M., ... Van Der Kraak, G. (2011). Fathead minnow (*Pimephales promelas*) reproduction is impaired in aged oil sands process-affected waters. *Aquatic Toxicology*, 101, 214-220.
- Kuo, S. (1996). Phosphorus in methods of soil analysis: Part3. *Chemical methods* (pp. 869-919). Madison, Wisconsin: SSSA.

- Lai, J.W., Pinto, L.J., Kiehlmann, E., Bendell-Young, L.I., & Moore, M.M. (1996). Factors that affect the degradation of naphthenic acids in oil sands wastewater by indigenous microbial communities. *Environmental Toxicology and Chemistry*, 15 (9), 1482–1491.
- Langley, S., Gault, A.G., Ibrahim, A., Takahashi, Y., Renaud, R., Fortin, D., Clark, L.D., & Ferris, F.G. (2009). Strontium desorption from bacteriogenic iron oxides (BIOS) subjected to microbial Fe(III) reduction. *Chemical Geology*. 262(3), 217–228
- Leuz, A.K., Monch, H., & Johnson, C.A. (2006). Sorption of Sb (III) and Sb(V) to goethite: influence on Sb(III) oxidation and mobilization. *Environmental Science and Technology*. 40(23), 7277 –7282.
- Li, J., Wang, Q., Oremland, R.S., Kulp, T.R., Rensing, C., Wang, G., & Drake, H.L. (2016). Microbial antimony biogeochemistry: enzymes, regulation, and related metabolic pathways. *Applied and Environmental Microbiology*, 82, 5482-5495.
- Lovley, D.R., & Phillips, E.J.P. (1986). Organic matter mineralization with reduction of ferric iron in anaerobic sediments. *Applied and Environmental Microbiology*, 51, 683–689.
- Marwijk, J.V., Opperman, D.J., Piater, L.A., & Heerden, E.V. (2009). Reduction of vanadium (V) by *Enterobacter cloacae* EV-SA01 isolated from a South African deep gold mine *Biotechnology Letters*, 31(6), 845-849
- McManus, J., Berelson, W. M., Severmann, S., Poulson, R. L., Hammond, D. E., Klinkhammer, G. P., & Holm, C. (2006). Molybdenum and uranium geochemistry in continental margin sediments: Paleoproxy potential. *Geochimica et Cosmochimica Acta*, 70(18), 4643–4662.
- Mitsunobu, S., Takahashi, Y., & Sakai, Y. (2008). Abiotic reduction of antimony (V) by green rust (Fe<sub>4</sub>(II)Fe<sub>2</sub>(III)(OH)<sub>12</sub>SO<sub>4</sub>·3H<sub>2</sub>O). *Chemosphere*. 70(5), 942 –947.
- Mohamad Shahimin, M.F., & Siddique, T. (2017a) .Methanogenic biodegradation of paraffinic solvent hydrocarbons in two different oil sands tailings. *Science of the Total Environment*. 583,115–122
- Mohamad Shahimin, M.F., & Siddique, T. (2017b). Sequential biodegradation of complex naphtha hydrocarbons under methanogenic conditions in two different oil sands tailings. *Environmental Pollution*, 221, 398–406
- Morse, J. W., Millero, F. J., Cornwell, J. C. & Rickard, D. (1987). The Chemistry of the hydrogen sulfide and iron sulfide systems in natural waters. *Earth Science Reviews*, 24(42), 1–42.

- Morse, J.W., R.S., Arvidson, A., & Luttge. (2007). Calcium carbonate formation and dissolution. *Chemical Reviews*, 107(2), 342–381. Doi: 10.1021/cr050358j
- Moulin, E., A. Jordens, & R. Wollast. (1985). Influence of the aerobic bacterial respiration on the early dissolution of carbonates in coastal sediments. In R., Van Grieken, and R. Wollast (Ed.), *Progress in belgian oceanographic research* (pp. 196–208). Brussels, Belgium: University of Antwerpen.
- O'Day, P.A. Vlassopoulos, D., Root, R., & Rivera, N. (2004). The influence of sulfur and iron on dissolved arsenic concentrations in the shallow subsurface under changing redox conditions. *Proceedings of the National Academy of Sciences of the United States of America*. 101(38), 13703–13708
- Osacky, M., Geramian, M., Dyar, M.D., Sklute, E.C., Valter, M., Ivey, D.G., Liu, Q., & Etsell, T.H. (2013). Characterization of petrologic end members of oil sands from the Athabasca region, Alberta, Canada. *The Canadian Journal of Chemical Engineering*, 91(8), 1402-1415.
- Oremland, R.S., & Stolz, J.F. (2005). Arsenic, microbes and contaminated aquifers. *Trends in Microbiology*, 13(2), 45–49.
- Pansu, M., Gautheyrou, J. (2006). *Handbook of soil analysis. Mineralogical, organic and inorganic methods*. Berlin; Heidelberg: Springer- Verlag. Doi:10.1007/978-3-540-31211-6
- Penner, T. J., Foght, J. M. (2010). Mature fine tailings from oil sands processing harbor diverse methanogenic communities. *Canadian Journal of Microbiology*, 56, 459–470. doi:10.1139/W10-029
- Polack, R., Chen, Y.W., & Belzile, N. (2009). Behavior of Sb(V) in the presence of dissolved sulfide under controlled anoxic aqueous conditions. *Chemical Geology*, 694(262), 179 –185.
- Ramos-Padrón, E., Bordenave, S., Lin, S., Bhaskar, I.M., Dong, X., Sensen, C.W., Fournier, J., Voordouw, G. & Gieg, L.M. (2011). Carbon and sulfur cycling by microbial communities in a gypsum-treated oil sands tailings pond. *Environmental Science & Technology*, 45(2):439-446.
- Rauret, G., Lo'pez-Sa'nchez, J.F., Sahuquillo, A., Rubio, R., Davidson, C.M., Ure, A., Quevauviller, P. (1999). Improvement of the BCR three step sequential extraction procedure prior to the certification of new sediment and soil reference materials. *Journal of Environmental Monitoring*, 1, 57 – 61.

- Robins, C.R., Brock-Hon, A.L., & Buck, B.J. (2012). Conceptual Mineral Genesis Models for Calcic Pendants and Petrocalcic Horizons, Nevada. *Soil Use and Management*, 29(2), 295-295.
- Sarkar, J., Kazy, S. K., Gupta, A., Dutta, A., Mohapatra, B., Roy, A., Bera, P., Mitra, A., & Sar, P. (2016). Biostimulation of Indigenous Microbial Community for Bioremediation of Petroleum Refinery Sludge. *Frontiers in Microbiology*. 7, 1407. doi: 10.3389/fmicb.2016.01407.
- Scandella, B.P., Varadharajan, C., Hemond, H.F., Ruppel, C. & Juanes, R. (2011). A conduit dilation model of methane venting from lake sediments. *Geophysical Research Letters*, 38(6), L06408.
- Siddique, T., Fedorak, P.M., & Foght, J.M. (2006). Biodegradation of short-chain n-alkanes in oil sands tailings under methanogenic conditions, *Environmental Science and Technology*, 40, 5459-5464.
- Siddique, T., Fedorak, P.M., MacKinnon, M.D., & Foght, J.M. (2007). Metabolism of BTEX and naphtha compounds to methane in oil sands tailings, *Environmental Science and Technology*, 41, 2350-2356.
- Siddique, T., P. Kuznetsov, A. Kuznetsova, N. Arkell, R. Young, S. Guigard, & J.M. Foght. (2014a). Microbially accelerated consolidation of oil sands tailings. Pathway I: Changes in porewater chemistry. *Frontiers in Microbiology*, 5,106. doi:10.3389/fmicb.2014.00106
- Siddique, T., Kuznetsov, P., Kuznetsova, A., Li, C., Young, R., Arocena, J.M., & Foght, J.M. (2014b). Microbially-accelerated consolidation of oil sands tailings. Pathway II: solid phase biogeochemistry. *Frontiers in Microbiology*, 5,107. doi: 10.3389/fmicb.2014.00107
- Siddique, T., Penner, T., Semple, K., & Foght, J. M. (2011). Anaerobic biodegradation of longerchainn-alkanes coupled to methane production in oil sands tailings. *Environmental Science & Technology*, 45(13), 5892–5899. Doi: 10.1021/es200649t
- Siddique, T., Stasik, S., Mohamad Shahimin, M. F., & Wendt-Potthoff, K. (2018). Microbial communities in oil sands tailings: Their implications in biogeochemical processes and tailings management. In T. J. McGenity (Ed.), *Microbial communities utilizing hydrocarbons and lipids: Members, metagenomics and ecophysiology* (pp. 1-33) Springer.
- Smedley, P.L., & Kinniburgh, D.G. (2017). Molybdenum in natural waters: A review of occurrence, distributions and controls. *Applied Geochemistry*, 84, 387-432.

- Sorensen, J. (1982). Reduction of ferric iron in anaerobic, marine sediment and interaction with reduction of nitrate and sulfate. *Applied & Environmental Microbiology*, 43, 319–324.
- Stasik, S., Loick, N., Knoeller, K., Weisener, C. & Wendt-Potthoff, K. (2014). Understanding biogeochemical gradients of sulfur, iron and carbon in an oil sands tailings pond. *Chemical Geology*, 382, 44-53.
- Stasik, S., & Wendt-Potthoff, K. (2014). Interaction of microbial sulphate reduction and methanogenesis in oil sands tailings ponds. *Chemosphere*, 103, 59-66.
- Stat Soft, I. (2011). *STATISTICA (data analysis software system)*
- Sun, W. J., Sierra, R., & Field, J. A. (2008). Anoxic oxidation of arsenite linked to denitrification in sludges and sediments. *Water Resources*, 42, 4569–4577.
- Thorpe, C.L., Lloyd, J.R., Law, G.T.W., Burke, I.T., Shaw, S., Bryan, N.D., & Morris, K. (2012). Strontium sorption and precipitation behaviour during bioreduction in nitrate impacted sediments,” *Chemical Geology*, (306–307), 114–122.
- Tonkin, J.W., Balistrieri, L.S., & Murray, J.W (2004). Modeling sorption of divalent metal cations on hydrous manganese oxide using the diffuse double layer model. *Applied Geochemistry*, 19, 29–53.
- Toor, N.S., Franz, E.D., Fedorak, P.M., MacKinnon, M.D., & Liber, K., 2013. Degradation and aquatic toxicity of naphthenic acids in oil sands process-affected waters using simulated wetlands. *Chemosphere*, 90, 449–458.
- US EPA. (1974). *Method 310.2. Alkalinity (colorimetric, automated, methyl orange)*. Retrieved from [http://water.epa.gov/scitech/methods/cwa/methods\\_index.cfm](http://water.epa.gov/scitech/methods/cwa/methods_index.cfm)
- US EPA. (2007). *Method 3050B. Acid Digestion of Sediments, Sludges, and Soils*. Retrieved from [http://www.epa.gov/wastes/hazard/testmethods/sw846/online/3\\_series.htm](http://www.epa.gov/wastes/hazard/testmethods/sw846/online/3_series.htm)
- Voordouw, G. (2013). Interaction of oil sands tailings particles with polymers and microbial cells: First steps toward reclamation to soil. *Biopolymers*, 99, 257–262. doi:10.1002/bip.22156
- Vorlicek, T.P., Kahn, M.D., Kasuya, Y., & Helz, G.R. (2004). Capture of molybdenum in pyrite-forming sediments: role of ligand-induced reduction by polysulfides. *Geochimica et Cosmochimica Acta*, 68, 547-556
- Wallace, S.H., Shaw, S., Morris, K., Small, J.S., Fuller, A.J., & Burke, I.T. (2012). Effect of groundwater pH and ionic strength on strontium sorption in aquifer sediments: Implications for <sup>90</sup>Sr mobility at contaminated nuclear sites. *Applied Geochemistry*, 27(8)1482–1491.

- Wang, H., Chen, F., Mu, S., Zhang, D., Pan, X., Lee, D.J., & Chang, J.S. (2013). Removal of antimony (Sb(V)) from Sb mine drainage: biological sulfate reduction and sulfide oxidation-precipitation. *Bioresource technology*, *146*, 799–802.
- Wersin, P., Leupin, O.X., Mettler, S., Gaucher, E.C., Mader, U., De Canniere, P., ... Eichinger, L. (2011). Biogeochemical processes in a clay formation in situ experiment: Part A. Overview, experimental design and water data of an experiment in the opalinus clay at the Mont terri underground research laboratory, Switzerland. *Applied Geochemistry*, *26*, 931–953. doi: 10.1016/j. apgeochem.2011.03.004
- Westcott, F. (2007). *Oil sands end pit lakes: A review to 2007*. (). Fort McMurray, AB, Canada: Cumulative Environmental Management Association End Pit Lakes Subgroup.
- White, K.B. (2017). Characterizing annual changes in the chemistry and toxicity of surface water from Base Mine Lake, an Alberta oil sands End Pit Lake. M.Sc. Thesis. University of Saskatchewan
- Yelton, A.P., Williams, K.H., Fournelle, J., Wrighton, K.C., Handley, K.M., & Banfield, J.F. (2013). Vanadate and acetate biostimulation of contaminated sediments decreases diversity, selects for specific taxa, and decreases aqueous V<sup>5+</sup> concentration. *Environmental Science and Technology*, *47*, 6500-6509.
- Zhang, J., Dong, H.L., Zhao, L.D., McCarrick, R., & Agrawal, A.(2014). Microbial reduction and precipitation of vanadium by mesophilic and thermophilic methanogens. *Chemical Geology*, *370*, 29-39.
- Zhang, Y. (2016). Development and Application of Fenton and UV-Fenton Processes at Natural pH Using Chelating Agents for the Treatment of Oil Sands Process-affected Water. PhD. Thesis. Alta University.

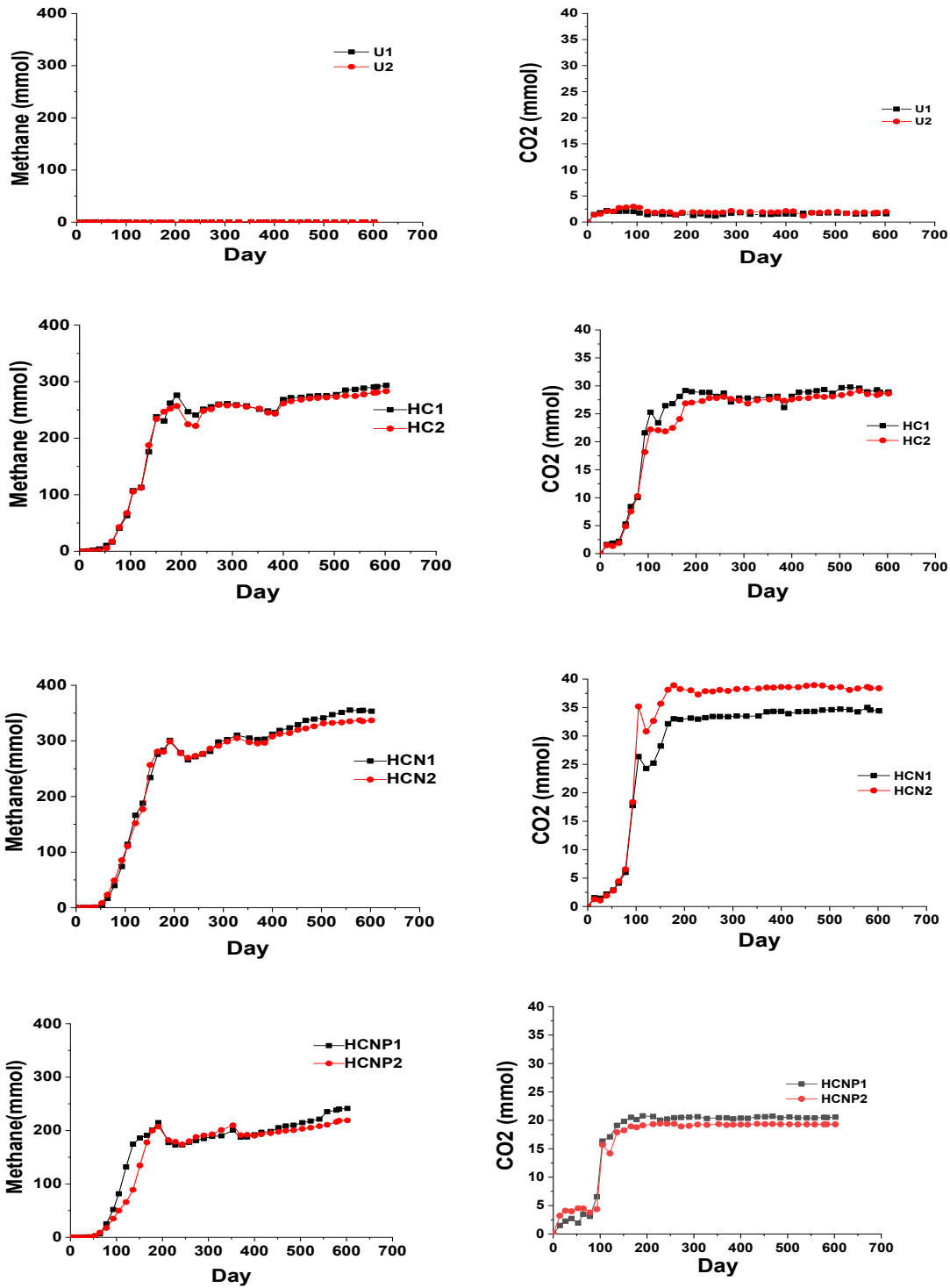


Figure 3-1. Cumulative emitted Methane (CH<sub>4</sub>) and carbon dioxide (CO<sub>2</sub>) measured in the headspace of methanogenic unamended and amended columns (2 columns per each treatment); U: unamended columns; HC: columns amended with hydrocarbon mixture; HCN: columns amended with hydrocarbon plus nitrogen; HCNP: columns amended with hydrocarbon plus nitrogen plus phosphorus

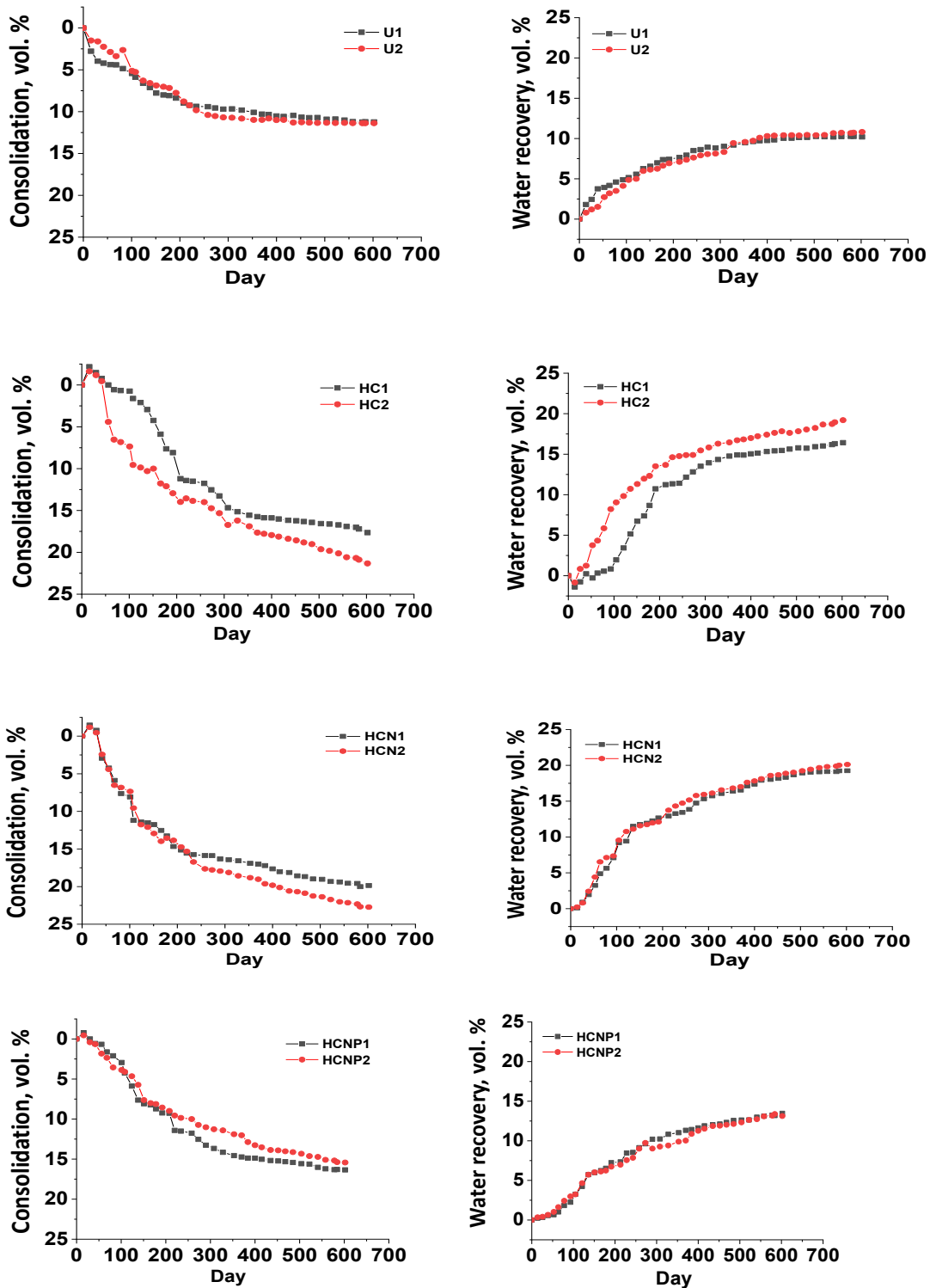


Figure 3-2. Consolidation and recovery of water in unamended (U) and amended (HC, HCN, HCNP) FFTs over incubation period. U: unamended columns; HC: columns amended with hydrocarbon mixture; HCN: columns amended with hydrocarbon plus nitrogen; HCNP: columns amended with hydrocarbon plus nitrogen plus phosphorus

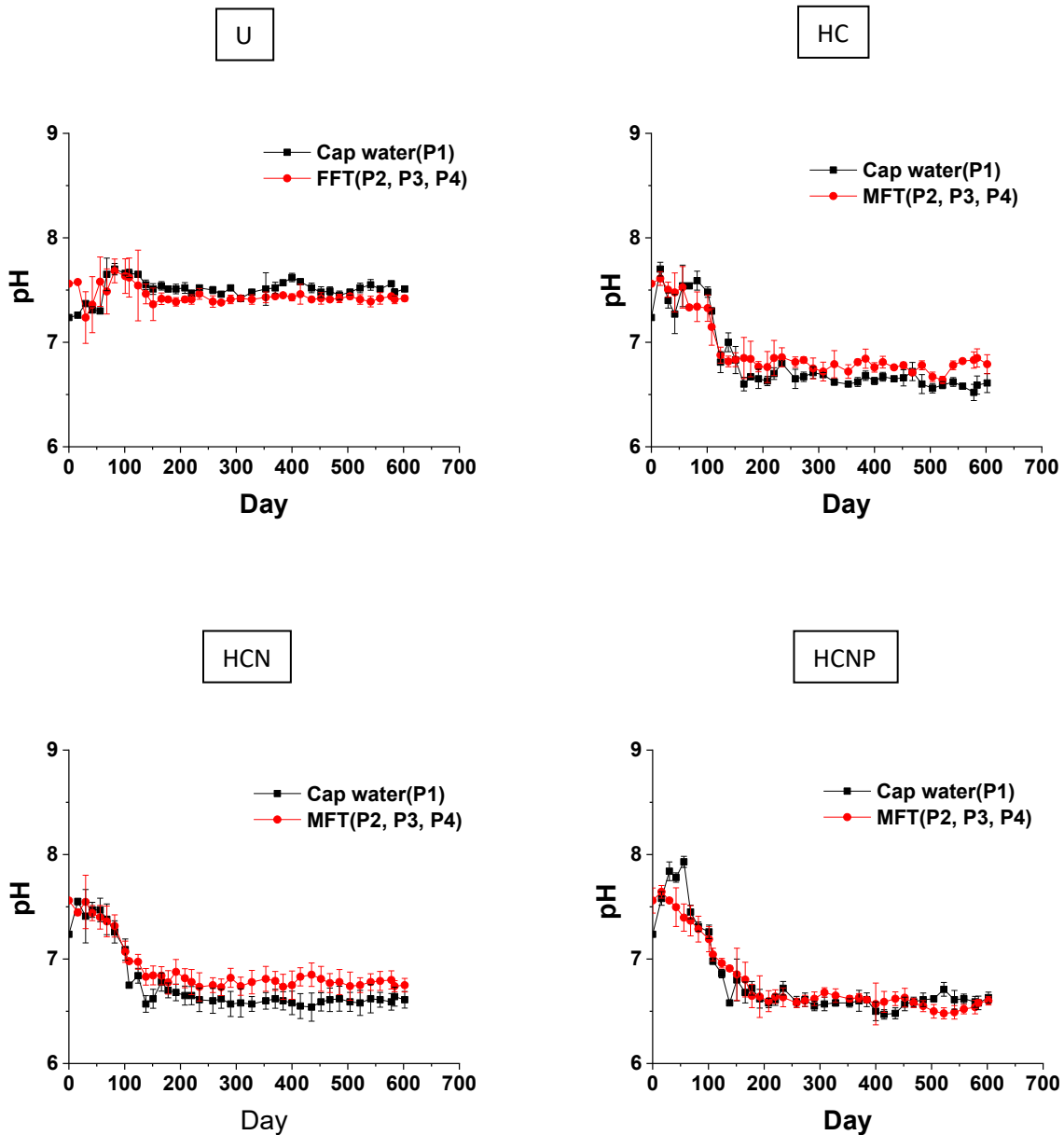


Figure 3-1 pH values in the pore- and cap-water of unamended (U) and amended (HC, HCN, and HCNP) columns. P1 refers to Port 1 located in the capwater and P2, P3, and P4 were below the mudline and accessed FFT (see Fig 2.1. at chapter 2). pH values measured at P1 (capwater) and at P2, P3, and P4 (the mean pH value of these 3 ports is given as a representative of pH in the FFT porewater per sampling time; error bars, where visible, represent 1 standard deviation).

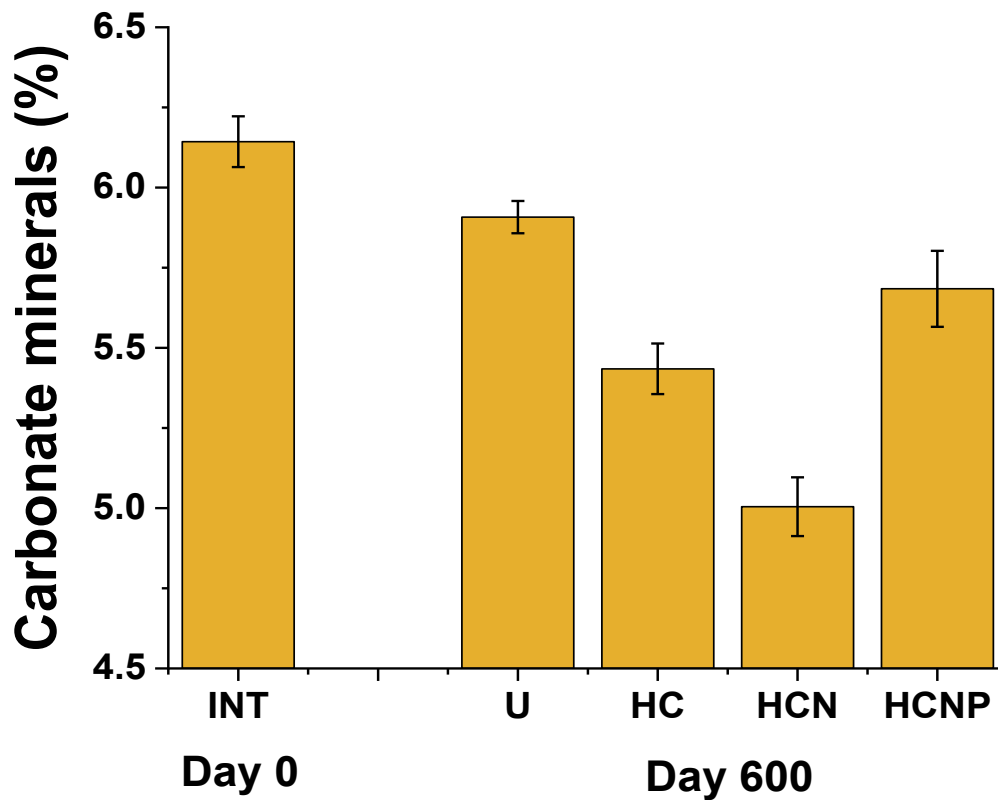


Figure 3-2. Carbonate mineral content in unamended (U) and amended (HC, HCN, HCNP) FFTs at day 0 and 600 days incubation. Bars represent the mean value from analysis of four replicates taken from port 4 of each column and the error bars, where visible, represent 1 standard deviation; U: unamended columns; HC: columns amended with hydrocarbon mixture; HCN: columns amended with hydrocarbon plus nitrogen; HCNP: columns amended with hydrocarbon plus nitrogen plus phosphorus

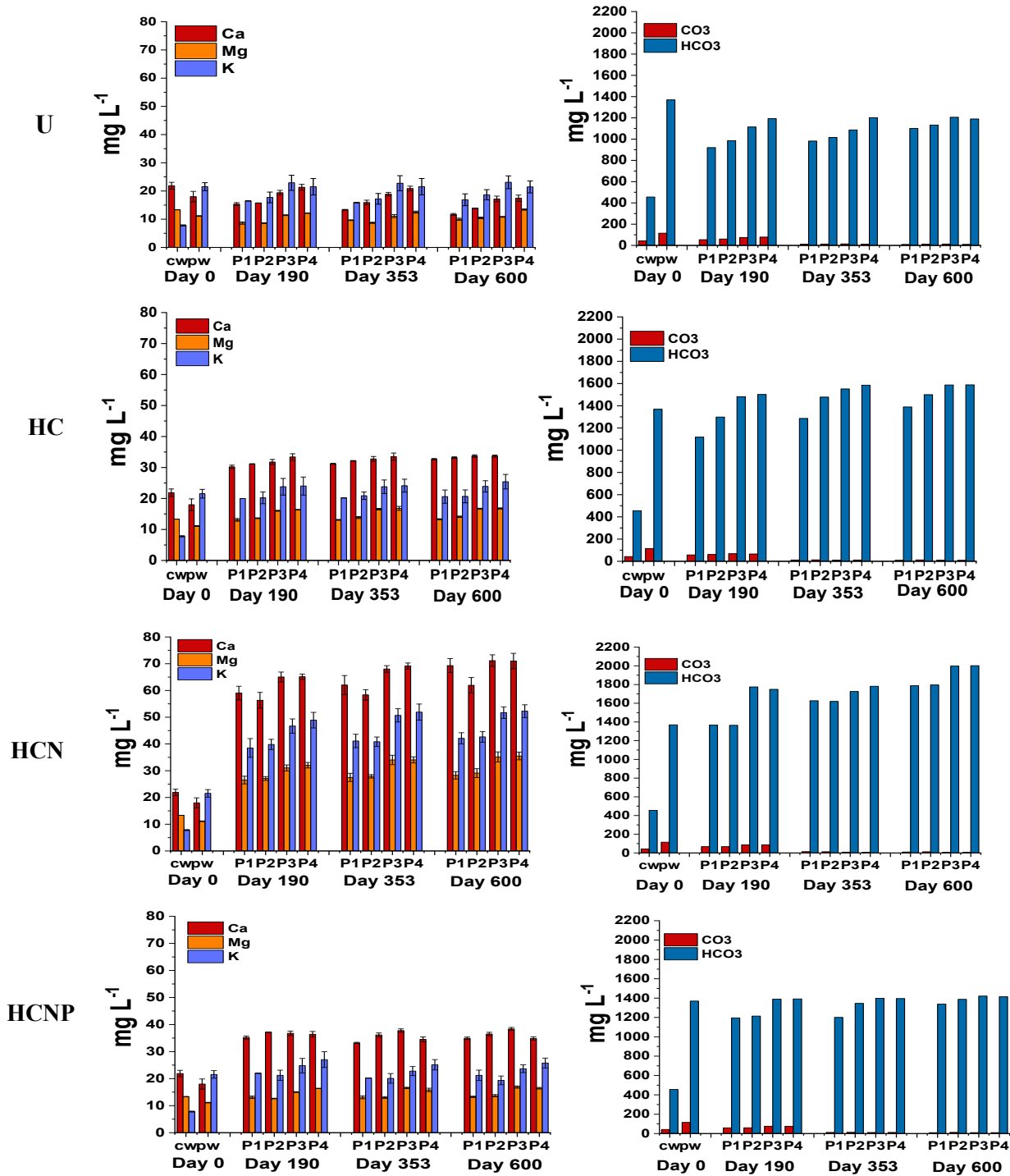


Figure 3-3. The concentrations of soluble cations and anions in the pore- and cap-water of unamended (U) and amended (HC, HCN, and HCNP) columns. P1 refers to Port 1 located in the capwater and P2, P3, and P4 were below the mudline and accessed FFT (see Fig 2.1. at Chapter 2). Left: Concentrations of major soluble cations in the cap- and porewater (Bars represent the mean from analysis of three replicates taken from each port and the error bars, where visible, represent 1 standard deviation). Right: Concentrations of major soluble carbonate and bicarbonate in the cap- and porewater.

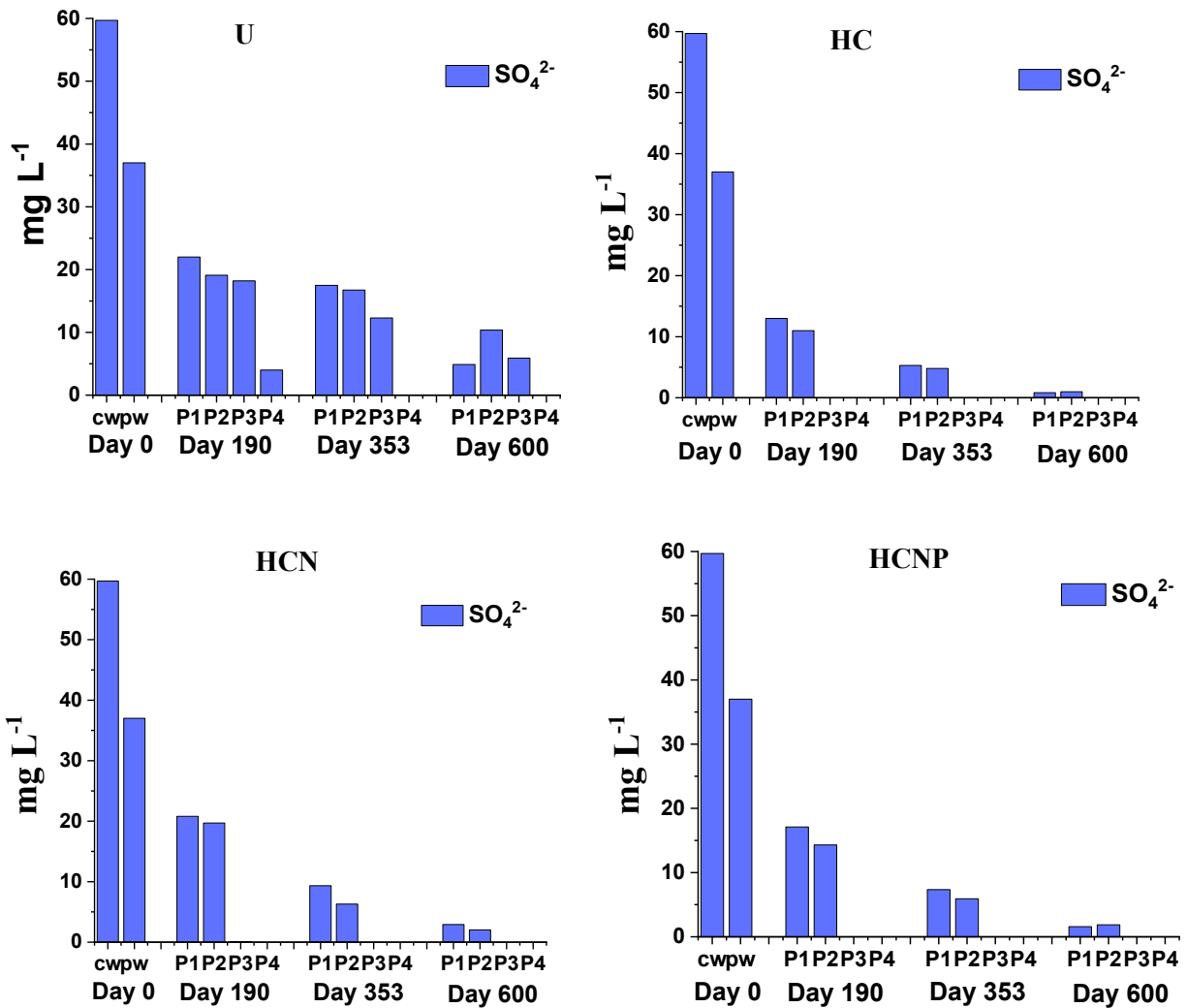


Figure 3-4. The concentration of sulfate in the pore- and cap-water of unamended (U) and amended (HC, HCN, and HCNP) columns. P1 refers to Port 1 located in the capwater and P2, P3, and P4 were below the mudline and accessed FFT (see Fig 2.1. at Chapter2).

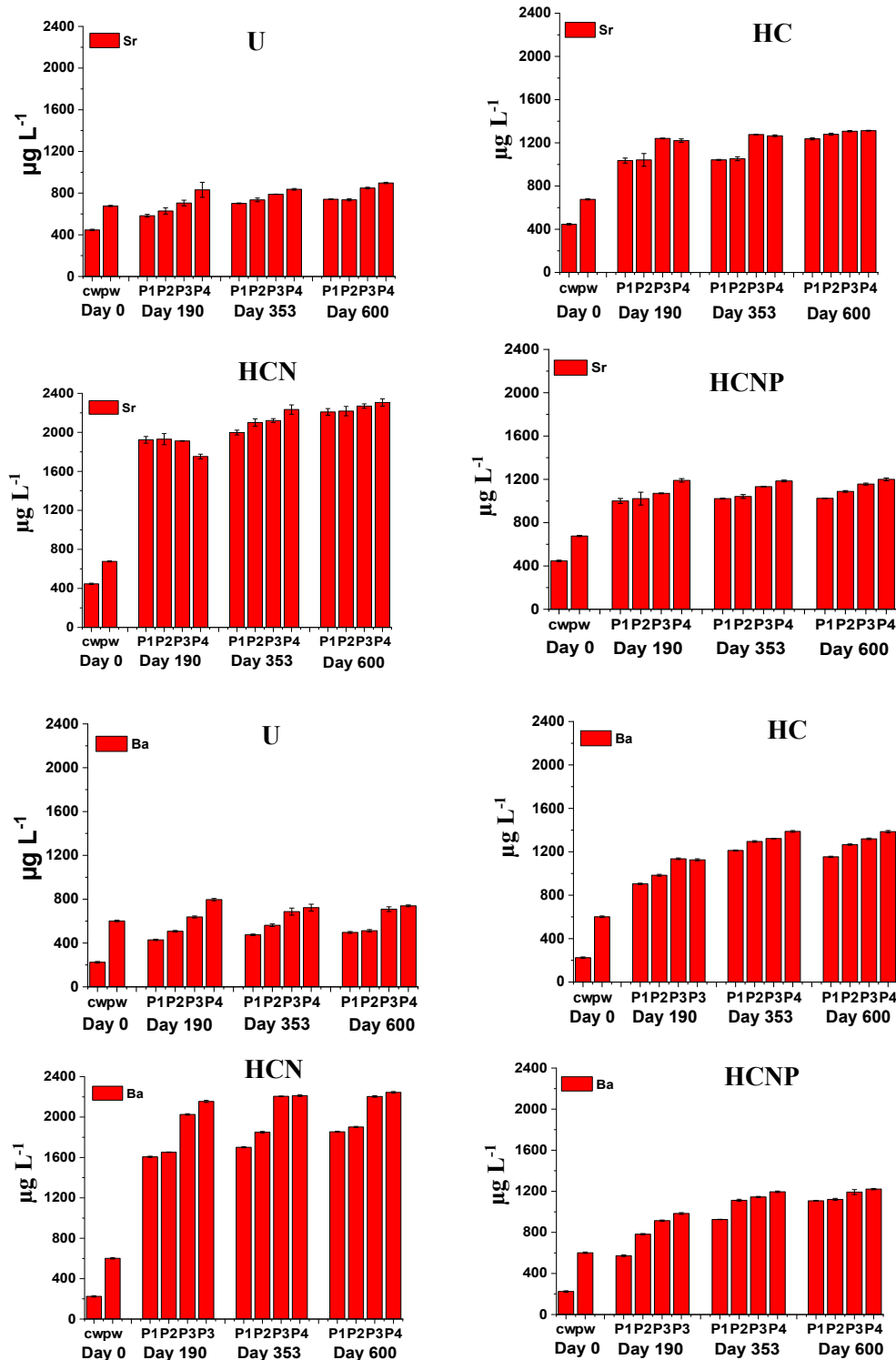


Figure 3-7. Total Sr and Ba concentrations in the capwater (cw) and porewater (pw) of unamended (U) and amended (HC, HCN, and HCNP) columns. HC, HCN, and HCNP respectively represent columns amended by hydrocarbon, hydrocarbon plus nitrogen, and hydrocarbon plus nitrogen plus phosphorous. P1 refers to Port 1 located in the capwater and P2, P3, and P4 were below the mudline and accessed FFT (see Fig 2.1. at chapter 2). Bars represent the mean from analysis of three replicates taken from the same ports in two replicated columns and the error bars, where visible, represent 1 standard deviation.

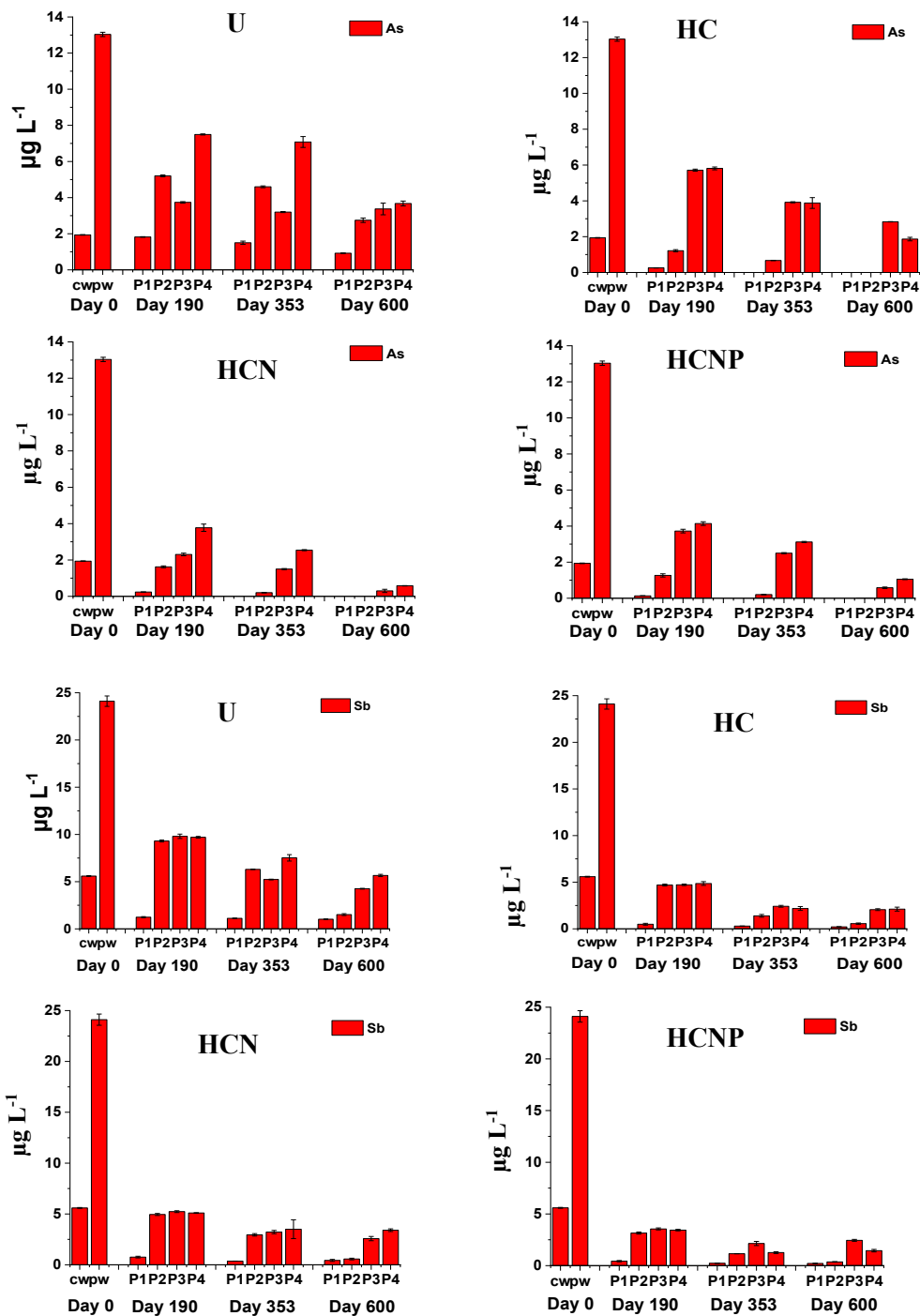
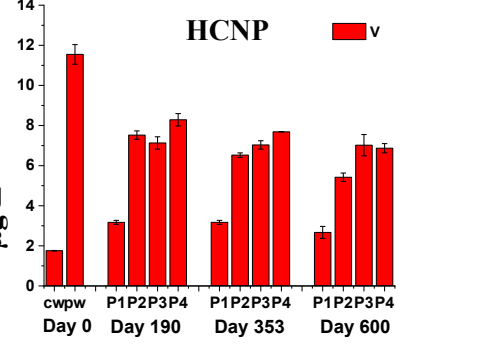
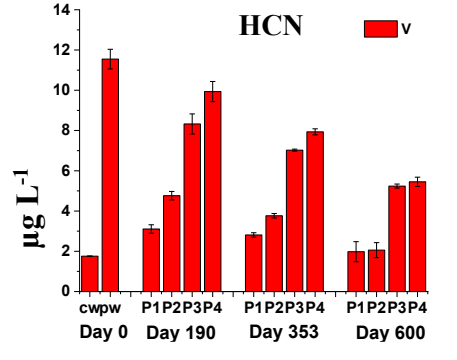
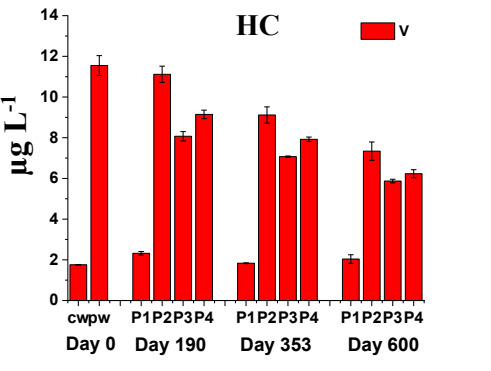
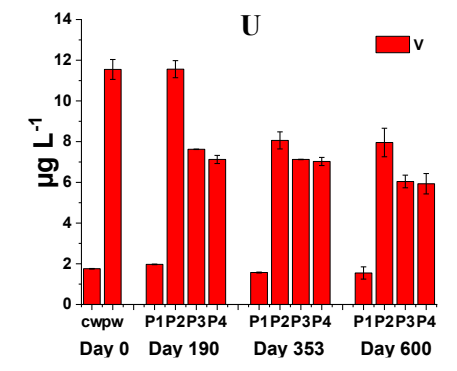
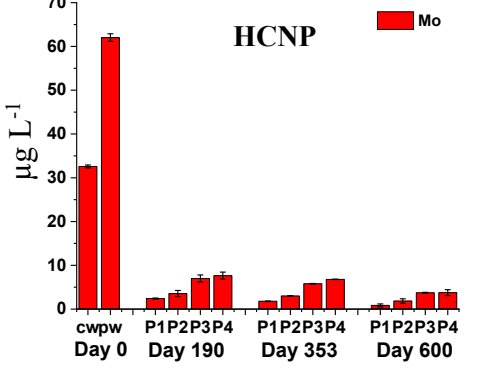
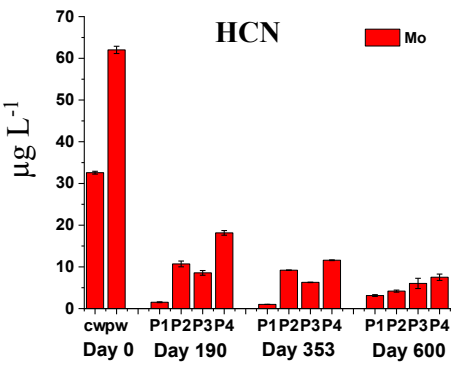
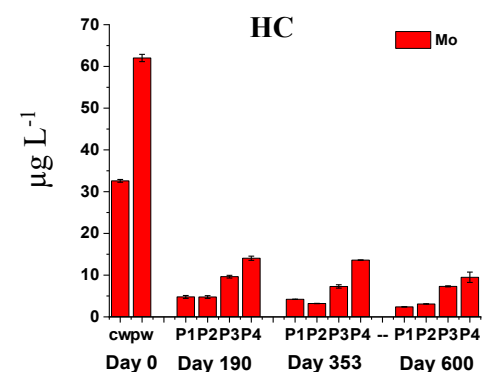
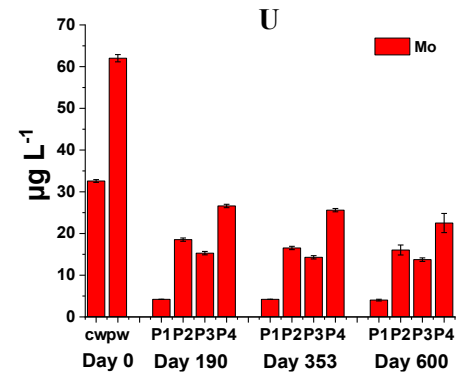


Figure 3-8. Total As and Sb concentrations in the capwater (cw) and porewater (pw) of unamended (U) and amended (HC, HCN, and HCNP) columns. HC, HCN, and HCNP respectively represent columns amended by hydrocarbon, hydrocarbon plus nitrogen, and hydrocarbon plus nitrogen plus phosphorous. P1 refers to Port 1 located in the capwater and P2, P3, and P4 were below the mudline and accessed FFT (see Fig 2.1. at chapter 2). Bars represent the mean from analysis of three replicates taken from the same ports in two replicated columns and the error bars, where visible, represent 1 standard deviation.



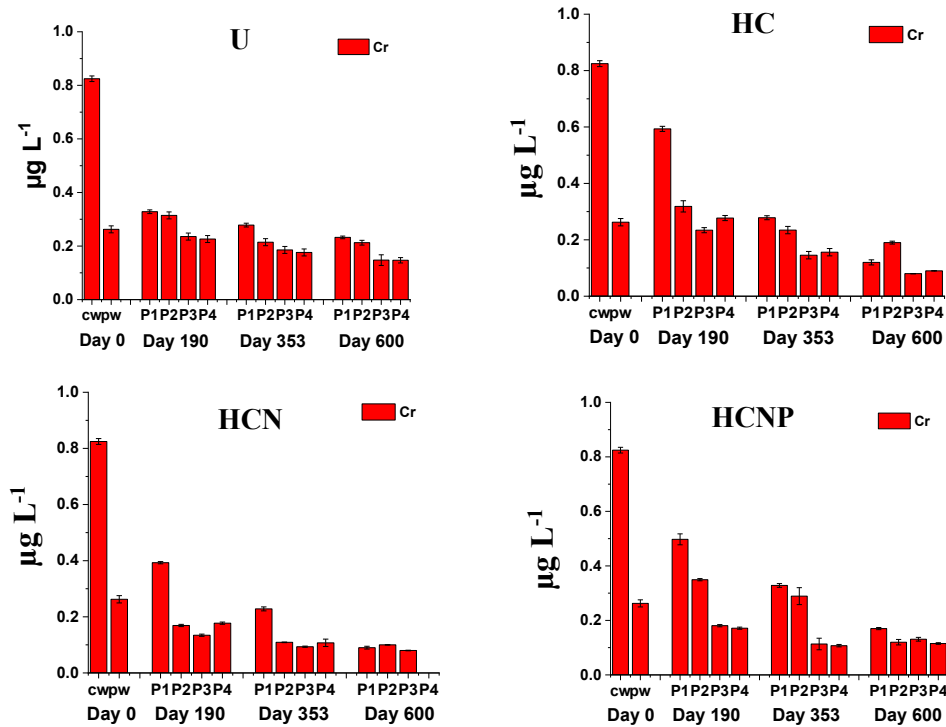


Figure 3-5. Total Mo, V, and Cr concentrations in the capwater (cw) and porewater (pw) of unamended (U) and amended (HC, HCN, and HCNP) columns. HC, HCN, and HCNP respectively represent columns amended by hydrocarbon, hydrocarbon plus nitrogen, and hydrocarbon plus nitrogen plus phosphorous. P1 refers to Port 1 located in the capwater and P2, P3, and P4 were below the mudline and accessed FFT (see Fig 2.1. at chapter 2). Bars represent the mean from analysis of three replicates taken from the same ports in two replicated columns and the error bars, where visible, represent 1 standard deviation.

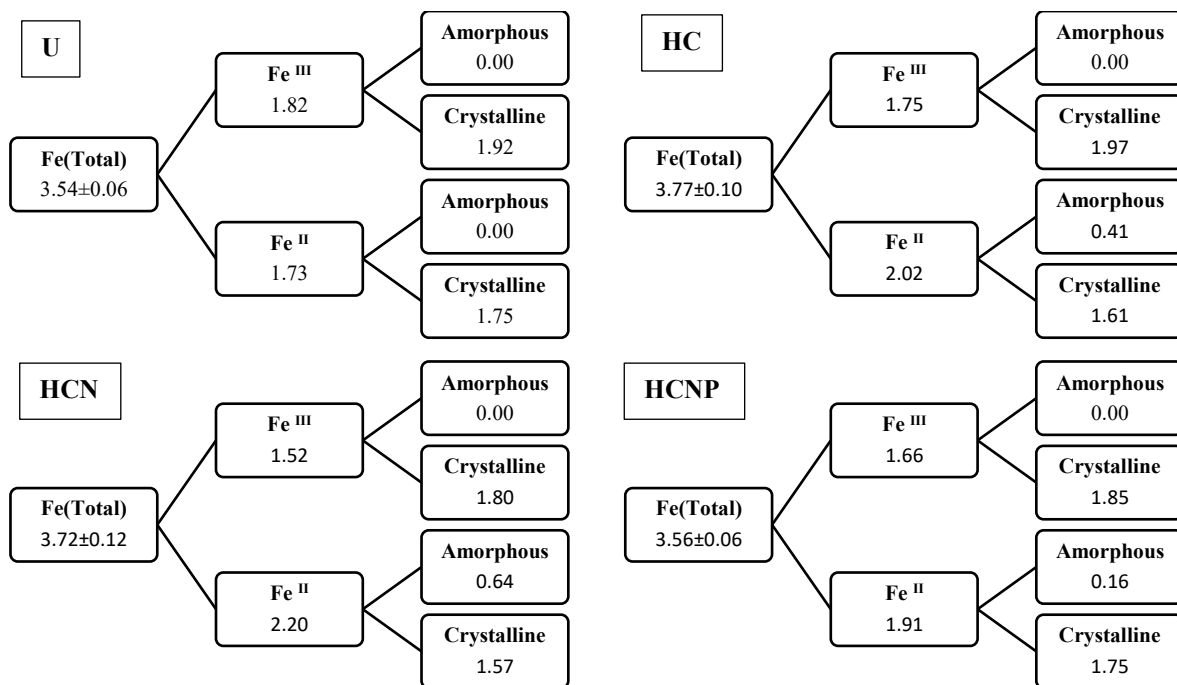


Figure 3-6. Transformation of Iron (Fe) in unamended (U) and amended (HC, HCN, HCNP) FFTs at day 0 and 600 days incubation. HC, HCN, and HCNP respectively represent columns amended by hydrocarbon, hydrocarbon plus nitrogen, and hydrocarbon plus nitrogen plus phosphorous and INT, represent the initial FFT. The data relative to iron fractionation has given at table 3.1. Fe (total) = Fe obtained from acid digestion method; Fe<sup>III</sup> = Fe (DCB) – Fe<sup>II</sup> (ferrozine); Fe<sup>III</sup> (amorphous) = Fe (AOD) – Fe (siderite) – Fe (acid volatile sulfides, AVS) – Fe (ferrozine); Fe<sup>III</sup> (crystalline) = Fe<sup>III</sup> – Fe<sup>III</sup> (amorphous); Fe<sup>II</sup> (crystalline) = Fe (pyrite) + Fe (vivianite) + Fe (siderite); and Fe<sup>II</sup> (amorphous) = Fe<sup>II</sup> – Fe<sup>II</sup> (crystalline).

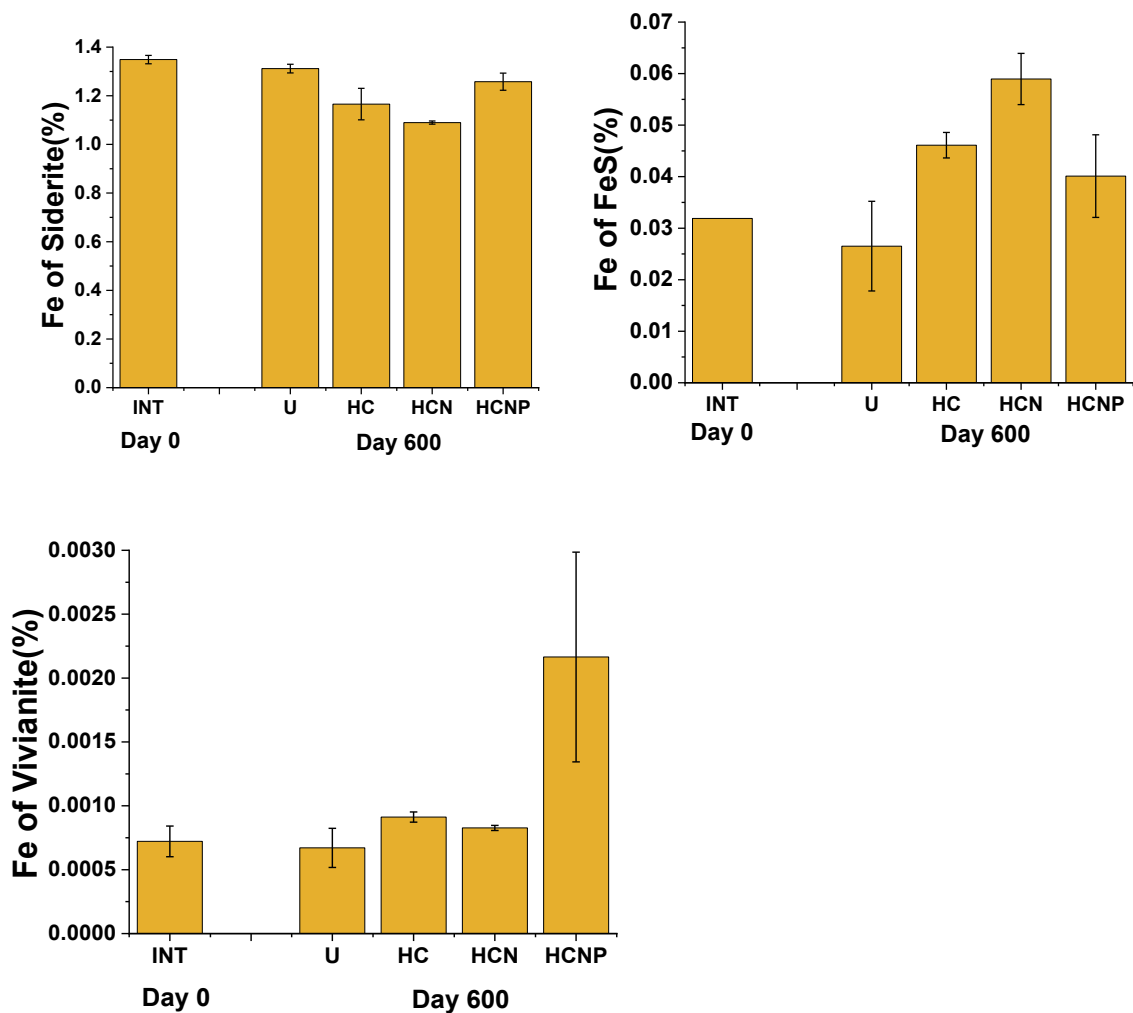


Figure 3-7. Transformation of Iron (Fe) in unamended (U) and amended (HC, HCN, HCNP) FFTs at day 0 and 600 days incubation. HC, HCN, and HCNP respectively represent columns amended by hydrocarbon, hydrocarbon plus nitrogen, and hydrocarbon plus nitrogen plus phosphorous and INT, represent the initial FFT. The data relative to iron fractionation has given at table 3.1. Siderite represent  $\text{FeCO}_3$ , and amorphous sulfides ( $\text{FeS}$ ), and vivianite ( $\text{Fe}_3(\text{PO}_4)_2 \cdot 8\text{H}_2\text{O}$ ) represent the iron content in newly formed  $\text{Fe}^{\text{II}}$  minerals. Bars represent the mean from analysis of three replicates taken from the port 4 of each column and the error bars, where visible, represent 1 standard deviation.

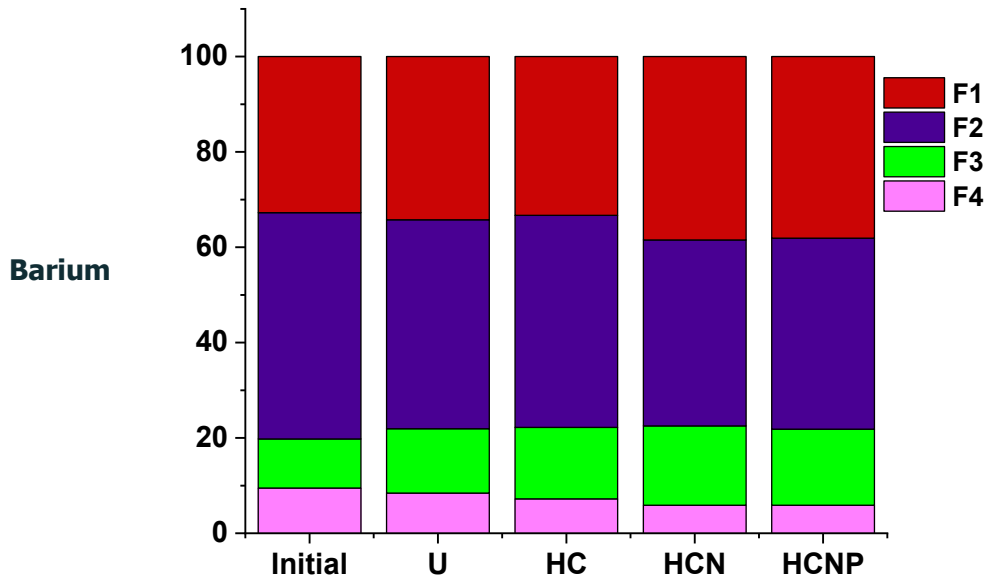
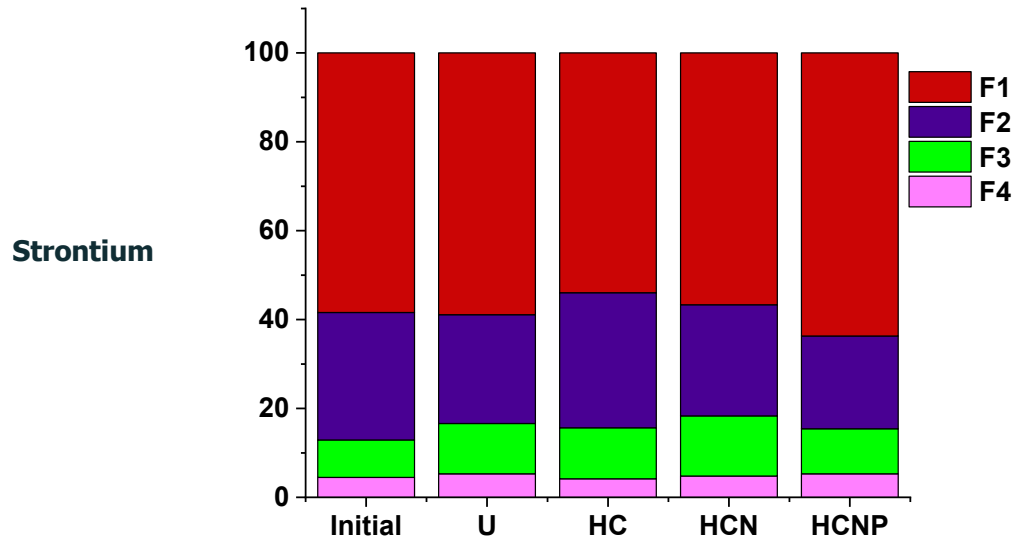


Figure 3-12. Relative distributions of Sr, and Ba in initial, unamended (U) and amended FFTs (HC, HCN, and HCNP) according to BCR sequential extraction procedures; F1: soluble, weak acid soluble, carbonate bound; F2: Fe and Mn bound, F3: organic matter and sulfide bound; F4: Residual

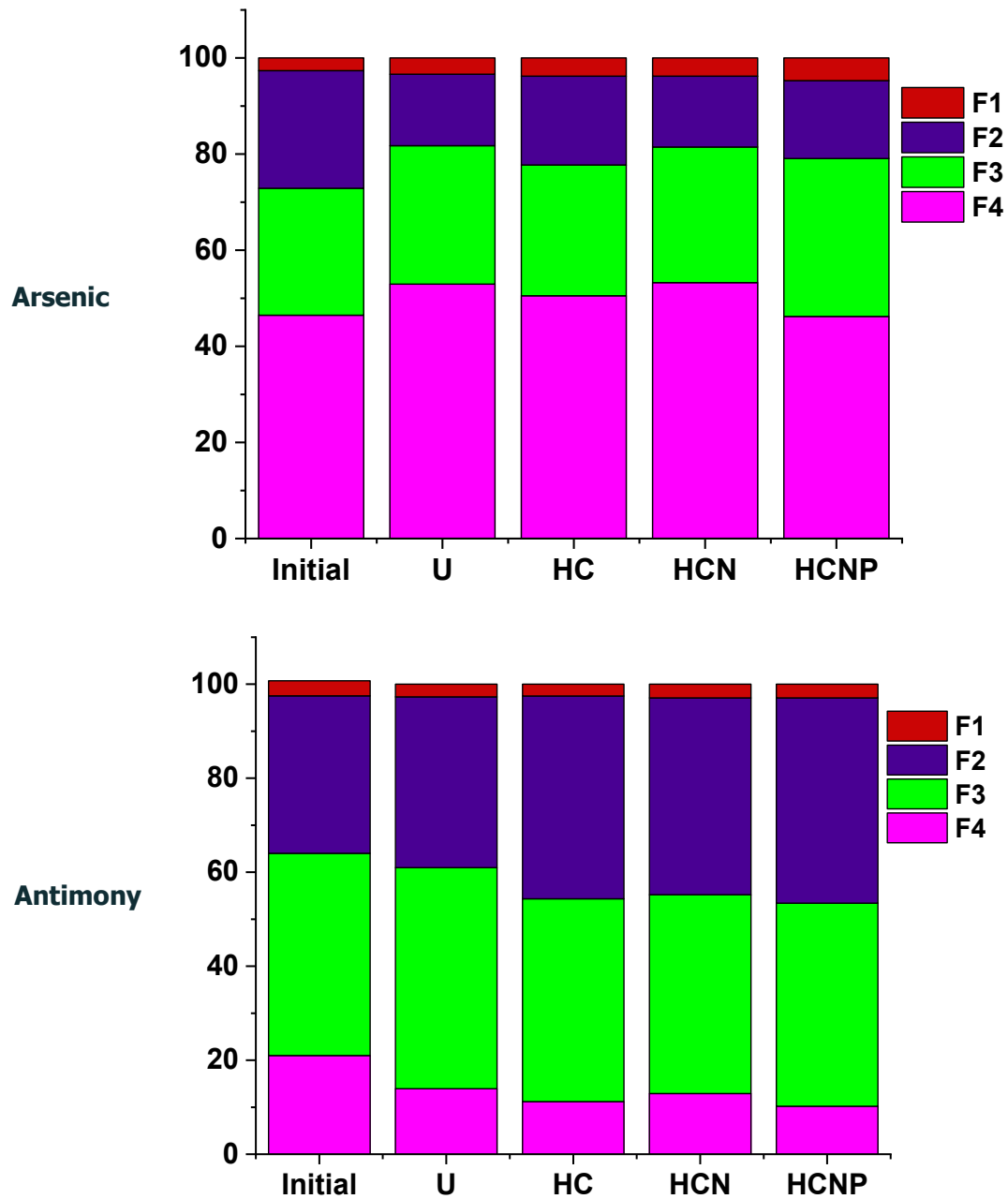


Figure 3-13. Relative distributions of As, and Sb in initial, unamended (U) and amended FFTs (HC, HCN, and HCNP) according to BCR sequential extraction procedures; F1: soluble, weak acid soluble, carbonate bound; F2: Fe and Mn bound, F3: organic matter and sulfide bound; F4: Residual

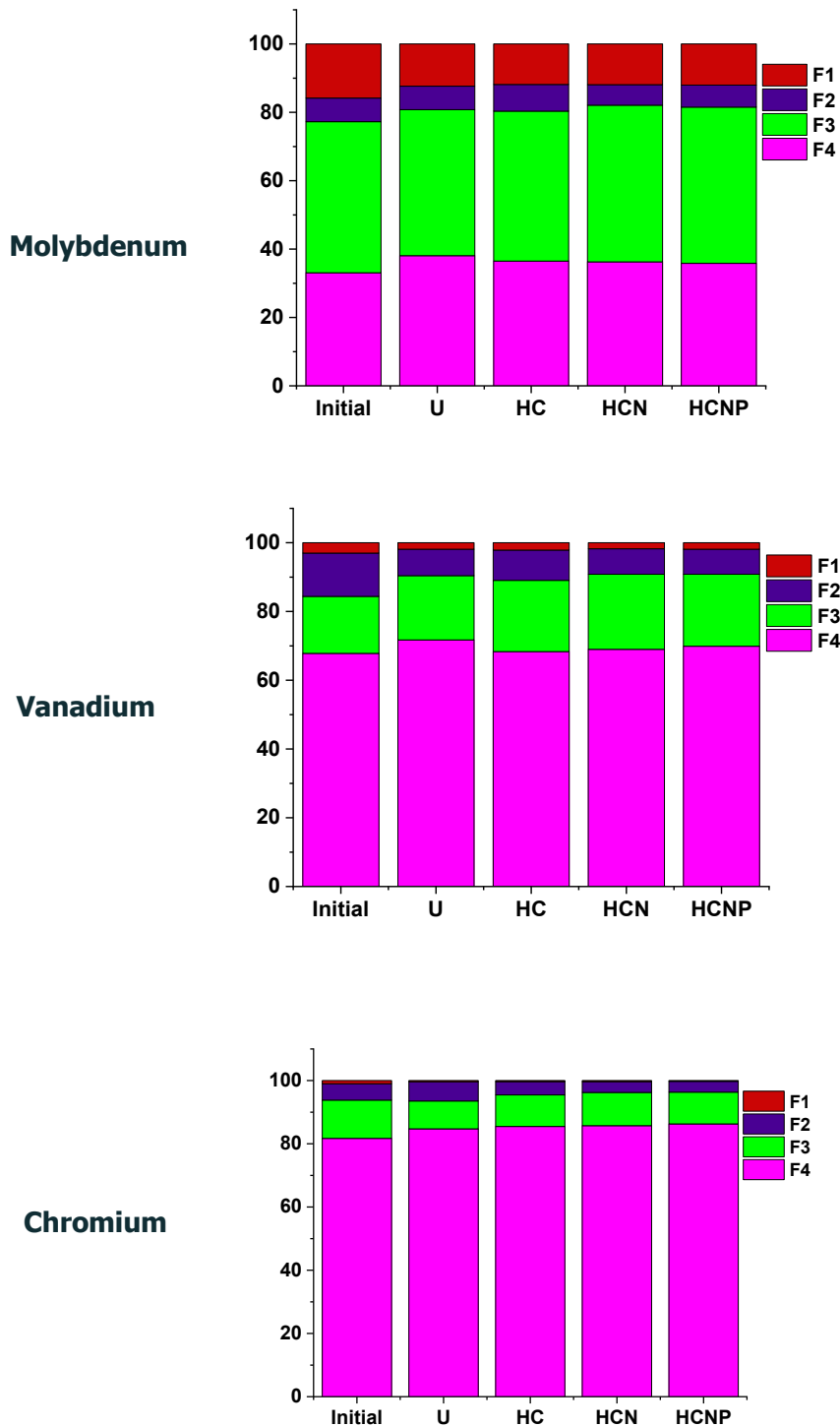


Figure 3-8. Relative distributions of Mo, V, and Cr in initial, unamended(U) and amended FFTs (HC, HCN, and HCNP) according to BCR sequential extraction procedures; F1: soluble, weak acid soluble, carbonate bound; F2: Fe and Mn bound, F3: organic matter and sulfide bound; F4: Residual

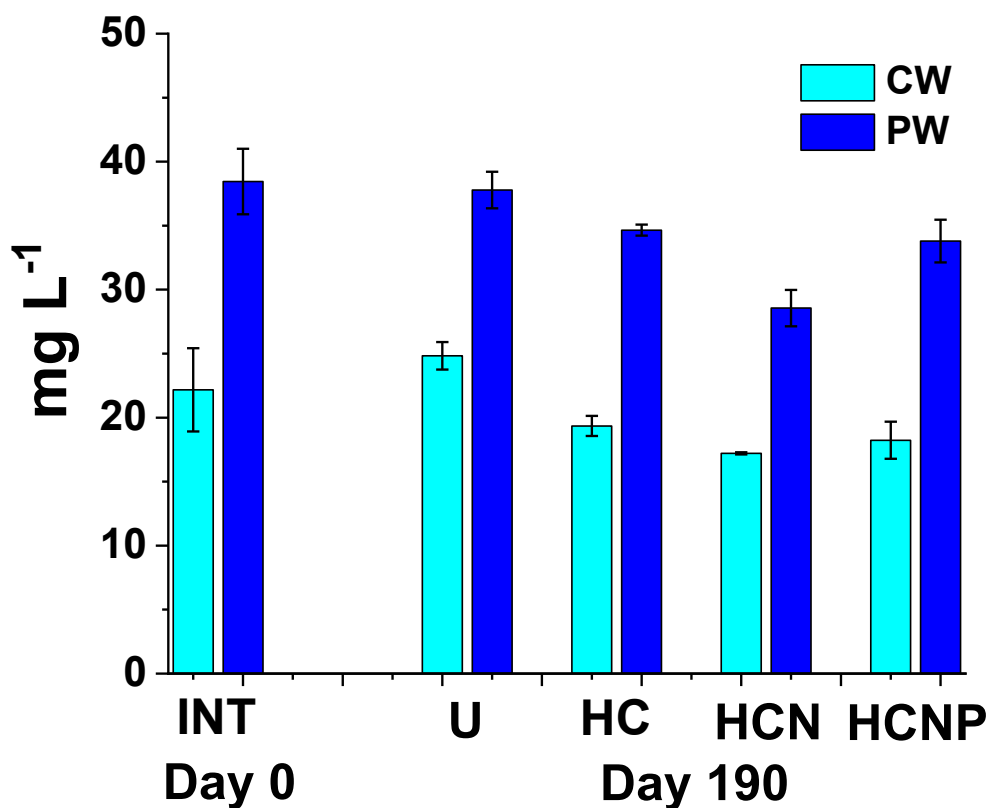


Figure 3-15. The concentrations of Naphthenic acid, in the pore and cap water of unamended (U) and amended (HC, HCN, and HCNP) columns at day 0 and 190 days incubation. Bars represent the mean value from the analysis of three replicates taken from port 1 (cap water) and port 4 (pore water) of each column, and the error bars, where visible, represent 1 standard deviation; U: unamended columns; HC: columns amended with hydrocarbon mixture; HCN: columns amended with hydrocarbon plus nitrogen; HCNP: columns amended with hydrocarbon plus nitrogen plus phosphorus

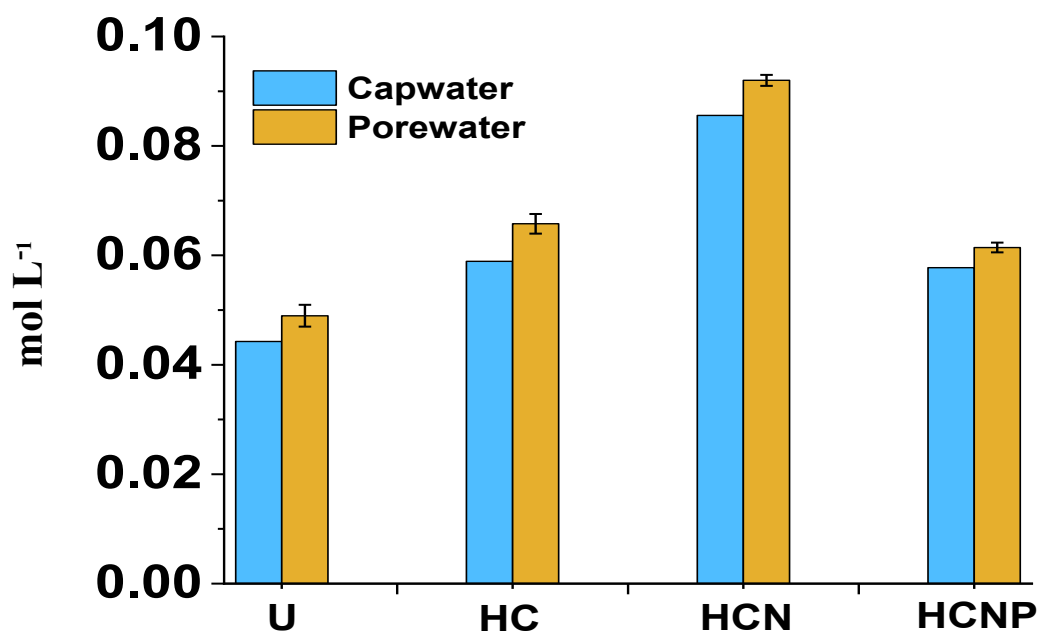


Figure 3-9. Calculated ionic strength of the porewater and capwater in unamended (U) and amended (HC, HCN, and HCNP) columns. Ionic strength was calculated using the cations and anions concentrations at P1 (capwater) and at P2, P3, and P4 (the mean ionic strength value of these 3 ports is given as a representative of ionic strength in the FFT porewater; error bars, where visible, represent 1 standard deviation) after 600 days incubation.

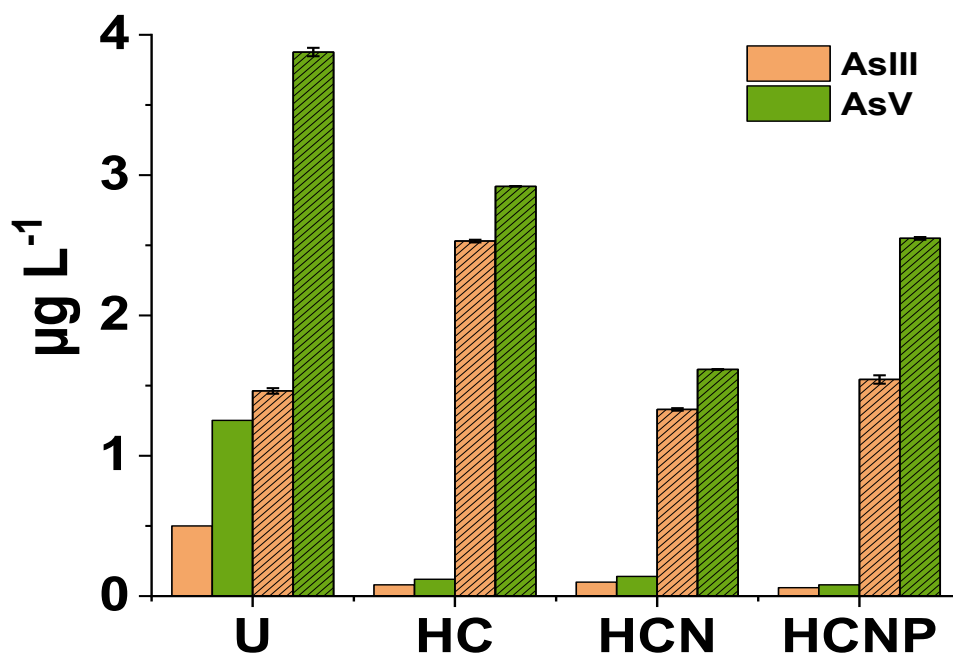


Figure 3-17. The concentrations of As species, As III and As V, in the pore and capwater of unamended (U) and amended (HC, HCN, and HCNP) columns after 190 incubation. Soil bars represent capwater, hatched bars represent porewater. The species of As was measured at at P1 (capwater) and at P2, P3, and P4 (the mean value of these 3 ports is given as a representative of As species in the FFT porewater; error bars, where visible, represent 1 standard deviation)

Table 3-1. Fractionation iron (Fe) in initial FFT prior to amendment and incubation at day 0 and in unamended (U) and amended (HC, HCN, HCNP) FFTs at 600 days incubation. Data represent the mean ( $\pm$  standard deviation, SD) of replicates taken from the port 4 of each column.

Fe fractionation (% in dry FFT) <sup>a</sup>	Initial	U	HC	HCN	HCNP
Total Fe <sup>b</sup> in solid phase; n=3	3.32 $\pm$ 0.13	3.54 $\pm$ 0.06	3.77 $\pm$ 0.10	3.72 $\pm$ 0.12	3.56 $\pm$ 0.06
Fe -AOD <sup>c</sup> ; n=2	1.14 $\pm$ 0.21	1.06 $\pm$ 0.25	1.06 $\pm$ .21	1.07 $\pm$ 0.17	1.20 $\pm$ 0.03
Fe-DCB <sup>d</sup> in solid phase; n=2	1.92 $\pm$ 0.24	1.98 $\pm$ 0.10	1.97 $\pm$ 0.02	1.80 $\pm$ 0.05	1.85 $\pm$ 0.08
Fe of FeS <sup>e</sup> ; n=2	0.03	0.026 $\pm$ 0.009	0.046 $\pm$ 0.002	0.056 $\pm$ 0.005	0.040 $\pm$ 0.008
Fe of pyrite; n=2	0.408 $\pm$ 0.002	0.441 $\pm$ 0.003	0.438 $\pm$ 0.01	0.477 $\pm$ 0.01	0.488 $\pm$ 0.045
Fe <sup>IIe</sup> in solid phase; n=3	0.179 $\pm$ 0.004	0.167 $\pm$ 0.02	0.215 $\pm$ 0.015	0.281 $\pm$ 0.028	0.195 $\pm$ 0.017
Fe of carbonate; n=4	1.349 $\pm$ 0.0172	1.312 $\pm$ 0.0179	1.166 $\pm$ 0.0647	1.089 $\pm$ 0.0064	1.258 $\pm$ 0.0352
Fe, related to Phosphorus; n=3	0.000722 $\pm$ 0.00012	0.000671 $\pm$ 0.000153	0.000912 $\pm$ 0.00004	0.000827 $\pm$ 0.00002	0.002165 $\pm$ 0.000821

<sup>a</sup> Oven dry weight of FFT was used for the calculation; <sup>b</sup> Total iron (US EPA, 2007); <sup>c</sup> Ammonium oxalate extractable iron; <sup>d</sup> Dithionite- citrate- bicarbonate extractable iron; <sup>e</sup> Fe<sup>II</sup> of amorphous sulfides.

Table 3-2. Relative distributions of Sr (a), Ba (b), As (c), Sb (d), Mo (e), V (f), and Cr (g) in initial, unamended(U) and amended FFTs (HC, HCN, and HCNP) according to BCR sequential extraction procedures; F1: soluble, weak acid soluble, carbonate bound; F2: Fe and Mn bound, F3: organic matter and sulfide bound; F4: Residual

		F1	F2	F3	F4
Sr	Initial	58.40	28.69	8.43	4.48
	U	58.90	24.50	11.32	5.28
	HC	53.95	30.40	11.49	4.16
	HCN	56.66	25.00	13.54	4.80
	HCNP	63.70	20.88	10.13	5.29
Ba	Initial	32.74	47.48	10.29	9.49
	U	34.23	43.82	13.50	8.44
	HC	33.30	44.50	14.97	7.23
	HCN	38.48	38.98	16.66	5.88
	HCNP	38.10	40.05	15.97	5.88
As	Initial	2.63	24.49	26.42	46.47
	U	3.38	14.87	28.80	52.95
	HC	3.78	18.47	27.21	50.53
	HCN	3.78	14.75	28.21	53.26
	HCNP	4.70	16.21	32.85	46.24
Sb	Initial	3.19	33.50	43.02	21.01
	U	2.70	36.32	47.04	13.93
	HC	2.51	43.15	43.12	11.21
	HCN	2.92	41.87	42.30	12.92
	HCNP	2.92	43.67	43.21	10.20
Mo	Initial	15.81	6.93	44.21	33.06
	U	12.34	6.88	42.69	38.09
	HC	11.83	7.81	43.87	36.49
	HCN	11.89	6.00	45.84	36.27
	HCNP	12.03	6.44	45.68	35.85
V	Initial	3.00	12.61	16.57	67.82
	U	1.90	7.66	18.72	71.72
	HC	2.12	8.83	20.69	68.36
	HCN	1.75	7.41	21.84	69.00
	HCNP	1.89	7.26	20.93	69.92
Cr	Initial	0.97	5.20	12.11	81.72
	U	0.35	6.10	8.81	84.74
	HC	0.33	4.20	9.98	85.49
	HCN	0.32	3.41	10.54	85.72
	HCNP	0.25	3.40	10.06	86.29

## 4 General Conclusions

### 4.1 Research Summary

EPLs as a developed reclamation strategy for the management of oil sands tailings and process affected waters are expected to become a biologically active, self-sustaining, and functional ecosystem. However, one of the potential issues that can affect water quality of EPL is the movement of constituents of concerns from FFT to the overlying water cap. The biogeochemical processes in FFT including microbial hydrocarbon degradation and biogenic gas production, mineral dissolution and precipitation, ion exchange, and metal adsorption, desorption, precipitation and co-precipitation in tailings influence the partitioning of constituents of concerns between the solid and aqueous phases of FFT and their subsequent transport to the cap water in EPLs. To determine the feasibility of EPLs for tailings reclamation, chemical, mineralogical, and molecular microbiological approaches were employed in this study at laboratory scale (simulating EPL) to investigate how biogeochemical processes in FFT affect the quality of cap water in EPL. The specific goal of this research was to investigate the effect of nutrients (nitrogen, N and phosphorus, P) on methanogenesis that ultimately affects the quality of cap water under EPL scenario. Our hypothesis was that N and P are essential nutrients for the microbial metabolisms and the addition of N will enhance methanogenesis (biogenic gas production) if the FFT is deficient in N. Methanogenesis drives biogeochemical processes in FFT that aid in dewatering and consolidation of tailings and can enhance the release of constituents of concerns (COCs) (ions and trace metals) into the FFT porewater and ultimately increase the flux of COCs from FFT to cap water. The research objectives were to: (1) determine the effect of nutrients (N and P) on methanogenesis and microbial community compositions and functions in FFT and (2) investigate the effect of methanogenesis on the mineral transformations in solid phase of FFT, the chemical composition of FFT porewater, and the flux of inorganic ions and trace metals from FFT to capwater. The conclusions drawn from this study are listed below:

The data collected and described in chapter 2 showed that (a) increasing the supply of nitrogen ( $\text{NH}_4^+$ ) to FFT mitigates N limitation, favors indigenous methanogenic microbial community and leads to enhanced rate of hydrocarbon metabolism into biogases ( $\text{CH}_4$  and  $\text{CO}_2$ ) production. The addition of N and P slowed the methanogenesis performance down and decreased the abundance of syntrophic bacteria and archaea. Therefore, it may be concluded that P might act as an effective agent for slowing  $\text{CH}_4$  production in FFT. The functional genes (*nifH*, *nirS*, *nosZ*,

and *nrfA*) involved in N transformation in the FFT were found in FFT microbial community. Also, methanogenic archaea were found as a key group harboring *nifH* gene involved in N<sub>2</sub>-fixation. The results show the potential for coupling of CH<sub>4</sub> and N cycling. These findings are important in understanding methanogenesis in tailings ponds, EPLs and wetlands.

The data presented in chapter 3 revealed that (a) stimulated methanogenesis with the addition of N resulted in significant increase in the concentrations of Ca<sup>2+</sup>, Mg<sup>2+</sup>, and HCO<sub>3</sub><sup>-</sup> in FFT porewater via enhanced biogenic CO<sub>2</sub> production that lowered the FFT porewater pH resulting in dissolution of carbonate minerals in FFT; (b) stimulated methanogenesis also increased the mobilization of Sr and Ba while diminishing the mobilization of As, Sb, Mo, V, and Cr. The results of the fractionations of Sr and Ba showed that two major phases including 1) soluble, weak acid soluble and carbonate, and 2) Fe and Mn oxides minerals contained the higher proportion of Sr and Ba. Under stimulated methanogenesis, the dissolution of carbonate minerals significantly increased the Sr and Ba mobilization in FFT porewater. Because the FFT mineral and cap water phases are in equilibrium across the water: solids interface (mudline), the significantly increased concentrations of ions, Sr and Ba were also detected in the water (cap water) above the mudline. The concentrations of As, Sb, Mo, V, and Cr decreased in the FFT pore water during methanogenesis. The fractionation of these elements in FFT solid phase was also investigated to determine host phases of these metals. As mainly associated with organic matter, and sulfide minerals and residual fractions. A positive correlation of Mo with As was observed in FFT samples. Sb showed a higher association with Fe and Mn minerals, and organic matter and sulfide minerals. Higher proportion of V and Cr were associated with residual fraction. The decrease in the concentrations of these metals in the porewater of all amended FFT was probably due to the precipitation or co-precipitation with the formation of newly formed Fe and sulfide minerals. Also, the biostimulation of FFT with hydrocarbon, nitrogen and phosphorous resulted in the decrease of NAs concentrations in the porewater and the capwater of all amended columns tested. The results of this study will help understand the extent of ions and Sr and Ba release during stimulated methanogenesis so that management strategy could be developed to improve the quality of EPLs surface water. However, more detailed study must be taken to determine the exact processes which controls the fate of each trace metals in the complex FFT.

## 4.2 Recommendation for the future studies

- It was the first time that the effect of nutrients (N and P) was assessed on the methanogenic activities in FFT. It is suggested that in a mesocosm experiment, different concentrations of nutrients, particularly P are used to determine its effect on stimulation or suppression of the methanogenesis.
- In the current study, three treatments were used: FFT amended with hydrocarbon (HC), FFT amended with hydrocarbon plus nitrogen (HCN) and the FFT amended with hydrocarbon plus nitrogen plus phosphorus (HCNP). In future experiment, the effect of phosphorus alone on the methanogenesis should be determined by including the treatment (FFT amended with hydrocarbon plus phosphorus).
- To explore the potential linkage between the methanogenesis and N-cycling, the assessment of the various steps of N-cycling through the determination of copy number of *nifH*, *nirS*, *nosZ*, and *nrfA* genes and their expression is needed.
- The application of metal stable isotope as a tracer in the biogeochemical processes occurring in FFT will help determine the fate of trace metals in FFT porewater and their flux to cap water.
- The assessment of speciation of redox sensitive metals in the porewater of FFT is needed to identify the mechanisms of their mobility and precipitation.
- The assessment of S-cycle and its relation to partitioning of the trace metals in FFT and cap water is needed to comprehend metals' mobility.

## Bibliography

- Abu Laban, N., Dao, A., & Foght, J. (2015). DNA stable-isotope probing of oil sands tailings pond enrichment cultures reveals different key players for toluene degradation under methanogenic and sulfidogenic conditions. *FEMS Microbiology Ecology*, *91*(5), fiv039. <https://doi.org/10.1093/femsec/fiv039>.
- Abu Laban, N., Dao, A., Semple, K., & Foght, J. M. (2014). Biodegradation of C7 and C8 isoalkanes under methanogenic conditions. *Environmental Microbiology*, *17* (12), 4898–4915. doi:10.1111/1462-2920.12643
- AEP. (2015a). Total area of the oil sands tailings ponds over time. Retrieved from <http://osip.alberta.ca/library/Dataset/Details/542>
- AEP. (2015b). Historical Water use per Barrel of Oil Produced. Retrieved from <http://osip.alberta.ca/library/Dataset/Details/117>
- Ahern, C.R., McElnea, A.E., & Sullivan, L.A. (1998). *Acid sulfate soils laboratory methods guidelines*. Wollongbar, NSW: Acid Sulfate Soil Management Advisory Committee.
- Alberta Government. (2015). Alberta's Oil Sands – about the Resource. Retrieved from <http://oilsands.alberta.ca/resource.html>.
- Allen, E.W. (2008). Process water treatment in Canada's oil sands industry: I. Target pollutants and treatment objectives. *Journal of Environmental Engineering and Science*, *7*(2), 123–138. Doi.org/10.1139/S07-038.
- Anderson, J.C., Wiseman, S.B., Moustafa, A., Gamal El-Din, M., Liber, K., & Giesy, J.P. (2012). Effects of exposure to oil sands process-affected water from experimental reclamation ponds on *Chironomus dilutus*. *Water Research*, *46*(6), 1662-1672.
- Anderson, O.R.T., Vrionis, H.A., Lovley, D.R. (2004). Vanadium respiration by *Geobacter metallireducens*: novel strategy for in situ removal of vanadium from groundwater. *Applied Environmental Microbiology*, *70*, 3091-3095.
- ARE. (2017). Tailings. Retrieved from <https://www.aer.ca/providing-information/by-topic/tailings>
- Arkell, N., Kuznetsov, P., Kuznetsova, A., Foght, J. M., & Siddique, T. (2015). Microbial metabolism alters pore water chemistry and increases consolidation of oil sands tailings. *Journal of Environmental Quality*, *44*(1), 145–153. doi:10.2134/jeq2014.04.0164

- Arshad, M., Khosa, M. A., Siddique, T., & Ullah, A. (2016). Modified biopolymers as sorbents for the removal of naphthenic acids from oil sands process affected water (OSPW). *Chemosphere*, *163*, 334-341.
- Bae, H. S., Morrison, E., Chanton, J.P., & Ogram, A. (2018). Methanogens are major contributors to nitrogen fixation in soils of the Florida Everglades. *Applied and Environmental Microbiology*, *84*(7):e02222-17. <https://doi.org/10.1128/AEM.02222-17>.
- BGC Engineering Inc. (2010). *Review of reclamation options for oil sands tailings substrates*. (No. OSRIN Report No. TR-2). BGC Engineering Inc., University of Alberta, Oil Sands Research and Information Network.
- Bodelier, P. L. E., & Steenbergh, A. K. (2014). Interactions between methane and the nitrogen cycle in light of climate change. *Current Opinion in Environmental Sustainability*, *9*(10): 26–36.
- Boe, K. (2006). Online monitoring and control of the biogas process. PhD. Thesis. Technical University of Denmark.
- Bolliger, C., Schroth, M. H., Bernasconi, S. M., Kleikemper, J. & Zeyer, J. (2001). Sulfur isotope fractionation during microbial reduction by toluene-degrading bacteria. *Geochimica et Cosmochimica Acta*, *65* (19), 3289–3298.
- Boonsawang, P., Rerngnarong, A., Tongurai, C., & Chairapat, S. (2014). Effect of nitrogen and phosphorus on the performance of acidogenic and methanogenic reactors for treatment of biodiesel wastewater. *Songklanakarinn Journal of Science and Technoly*, *36*(6), 643-649.
- CAPP. (2017). Crude Oil: Forecast, Markets, and Transportation. Canadian Association of Petroleum Producers. Retrieved from <https://www.capp.ca/publications-and-statistics/publications>
- Canadian Council of Ministers of the Environment. (1997). *Canadian water quality guidelines: Arsenic, bromacil, carbaryl, chlorpyrifos, deltamethin, and glycols*. Winnipeg: Canadian Council of Ministers of the Environment.
- CEC. (1998). *The quality of water intended for human consumption*. Brussels, Belgium: Council of the European Communities.
- Cumulative Environmental Management Association. (2012a). *Experiences from non-oil sands pit lakes*. Fort McMurray, AB, Canada: CEMA.

- Cumulative Environmental Management Association. (2012b). *End pit lakes guidance document*. (No. 37(12)). Fort McMurray, AB, Canada: CEMA.
- Chalaturnyk, R. J., Scott, J., & Özü, B. (2002). Management of oil sands tailings. *Petroleum Science and Technology*, 20(9-10), 1025–1046. doi:10.1081/LFT 120003695
- Charette, M.A., & Sholkovitz, E.R. (2006). Trace element cycling in a subterranean estuary: Part 2. Geochemistry of the pore water. *Geochimica et Cosmochimica Acta*, 70, 811–826.
- Cheng, L., Ding, C., Li, Q., He, Q., Dai, L.R., & Zhang, H. (2013). DNA-SIP reveals that *Syntrophaceae* play an important role in methanogenic hexadecane degradation. *Plos One*, 8(7), e66784. doi:10.1371/journal.pone.0066784
- Chen, M., Walshe, G., Chi Fru, E., Ciborowski, J.J.H. & Weisener, C.G. (2013). Microcosm assessment of the biogeochemical development of sulfur and oxygen in oil sands fluid fine tailings. *Applied Geochemistry*, 37, 1-11.
- Chou, L., R.M. Garrels, & R. Wollast. (1989). Comparative study of the kinetics and mechanisms of dissolution of carbonate minerals. *Chemical Geology*. 78(3-4), 269–282. doi: 10.1016/0009-2541(89)90063-6
- Clement, J.C., Shrestha, J., Ehrenfeld, J. G., & Jaffé, P. R. (2005). Ammonium oxidation coupled to dissimilatory reduction of iron under anaerobic conditions in wetland soils. *Soil Biology and Biochemistry*, 37(12), 2323-2328. <https://doi.org/10.1016/j.soilbio.2005.03.027>
- Clothier, L.N., & Gieg, L.M. (2016). Anaerobic biodegradation of surrogate naphthenic acids. *Water Resources*. 90, 156–166.
- Collins, V. C. E., Foght, J. M., & Siddique, T. (2016). Co-occurrence of methanogenesis and N<sub>2</sub> fixation in oil sands tailings. *Science of the Total Environment*, 565, 306–312. doi:10.1016/j.scitotenv.2016.04.154
- COSIA. (2012). *Technical guide for fluid fine tailings management*. Edmonton, AB: Canadian Oil Sands Innovation Alliance.
- Devi, M. P., Reddy, M. V., Juwarkar, A., Sarma, P. N. & Mohan, S. R. V. (2011). Effect of Co-culture and nutrients supplementation on bioremediation of crude petroleum sludge. *Clean Soil, Air, and Water*, 39 (10), 900–907.
- Dolfing, J., Larter, S.R., & Head, I.M. (2008). Thermodynamic constraints on methanogenic crude oil biodegradation. *ISME Journal*. 2(4), 442–452.

- Dompierre, K. A., Lindsay, M. B. J., Cruz-Hernández, P., & Halferdahl, G. M. (2016). Initial geochemical characteristics of fluid fine tailings in an oil sands end pit lake. *Science of the Total Environment*, 556, 157-177.
- Ebrahimi, P., & Vilcaez, J. (2018). Petroleum produced water disposal: Mobility and transport of barium in sandstone and dolomite rocks. *Science of the Total Environment*. 1(634), 1054-1063. doi:10.1016/j.scitotenv.2018.04.067.
- Edwards, B. R., Reddy, C. M., Camilli, R., Carmichael, C. A., Longnecker, K., & VanMooy, B. A. S. (2011). Rapid microbial respiration of oil from the Deepwater Horizon spill in offshore surface waters of the Gulf of Mexico. *Environmental Resources Letter*, 6 (3), 035301. doi: 10.1088/1748-9326/6/3/035301
- Elango, V., Urbano, M., Lemelle, K. R., & Pardue, J. H. (2014). Biodegradation of MC252 oil in oil: sand aggregates in a coastal headland beach environment. *Frontiers in Microbiology*, 5(161). doi: 10.3389/fmicb.2014.00161
- Engelbrektson, A., Kunin, V., Wrighton, K. C., Zvenigorodsky, N., Chen, F., & Ochman, H. (2010). Experimental factors affecting PCR-based estimates of microbial species richness and evenness. *The ISME Journal*, 4(5), 642–647.
- EPA. (1999). *National primary drinking water standards*. Washington, DC: US EPA Office of Water.
- EPA. (2014). *Announcement of preliminary regulatory determinations for contaminants*. (No. 79 (202)). Third Drinking Water Contaminant Candidate List.
- ERCB. (2009). *Directive 074 tailings performance criteria and requirements for oil sands mining schemes*. Calgary, Alberta: Energy Resources Conservation Board.
- Essington, M. E. (2004). *Soil and water chemistry: An integrative approach*. Boca Raton, FL: CRC.
- Fedorak, P. M., Coy, D. L., Dudas, M. J., Simpson, M. J., Renneberg, J., & MacKinnon, M. D. (2003). Microbially-mediated fugitive gas production from oil sands tailings and increased tailings densification rates. *Journal of Environmental Engineering & Science*, 2, 199–211. doi:10.1139/S03-022
- Finneran, K. T., Johnsen, C. V. & Lovley, D. R. (2003). *Rhodoferrax ferrireducens* sp. nov., a psychrotolerant, facultatively anaerobic bacterium that oxidizes acetate with the reduction of Fe (III). *International Journal of Systematic and Evolutionary Microbiology*, 53, 669–673.

- Foght, J., Aislabie, J., Turner, S., Brown, C.E., Ryburn, J., Saul, D.J., & Lawson, W. (2004). Culturable bacteria in subglacial sediments and ice from two Southern Hemisphere glaciers. *Microbial Ecology*, 47(4), 329–340.
- Foght, J.M., Gieg, L.M., & Siddique, T. (2017). The microbiology of oil sands tailings: past, present, future. *FEMS Microbiology Ecology*, 93, fix034. doi: 10.1093/femsec/fix034
- Fotidis, I. A., Karkashev, D., Kotsopounlos, T.A., Martzopoulos, G. G., & Angleildaki, I. (2013). Effect of ammonium and acetate on methanogenic pathway and methanogenic community composition. *FEMS Microbiology Ecology*, 83, 38-48.
- Fowler, S. J., Dong, X., Sensen, C. W., Suflita, J. M., & Gieg, L. M. (2012). Methanogenic toluene metabolism: community structure and intermediates. *Environmental Microbiology*, 14(3), 754–764. doi:10.1111/j.1462-2920.2011.02631.x
- Franke-Whittle, I. H., Walter, A., Ebner, C., & Insam, H. (2014). Investigation into the effect of high concentrations of volatile fatty acids in anaerobic digestion on methanogenic communities. *Waste management*, 34(11), 2080-9.
- Gray, N. D., Sherry, S., Grant, R.J., Rowan, A.K., Hubert, C.R.J., Callbeck, C.M., ... Larter, S.R., Head, I.M. (2011). The quantitative significance of *Syntrophaceae* and syntrophic partnerships in methanogenic degradation of crude oil alkanes. *Environmental Microbiology*, 13(11): 2957–2975. doi: 10.1111/j.1462-2920.2011.02570.x
- Guo, C. (2009). Rapid Densification of the oil sands mature fine tailings (MFT) by microbial activity. PhD. Thesis, University of Alberta.
- He, Y., Patterson, S., Wang, N., Hecker, M., Martin, J.W., Gamal El-Din, M., Giesy, J.P., & Wiseman, S.B. (2012). Toxicity of untreated and ozone-treated oil sands process-affected water (OSPW) to early life stages of the fathead minnow (*Pimephales promelas*). *Water Resources*. 46, 6359-6368.
- Helz, G.R., Vorlicek, T.P., & Kahn, M.D. (2004). Molybdenum scavenging by iron monosulfides. *Environmental Science & Technology*, 38, 4263-4268.
- Herman, D.C., Fedorak, P.M., MacKinnon, M.D., & Costerton, J.W. (1994). Biodegradation of naphthenic acids by microbial populations indigenous to oil sands tailings. *Canadian Journal of Microbiology*, 40, 467–477.

- Hester, E. R., Harpenslager, S. F., van Diggelen, J., Lamers, L. L., Jetten, M., Lüke, C., Lückner, S., & Welte, C. U. (2018). Linking Nitrogen Load to the Structure and Function of Wetland Soil and Rhizosphere Microbial Communities. *M Systems*, 3(1), e00214-17.
- Holowenko, F. M., MacKinnon, M. D., & Fedorak, P. M. (2000). Methanogens and sulfate reducing bacteria in oil sands fine tailings waste. *Canadian Journal of Microbiology*, 46(10), 927–937.
- Holowenko, F.M., Mackinnon, M.D., & Fedorak, P.M. (2001). Naphthenic acids and surrogate naphthenic acids in methanogenic microcosms. *Water Resources*. 35(2), 595-606.
- Houlihan, R.H., & Hale, C.E. (2011). Alberta mine reclamation and abandonment requirements. Paper presented at the *Sixth International Conference on Mine Closure*, 13-22.
- Hu, M., Li, F., Liu, C., & Wu, W. (2015). The diversity and abundance of As (III) oxidizers on root iron plaque is critical for arsenic bioavailability to rice. *Scientific Reports*, 5, 13611. doi: 10.1038/srep13611
- Huerta-Diaz, M. A., Carignan, R., & Tessier, A. (1993). Measurement of trace metals associated with acid volatile sulfides and pyrite in organic freshwater sediments. *Environmental Science & Technology*, 27, 2367–2372.
- Hull, L.C., & Schafer, A.L. (2008). Accelerated transport of Sr-90 following a release of high ionic strength solution in vadose zone sediments. *Journal of Contaminant Hydrology*, 97, 135-157.
- Jivraj, M., MacKinnon, M., & Fung, B.(1995). Naphthenic acid extraction and quantitative analysis with FT-IR spectroscopy. *Syncrude analytical manuals*. Edmonton, AB: Syncrude Canada Ltd.
- Kabwe, L.K., Scott, J.D., Beier, N.A., Wilson, G.W., & Jeeravipoolvarn, S. (2018). Environmental implications of end pit lakes at oil sand mines in Alberta, Canada. *Environmental Geotechnics*, 1-8. <https://doi.org/10.1680/jenge.17.00110>
- Kalvelage, T., Lavik, G., Jensen, M. M., Revsbech, N.P., Löscher, C., Schunck, H.,...Kuypers, M. M. M. (2015). Aerobic microbial respiration in oceanic oxygen minimum zones. *Plos One*. 10:e0133526 DOI 10.1371/journal.pone.0133526.
- Kasperski, K. L., & Mikula, R. J. (2011). Waste streams of mined oil sands: characteristics and remediation. *Elements*, 7(6), 387–392. doi:10.2113/gselements.7.6.387

- Kavanagh, R. J., Frank, R.A., Oakes, K.D., Servos, M.R., Young, R.F., Fedorak, P.M., ... Van Der Kraak, G. (2011). Fathead minnow (*Pimephales promelas*) reproduction is impaired in aged oil sands process-affected waters. *Aquatic Toxicology*, *101*, 214-220.
- Khanal, S. K. (2008). *Anaerobic biotechnology for bioenergy production: Principles and applications*. Singapore: Wiley Blackwell, John Wiley & Sons, Inc.
- Kloos, K., Mergel, A., Rösch, C., & Bothe, H. (2001). Denitrification within the genus *Azospirillum* and other associative bacteria. *Australian Journal of Plant Physiology*, *28*(9), 991–998.
- Kuo, S. (1996). Phosphorus in methods of soil analysis: Part3. *Chemical methods* (pp. 869–919). Madison, Wisconsin: SSSA.
- Kuypers, M. M. M., Sliemers, A. O., Lavik, G., Schmid, M., Jorgensen, B. B., Kuenen, J. G., ... Jetten, M. S. M. (2003). Anaerobic ammonium oxidation by anammox bacteria in the Black Sea. *Nature*, *422*, 608-611. DOI 10.1038/nature01472.
- Lai, J.W., Pinto, L.J., Kiehlmann, E., Bendell-Young, L.I., & Moore, M.M. (1996). Factors that affect the degradation of naphthenic acids in oil sands wastewater by indigenous microbial communities. *Environmental Toxicology and Chemistry*, *15* (9), 1482–1491.
- Langley, S., Gault, A.G., Ibrahim, A., Takahashi, Y., Renaud, R., Fortin, D., Clark, L.D., & Ferris, F.G. (2009). Strontium desorption from bacteriogenic iron oxides (BIOS) subjected to microbial Fe(III) reduction. *Chemical Geology*. *262*(3), 217–228
- Leclair, L.A., MacDonald, G.Z., Phalen, L.J., Kollner, B., Hogan, N.S., & van den Heuvel, M.R. (2013). The immunological effects of oil sands surface waters and naphthenic acids on rainbow trout (*Oncorhynchus mykiss*). *Aquatic Toxicology*, *142-143*, 185-194.
- Leigh, J.A. (2000). Nitrogen fixation in methanogens: the archaeal perspective. *Current Issues in Molecular Biology*, *2*(4), 125–131.
- Leilei, X., Baohua, X., Jinchao, L., Hongxia, Z., Guangxuan, H., Oumei, W., & Fanghua, L. (2017). Stimulation of long-term ammonium nitrogen deposition on methanogenesis by Methanocellaceae in a coastal wetland. *Science of the Total Environment*, *595*, 337–343.
- Leuz, A.K., Monch, H., & Johnson, C.A. (2006). Sorption of Sb (III) and Sb(V) to goethite: influence on Sb(III) oxidation and mobilization. *Environmental Science and Technology*. *40*(23), 7277 –7282.

- Li, C. (2010). Methanogenesis in oil sands tailings: An analysis of the microbial community involved and its effects on tailings densification. M.Sc. Thesis, University of Alberta.
- Li, C., Fub, L., Stafford, J., Belosevic, M., & El-Din, M. G. (2017). The toxicity of oil sands process-affected water (OSPW): A critical review. *The science of the Total Environment*, 601-602, 1785-1802.
- Li, J., Wang, Q., Oremland, R.S., Kulp, T.R., Rensing, C., Wang, G., & Drake, H.L. (2016). Microbial antimony biogeochemistry: enzymes, regulation, and related metabolic pathways. *Applied and Environmental Microbiology*, 82, 5482-5495.
- Liang, Y., Van Nostrand, J.D., Deng, Y., He, Z., Wu, L., Zhang, X., Li, G., & Zhou, J. (2011). Functional gene diversity of soil microbial communities from five oil-contaminated fields in China. *The ISME Journal*, 5 (3), 403-413.
- Lovley, D.R., & Phillips, E.J.P. (1986). Organic matter mineralization with reduction of ferric iron in anaerobic sediments. *Applied and Environmental Microbiology*, 51, 683–689.
- Mahaffey, A., & Dube, M. (2016). Review of the composition and toxicity of oil sands process affected water. *Environ. Reviews*, 25(1), 97-114. <http://dx.doi.org/10.1139/er-2015-0060>.
- Mancipe-Jiménez, D.C., Costa, C., Márquez, M. C. (2017). Methanogenesis inhibition by phosphorus in anaerobic liquid waste treatment. *Liquid Waste Recovery*. 2, 1–8. doi.10.1515/lwr-2017-0001
- Marwijk, J.V., Opperman, D.J., Piater, L.A., & Heerden, E.V. (2009). Reduction of vanadium (V) by *Enterobacter cloacae* EV-SA01 isolated from a South African deep gold mine *Biotechnology Letters*, 31(6), 845-849
- McLean, K. M. (1995). High-rate anaerobic digestion: A review. In Kolarik, L.O. and Priestley, A.J. (Ed.), *Modern techniques in water and wastewater treatment* (pp. 133-140). Melbourne. CSIRO.
- McManus, J., Berelson, W. M., Severmann, S., Poulson, R. L., Hammond, D. E., Klinkhammer, G. P., & Holm, C. (2006). Molybdenum and uranium geochemistry in continental margin sediments: Paleoproxy potential. *Geochimica et Cosmochimica Acta*, 70(18), 4643–4662.
- McQueen, A.D., Kinley, C.M., Hendrikse, M., Gaspari, D.P., Calomeni, A.J., Iwinski, K.J. ...Rodgers, J.H. (2017). A risk-based approach for identifying constituents of concern in oil sands process-affected water from the Athabasca Oil Sands region. *Chemosphere*, 173, 340-350.

- MacKinnon, M. D. (1989). Development of the tailings pond at Syncrude's oil sands plant: 1978-1987. *AOSTRA Journal of Research*, 5(1), 109 – 133.
- MacKinnon, M. D., Matthews, J. G., Shaw, W. H., & Cuddy, R. G. (2010). Water Quality Issues Associated With Composite Tailings (CT) Technology for Managing Oil Sands Tailings.
- McNeill, J., & Lothian, N. (2017). *Review of directive 085 tailings management plans*. Retrieved from <http://www.pembina.org/reports/tailings-whitepaper-d85.pdf>.
- Mendelsohn, I.A., Andersen, G.L., Baltz, D.M., Caffey, R.H., Carman, K.R., Fleeger, J.W. ... Rozas, L.P. (2012). Oil impacts on coastal wetlands: implications for the Mississippi River delta ecosystem after the deepwater horizon oil spill. *Bioscience*, 62 (6), 562-574.
- Mitsunobu, S., Takahashi, Y., & Sakai, Y. (2008). Abiotic reduction of antimony (V) by green rust (Fe 4(II) Fe 2(III) (OH) 12SO 4·3H 2O). *Chemosphere*. 70(5), 942 –947.
- Mohamad Shahimin, M.F., Foght, J.M., & Siddique, T. (2016). Preferential methanogenic biodegradation of short-chain n-alkanes by microbial communities from two different oil sands tailings ponds. *Science of the Total Environment*, 553, 250–257
- Mohamad Shahimin, M.F., & Siddique, T. (2017a) .Methanogenic biodegradation of paraffinic solvent hydrocarbons in two different oil sands tailings. *Science of the Total Environment*. 583,115–122
- Mohamad Shahimin, M.F., & Siddique, T. (2017b). Sequential biodegradation of complex naphtha hydrocarbons under methanogenic conditions in two different oil sands tailings. *Environmental Pollution*, 221, 398–406
- Morris, B. E. L., Herbst, F. A., Bastida, F., Seifert, J., von Bergen, M., Richnow, H. H., & Suflita, J. M. (2012). Microbial interactions during residual oil and n-fatty acid metabolism by a methanogenic consortium. *Environmental Microbiology Reports*, 4(3), 297–306. doi:10.1111/j.1758-2229.2012.00333.x
- Morse, J. W., Millero, F. J., Cornwell, J. C. & Rickard, D. (1987). The Chemistry of the hydrogen sulfide and iron sulfide systems in natural waters. *Earth Science Reviews*, 24(42), 1–42.
- Morse, J.W., R.S., Arvidson, A., & Luttge. (2007). Calcium carbonate formation and dissolution. *Chemical Reviews*, 107(2), 342–381. Doi: 10.1021/cr050358j
- Moulin, E., A. Jordens, & R. Wollast. (1985). Influence of the aerobic bacterial respiration on the early dissolution of carbonates in coastal sediments. In R., Van Grieken, and R. Wollast

- (Ed.), *Progress in belgian oceanographic research* (pp. 196–208). Brussels, Belgium: University of Antwerpen.
- Natural Resources Canada-Canmet, E. (2010). *Oil sands water toxicity: A critical review*. Devon AB: Natural Resources Canada-Canmet ENERGY.
- O'Day, P.A. Vlassopoulos, D., Root, R., & Rivera, N. (2004). The influence of sulfur and iron on dissolved arsenic concentrations in the shallow subsurface under changing redox conditions. *Proceedings of the National Academy of Sciences of the United States of America*. 101(38), 13703–13708
- Osacky, M., Geramian, M., Dyar, M.D., Sklute, E.C., Valter, M., Ivey, D.G., Liu, Q., & Etsell, T.H. (2013). Characterization of petrologic end members of oil sands from the Athabasca region, Alberta, Canada. *The Canadian Journal of Chemical Engineering*, 91(8), 1402-1415.
- Oremland, R.S., & Stolz, J.F. (2005). Arsenic, microbes and contaminated aquifers. *Trends in Microbiology*, 13(2), 45–49.
- Oren, A. (2014). The family Methanosarcinaceae. In Eugene Rosenberg, Edward F DeLong, Stephen Lory, Erko Stackebrandt & Fabiano Lopes Thompson (Eds.), *The prokaryotes : Other major lineages of bacteria and the archaea* (pp. 259-281) doi:10.1007/978-3-642-38954-2\_408
- OSTC, & COSIA. (2012). *Technical guide for fluid fine tailings management*. Calgary, Alberta: Oil Sands Tailings Consortium and Canada's Oil Sands Innovation Alliance. Retrieved from <http://www.cosia.ca/uploads/documents/id7/TechGuideFluidTailingsMgmt>
- Östeberg, T.L., Jonsson, A., & Lundström, U.S. (2006). Accelerated biodegradation of n-alkanes in aqueous solution by the addition of fermented whey. *International Biodeterioration & Biodegradation*, 57(3):190–194
- Pansu, M., Gautheyrou, J. (2006). *Handbook of soil analysis. Mineralogical, organic and inorganic methods*. Berlin; Heidelberg: Springer- Verlag. Doi: 10.1007/978-3-540-31211-6
- Penner, T.J. (2006). Analysis of methanogenic microbial communities from oil sands processing tailings. M.Sc. Thesis, University of Alberta.

- Penner, T. J., Foght, J. M. (2010). Mature fine tailings from oil sands processing harbor diverse methanogenic communities. *Canadian Journal of Microbiology*, 56, 459–470. doi:10.1139/W10-029
- Petersen, D., Blazewicz, S., Firestone, M., Herman, D., Turetsky, M., & Waldrop, M. (2012). Abundance of microbial genes associated with nitrogen cycling as indices of biogeochemical process rates across a vegetation gradient in Alaska. *Environmental Microbiology*, 4(4):993-1008.
- Polack, R., Chen, Y.W., & Belzile, N. (2009). Behavior of Sb(V) in the presence of dissolved sulfide under controlled anoxic aqueous conditions. *Chemical Geology*, 694(262), 179 –185.
- Prakash, S., Vandenberg, J.A., & Buchak, E. The oil sands pit Lake Model sediment diagenesis module. Paper presented at the Retrieved from <http://mssanz.org.au/modsim2011>
- Puttaswamy, N., & Liber, K. (2012). Influence of inorganic anions on metals release from oil sands coke and on toxicity of nickel and vanadium to *Ceriodaphnia dubia*. *Chemosphere*, 86 (5), 521–529. <http://dx.doi.org/10.1016/j.chemosphere.2011.10.018>.
- Ramos-Padrón, E., Bordenave, S., Lin, S., Bhaskar, I.M., Dong, X., Sensen, C.W., Fournier, J., Voordouw, G. & Gieg, L.M. (2011). Carbon and sulfur cycling by microbial communities in a gypsum-treated oil sands tailings pond. *Environmental Science & Technology*, 45(2):439-446.
- Rauret, G., Lo'pez-Sa'nchez, J.F., Sahuquillo, A., Rubio, R., Davidson, C.M., Ure, A., Quevauviller, P. (1999). Improvement of the BCR three step sequential extraction procedure prior to the certification of new sediment and soil reference materials. *Journal of Environmental Monitoring*, 1, 57 – 61.
- Robins, C.R., Brock-Hon, A.L., & Buck, B.J. (2012). Conceptual Mineral Genesis Models for Calcic Pendants and Petrocalcic Horizons, Nevada. *Soil Use and Management*, 29(2), 295-295.
- Rösch, C., Mergel, A. & Bothe, H. (2002). Biodiversity of denitrifying and dinitrogen-fixing bacteria in an acid forest soil. *Applied and Environmental Microbiology*, 68(8), 3818–3829.
- Sarkar, J., Kazy, S. K., Gupta, A., Dutta, A., Mohapatra, B., Roy, A., Bera, P., Mitra, A., & Sar, P. (2016). Biostimulation of Indigenous Microbial Community for Bioremediation of Petroleum Refinery Sludge. *Frontiers in Microbiology*. 7, 1407. doi: 10.3389/fmicb.2016.01407.

- Scandella, B.P., Varadharajan, C., Hemond, H.F., Ruppel, C. & Juanes, R. (2011). A conduit dilation model of methane venting from lake sediments. *Geophysical Research Letters*, 38(6), L06408.
- Sharma, J., & Singh, R. (2001). Effect of nutrients supplementation on anaerobic sludge development and activity for treating distillery effluent. *Bioresource Technology*. 79(2), 203-206.
- Siddique, T., Fedorak, P.M., & Foght, J.M. (2006). Biodegradation of short-chain n-alkanes in oil sands tailings under methanogenic conditions, *Environmental Science and Technology*, 40, 5459-5464.
- Siddique, T., Fedorak, P.M., MacKinnon, M.D., & Foght, J.M. (2007). Metabolism of BTEX and naphtha compounds to methane in oil sands tailings, *Environmental Science and Technology*, 41, 2350-2356.
- Siddique, T., Gupta, R., Fedorak, P. M., MacKinnon, M. D., & Foght, J. M. (2008). A first approximation kinetic model to predict methane generation from an oil sands tailings settling basin. *Chemosphere*, 72(10), 1573–1580. doi:10.1016/j.chemosphere.04.036
- Siddique, T., P. Kuznetsov, A. Kuznetsova, N. Arkell, R. Young, S. Guigard, & J.M. Foght. (2014a). Microbially accelerated consolidation of oil sands tailings. Pathway I: Changes in porewater chemistry. *Frontiers in Microbiology*, 5,106. doi:10.3389/fmicb.2014.00106
- Siddique, T., Kuznetsov, P., Kuznetsova, A., Li, C., Young, R., Arocena, J.M., & Foght, J.M. (2014b). Microbially-accelerated consolidation of oil sands tailings. Pathway II: solid phase biogeochemistry. *Frontiers in Microbiology*, 5,107. doi: 10.3389/fmicb.2014.00107
- Siddique, T., Mohamad Shahimin M.F., Zamir S., Semple, K., Li, C., & Foght, J.M. (2015). Long-term incubation reveals methanogenic biodegradation of C5 and C6 iso-alkanes in oil sands tailings. *Environmental and Science Technology*, 49, 14732–14739
- Siddique, T., Penner, T., Klassen, J., Nesbo, C., & Foght, J.M. (2012). Microbial communities involved in methane production from hydrocarbons in oil sands tailings, *Environmental and Science Technology*, 46, 9802-9810.
- Siddique, T., Penner, T., Semple, K., & Foght, J. M. (2011). Anaerobic biodegradation of longer chain n-alkanes coupled to methane production in oil sands tailings. *Environmental Science & Technology*, 45(13), 5892–5899. Doi: 10.1021/es200649t

- Siddique, T., Stasik, S., Mohamad Shahimin, M. F., & Wendt-Potthoff, K. (2018). Microbial communities in oil sands tailings: Their implications in biogeochemical processes and tailings management. In T. J. McGenity (Ed.), *Microbial communities utilizing hydrocarbons and lipids: Members, metagenomics and ecophysiology* (pp. 1-33) Springer.
- Siles, J. A., Martín, M. A., Chica, A. F., & Martín, A. (2010). Anaerobic co-digestion of glycerol and wastewater derived from biodiesel manufacturing. *Bioresource Technology*, *101*, 6315-6321.
- Smedley, P.L., & Kinniburgh, D.G. (2017). Molybdenum in natural waters: A review of occurrence, distributions and controls. *Applied Geochemistry*, *84*, 387-432.
- Smith, E., Thavamani, P., Ramadass, K., Naidu, R., Srivastava, P., & Megharaj, M. (2015). Remediation trials for hydrocarbon-contaminated soils in arid environments: evaluation of bioslurry and biopiling techniques. *International Biodeterioration & Biodegradation*, *101*, 56–65. doi:10.1016/j.ibiod.2015.03.029
- Sobkowicz, J. (2012). *Oil sands tailings technology deployment roadmap*. (No. 2). Calgary, Alberta, Canada: Golder Associates Ltd.
- Sorensen, J. (1982). Reduction of ferric iron in anaerobic, marine sediment and interaction with reduction of nitrate and sulfate. *Applied & Environmental Microbiology*, *43*, 319–324.
- Sreethawong, T., Niyamapa. T., Neramitsuk, H., Rangsunvigit, P., Leethochawalit, M., & Chavadej, S. (2010). Hydrogen production from glucose-containing wastewater using an anaerobic sequencing batch reactor: Effects of COD loading rate, nitrogen content, and organic acid composition. *Chemical Engineering Journal*, *160*, 322-332.
- Stackebrandt, E. (2014). The emended family peptococcaceae and description of the families' desulfitobacteriaceae, desulfotomaculaceae, and thermicolaceae. In Rosenberg, E., DeLong, E.F., Lory, S., Stackebrandt, E., Thompson, F. (Ed.), *The prokaryotes: Firmicutes and tenericutes* (pp. 285-290) Retrieved from <http://dx.doi.org/10.1007/978-3-642-30120-9>
- Stasik, S., Loick, N., Knöller, K., Weisener, C. & Wendt-Potthoff, K. (2014). Understanding biogeochemical gradients of sulfur, iron and carbon in an oil sands tailings pond. *Chemical Geology*, *382*, 44-53.
- Stasik, S., & Wendt-Potthoff, K. (2014). Interaction of microbial sulphate reduction and methanogenesis in oil sands tailings ponds. *Chemosphere*, *103*, 59-66.
- Stat Soft, I. (2011). *STATISTICA (data analysis software system)*

- Sun, W. J., Sierra, R., & Field, J. A. (2008). Anoxic oxidation of arsenite linked to denitrification in sludges and sediments. *Water Resources*, 42, 4569–4577.
- Symons, G. E., & Buswell, A. M. (1933). The methane fermentation of carbohydrates. *Journal of the American Chemical Society*, 55(5), 2028–2036. Doi.10.1021/ja01332a039
- Tan, B., Rozycki, T., & Foght, J.M. (2014). Draft genome sequences of three *Smithella* spp. obtained from a methanogenic alkane-degrading culture and oil field produced water. *Genome Announc*, 2(5), <http://dx.doi.org/10.1128/genomeA.01085-14> e01085e14.
- Tan, B., Semple, K., & Foght, J.M. (2015). Anaerobic alkane biodegradation by cultures enriched from oil sands tailings ponds involves multiple species capable of fumarate addition. *FEMS Microbiology Ecology*, 91(5), fiv042. doi: 10.1093/femsec/fiv042.
- The government of Alberta. (2017). *Alberta oil sands industry quarterly update*. Edmonton, AB: The government of Alberta.
- Thompson, D.K., Motta F.L., & Soares J.B.P. (2017). Investigation on the flocculation of oil sands mature fine tailings with alkoxy silanes. *Minerals Engineering*, 111, 90-99.
- Throback I. N., Enwall K., Jarvis A., & Hallin S. (2004). Reassessing PCR primers targeting *nirS*, *nirK* and *nosZ* genes for community surveys of denitrifying bacteria with DGGE. *FEMS Microbiology Ecology*, 49, 401–417.
- Thorpe, C.L., Lloyd, J.R., Law, G.T.W., Burke, I.T., Shaw, S., Bryan, N.D., & Morris, K. (2012). Strontium sorption and precipitation behaviour during bioreduction in nitrate impacted sediments,” *Chemical Geology*, (306–307), 114–122.
- Tonkin, J.W., Balistrieri, L.S., & Murray, J.W (2004). Modeling sorption of divalent metal cations on hydrous manganese oxide using the diffuse double layer model. *Applied Geochemistry*, 19, 29–53.
- Toor, N.S., Franz, E.D., Fedorak, P.M., MacKinnon, M.D., & Liber, K., 2013. Degradation and aquatic toxicity of naphthenic acids in oil sands process-affected waters using simulated wetlands. *Chemosphere*, 90, 449–458.
- US EPA. (1974). *Method 310.2. Alkalinity (colorimetric, automated, methyl orange)*. Retrieved from [http://water.epa.gov/scitech/methods/cwa/methods\\_index.cfm](http://water.epa.gov/scitech/methods/cwa/methods_index.cfm)
- US EPA. (2007). *Method 3050B. Acid Digestion of Sediments, Sludges, and Soils*. Retrieved from [http://www.epa.gov/wastes/hazard/testmethods/sw846/online/3\\_series.htm](http://www.epa.gov/wastes/hazard/testmethods/sw846/online/3_series.htm)

- Van den Heuvel, M.R., Hogan, N.S., Roloson, S.D., & Van Der Kraak, G.J. (2012). Reproductive development of yellow perch (*Perca flavescens*) exposed to oil sands-affected waters. *Environmental Toxicology and Chemistry*, 31, 654–662. <http://dx.doi.org/10.1002/etc.1732>.
- Van Hamme, J. D., & Ward, O. P. (2003). Recent advances in petroleum microbiology. *Microbiology and Molecular Biology Reviews*, 67(4): 503-549.
- Vidal, G., Carvalho, A., Méndez, R., & Lema, J. M. (2000). Influence of the content in fats and proteins on the anaerobic biodegradability of dairy wastewaters. *Bioresource Technology*, 74, 231-239
- Volke-Sepúlveda, T., Gutiérrez-Rojas, M., & Favela-Torres, E. (2006). Biodegradation of high concentrations of hexadecane by *Aspergillus niger* in a solid-state system: Kinetic analysis. *Bioresource Technology*, 94(14), 1583–1591
- Voordouw, G. (2013). Interaction of oil sands tailings particles with polymers and microbial cells: First steps toward reclamation to soil. *Biopolymers*, 99, 257–262. doi:10.1002/bip.22156
- Vorlicek, T.P., Kahn, M.D., Kasuya, Y., & Helz, G.R. (2004). Capture of molybdenum in pyrite-forming sediments: role of ligand-induced reduction by polysulfides. *Geochimica et Cosmochimica Acta*, 68, 547-556
- Wallace, S.H., Shaw, S., Morris, K., Small, J.S., Fuller, A.J., & Burke, I.T. (2012). Effect of groundwater pH and ionic strength on strontium sorption in aquifer sediments: Implications for <sup>90</sup>Sr mobility at contaminated nuclear sites. *Applied Geochemistry*, 27(8)1482–1491.
- Walworth, J., Pond, A., Snape, I., Rayner, J., Ferguson, S., & Harvey, P. (2007). Nitrogen requirements for maximizing petroleum bioremediation in a sub-Antarctic soil. *Cold Reg. Science Technology*, 48, 84–91.
- Wang, H., Chen, F., Mu, S., Zhang, D., Pan, X., Lee, D.J., & Chang, J.S. (2013). Removal of antimony (Sb(V)) from Sb mine drainage: biological sulfate reduction and sulfide oxidation-precipitation. *Bioresource technology*, 146, 799 –802.
- Welsh, A., Chee-Sanford, J., Connor, L., Löffler, F., & Sanford, R. (2014). Refined *nrfA* phylogeny improves PCR-based *nrfA* gene detection. *Applied and Environmental Microbiology*, 80(7), 2110-2119. doi:10.1128/AEM.03443-13.
- Wersin, P., Leupin, O.X., Mettler, S., Gaucher, E.C., Mader, U., De Canniere, P., ... Eichinger, L. (2011). Biogeochemical processes in a clay formation in situ experiment: Part A. Overview, experimental design and water data of an experiment in the opalinus clay at the Mont terri

- underground research laboratory, Switzerland. *Applied Geochemistry*, 26, 931–953. doi: 10.1016/j.apgeochem.2011.03.004
- Westcott, F. (2007). *Oil sands end pit lakes: A review to 2007*. (). Fort McMurray, AB, Canada: Cumulative Environmental Management Association End Pit Lakes Subgroup.
- White, K.B. (2017). Characterizing annual changes in the chemistry and toxicity of surface water from Base Mine Lake, an Alberta oil sands End Pit Lake. M.Sc. Thesis. University of Saskatchewan
- Widdel, F., Knittel, K., & Galushko, A. (2010). Anaerobic hydrocarbon-degrading microorganisms: An overview. *In Handbook of hydrocarbon and lipid microbiology* (pp.1997–2021). Berlin, Heidelberg: Springer. doi.org/10.1007/978-3-540-77587-4\_146
- Xu, R., & Obbard, J.P. (2003). Effect of Nutrient Amendments on Indigenous Hydrocarbon Biodegradation in Oil Contaminated Beach Sediments. *Journal of Environmental Quality*, 32(4):1234-43.
- Yelton, A.P., Williams, K.H., Fournelle, J., Wrighton, K.C., Handley, K.M., & Banfield, J.F. (2013). Vanadate and acetate biostimulation of contaminated sediments decreases diversity, selects for specific taxa, and decreases aqueous V<sup>5+</sup> concentration. *Environmental Science and Technology*, 47, 6500-6509.
- Zahr, J. P., Jenkins, B. D., Short, S. M., & Steward, G. F. (2003). Nitrogenase gene diversity and microbial community structure: a cross-system comparison. *Environmental Microbiology*, 5, 539 –554. <https://doi.org/10.1046/j.1462-2920.2003.00451.x>.
- Zhang, J., Dong, H.L., Zhao, L.D., McCarrick, R., & Agrawal, A.(2014). Microbial reduction and precipitation of vanadium by mesophilic and thermophilic methanogens. *Chemical Geology*, 370, 29-39.
- Zhang, Y. (2016). Development and Application of Fenton and UV-Fenton Processes at Natural pH Using Chelating Agents for the Treatment of Oil Sands Process-affected Water. PhD. Thesis. Alta University.

Zhang, Z., & Lo, I. M. (2015). Biostimulation of petroleum-hydrocarbon- contaminated marine sediment with co-substrate: involved metabolic process and microbial community. *Applied Microbiology and Biotechnology*, *99*, 5683–5696. doi: 10.1007/s00253-015-6420-9

Zhou, L., Li, K. P., Mbadinga, S. M., Yang, S. Z., Gu, J. D., & Mu, B. Z. (2012). Analyses of n-alkanes degrading community dynamics of a high-temperature methanogenic consortium enriched from production water of a petroleum reservoir by a combination of molecular techniques. *Ecotoxicology*, *21*, 1680–1691. <http://dx.doi.org/10.1007/s10646-012-0949-5>.

## Appendix A

Supporting Information for

Chapter 2. Nutrients' impact on the methanogenesis in oil sand tailings under End Pit Lake scenario: I: co-occurrence of N cycling and methanogenesis

### Details of raw gene sequence data analysis

After receiving the illumina sequencing files, separate these files into 2 folders, one folder for R1 and R2 files, and another folder for L1 and L2 files. Then, download and install a file compression program, such as Band zip (<https://www.bandisoft.com/bandizip/>). After selecting the R1 and R2 files, right click on them, and create an archive TAR-files of them. This compressed file is containing the sequencing data. Then, open an Excel file and make a mapping file. In Excel file, the 1<sup>st</sup>, 2<sup>nd</sup>, 3<sup>rd</sup>, 4<sup>th</sup>, and the 5<sup>th</sup> columns must be filled by the sample name, the treatment, the strand, and the names of read files Read 1 (R1), and Read 2(R2) (R1 and R2 must match the file names of the R1 and R2 Illumina files), respectively and the prepared mapping file must be saved as text file. Now, go to the Metamp website (<http://ebg.ucalgary.ca/metaamp/index.html>) and then enter the file name and email address. Then choose the Fastq and Paired-end and upload the compressed.tar file and the mapping file that you made previously. Now put in the forward and reverse primers for the one gene that you are looking for. For the 16S, rRNA gene and all other genes non-rRNA gene must be chosen. The maximum number of errors in overlap was chosen 50, for 16S gene based on the research of other data pipelines. The maximum expected error was used 1 as it is a usual number in analysis. The various trim amplicon was used to fixed length for each gene as below.

16S

F: AAACYAAAKGAATTGRCGG

R: ACGGGCGGTGTGTRC

Min Overlap 50

Max Diff 10

Errors in Primer sequence: 1

Trim amp 400

NifH

F: AAAGGYGGWATCGGYAARTCCACCAC

R: TTGTTSGCSGCRTACATSGCCATCAT

Min Overlap 50

Max Diff 10

Trim amp 385

NirS

F: G TSAACGTSAAGGARACSGG

R: GASTTCGGRTGSGTCTTGA

Min Overlap 50

Max Diff 10

Trim amp 375

NosZ

F: CGYTG TTCMTCGACAGCCAG

R: CGSACCTTSTTGCCSTYGCG

Min Overlap 50

Max Diff 10

Trim amp 275

NrfA

F: CARTGYCAYGTBGARTA

R: TWNGGCATRTGRCARTC

Min Overlap 200

Max Diff 10

Trim amp 235

After filling out the above information, click on “Get OTUs”. For each gene, the above information must be entered to metaamp site, separately. After receiving the data file through email, click on “Download a packaged file containing all results in this page”, and then download, and rename the file and chose the same analysis name that was used earlier and save the file wherever you want. For 16S, go to OTU\_and\_taxonomy folder, open the \*.taxonomy.summary file in Excel. This file show the number of the reads of each microorganism as aligned with the Silva\_123 database (the best database). Now the data is in Excel and easy to work with. Here, I determine the % of each type of microbe within a sample and compare to other samples. For all other genes (functional), go to the alpha\_and\_beta\_diversity folder and find the \*.shared file and open in Excel. This tells the number of reads for each OUT in each sample. Determine the % of each read in each sample and ignore any OUT at less than 2%. Go to the OTU\_and\_taxonomy folder, open the \*.OTUs.fasta file in Excel. This tells the sequence of each OTU. Copy the OUT sequence and go to

[https://blast.ncbi.nlm.nih.gov/Blast.cgi?PAGE=MegaBlast&PROGRAM=blastn&PAGE\\_TYPE=BlastSearch&BLAST\\_SPEC=\(BLASTn\)](https://blast.ncbi.nlm.nih.gov/Blast.cgi?PAGE=MegaBlast&PROGRAM=blastn&PAGE_TYPE=BlastSearch&BLAST_SPEC=(BLASTn)).

Paste one sequences into the Enter Query Sequence box and hit BLAST at the bottom. Only one OTU can be run at a time. After a while a list of potential matches are given. The gene is most closely to the top matches. The matches must be assessed one by one and then decide about the OTU. For example if the purpose is searching the NirS gene and the top matches are rRNA genes, then this OTU should be discarded because it is not a NirS gene. Also, if the top matches are complete Genome matches, the some low down might be NirS matches, it means that the NirS matches were somewhere within the complete genome. Also, it should be tried to find the matches with a name. This process is hand curating and must be done for each OTU of the relevant gene.